Chapter 8

PHENOMENA AFFECTING ELECTROMAGNETIC PROPAGATION[1]

INTRODUCTION

The two principal phenomena caused by a nuclear detonation that affect electromagnetic propagation are electromagnetic emissions and ionization of the atmosphere. The short duration electromagnetic pulse described in Chapter 7 is in the first category. Also included in this first category are continuing thermal radiation and emissions from various chemical reactions within the atmosphere. These radiations and emissions produce noise throughout the radio and optical spectra. The second phenomenon, atmospheric ionization, involves alterations of the electrical properties of the atmosphere that can affect the propagation of electromagnetic waves. Both types of effects are caused by energy radiated from the nuclear explosion, from the subsequent fireball, and from the radioactive debris. The severity of the effects on the propagation of electromagnetic waves may vary from being completely negligible to intolerable degradation of system performance.

For the purpose of discussing the effects on propagation, the electromagnetic spectrum is divided into two frequency bands: the radio band, which includes radar applications, and the optical band, as shown in Figure 8-1. The most important effects in the radio band usually are those that affect the propagation of the desired electromagnetic signal (effects that change the amplitude, phase, direction, etc.). Electromagnetic radiations from the fireball and other regions can interfere with desired signals, and in some cases, interference from other sources (e.g., atmospheric noise) will be enhanced or diminished. The most important effect in the optical band is radiation from the fireball and other regions that interferes with desired signals. The source of this radiation is described in Chapter 3.

The current state of knowledge concerning the effects of nuclear detonations on electromagnetic wave propagation stems from full scale tests, laboratory experiments, theoretical studies, and simulation with certain atmospheric phenomena. Meaningful testing of high-altitude nuclear weapon effects requires a sophisticated space capability (e.g., instrumented rocket probes), and only a relatively few high-altitudes tests were performed prior to the test moratorium in 1962.

While those tests provided information to develop models to calculate the various phenomena, considerable uncertainty exists in scaling to burst or atmospheric conditions that are much different from those of the tests. All of the high-altitude tests have been single bursts. Significant differences are expected when two or more nuclear detonations occur near one another in time and space.

Detailed theoretical descriptions for most burst phenomena are highly complex and require specification of poorly known parameters for quantitative results. Laboratory measurements have been used to obtain estimates of some parameters, but usually the results have to be scaled to conditions much different than those

[1] Although the English system of units for measuring distance is given priority throughout most chapters of this manual, wavelengths and other dimensions dealing with electromagnetic wave propagation usually are given in the metric system. Therefore, in this chapter and in Chapter 17, the metric system is used for distance dimensions. Conversion factors from the metric system to the English system are provided in Appendix B.

[redacted]

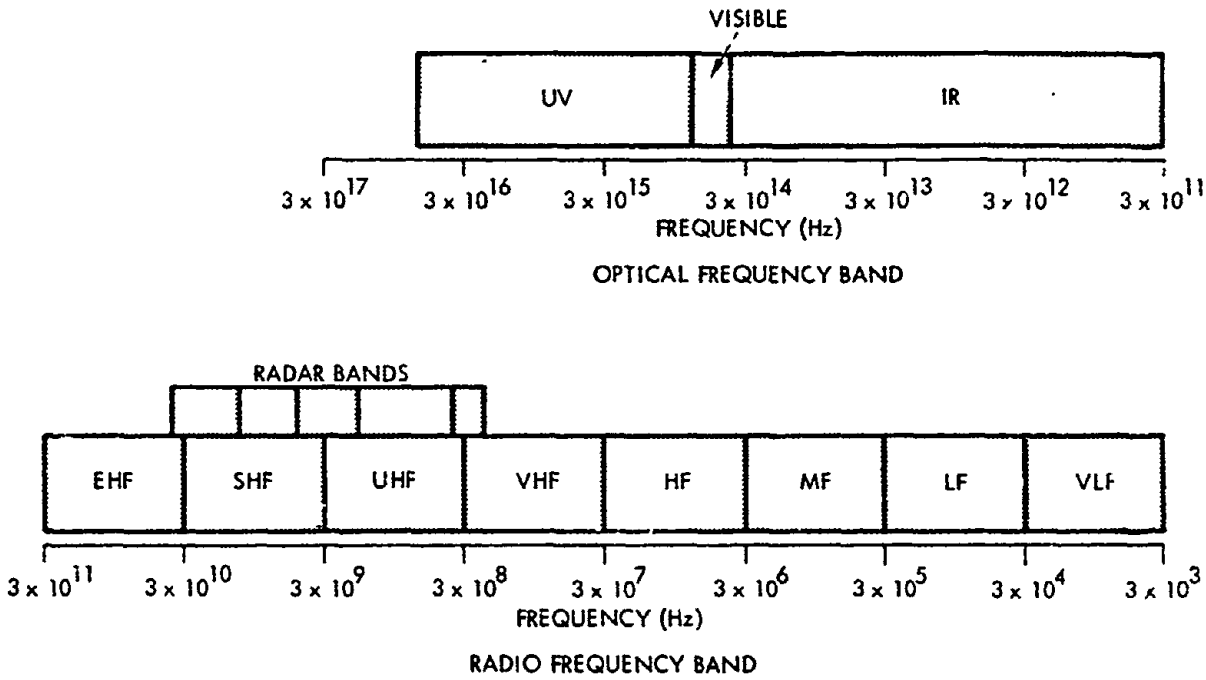

Figure 8-1. [redacted] Optical and Radio Frequency Bands [redacted]

[redacted]

used in the measurements. Some understanding of electromagnetic p.opagation in disturbed environments has been obtained from propagation measurements during eclipses, solar flares, and auroral disturbances. However, natural phenomena often involve the superposition of different phenomena than those brought about by nuclear bursts, and extrapolation to burst conditions can be misleading.

SECTION I
[redacted] PHENOMENA AFFECTING RADIO FREQUENCIES [redacted]

[redacted] The number of free electrons in the atmosphere is increased greatly by weapon radiations from high altitude bursts. These free electrons can absorb energy from electromagnetic waves and can change the phase velocity of the waves (changing the direction of propagation and signal characteristics). Electromagnetic radiations from heated regions and from trapped electrons are a source of noise.

[redacted] IONIZATION AND DEIONIZATION [redacted]

[redacted] Most of the energy of a nuclear detonation is emitted in forms that can produce ionization.[2] Some of this energy is in particulate matter (neutrons, beta particles, and high-speed debris that originally constituted the warhead and adjacent structure), and some is in photons (thermal radiation from the weapon case and gamma rays). Between 90 and 95 percent of the energy is emitted promptly (within a microsecond); about 5 to 10 percent is delayed radiation from the radioactive decay of fission debris.

[2]The ionization process is described in paragraph 6-4, Chapter 6.

[redacted]

[redacted] If a nuclear explosion occurred in a vacuum with no magnetic field, the flux of radiated energy would decrease as the square of the distance traveled. In the atmosphere, collisions and scattering processes absorb energy and produce ionization and excitation. (See Chapters 3, 4, and 5 for discussion of atmospheric absorption of photons, neutrons, and beta particles.)

[redacted] Radiation entering the atmosphere from above is absorbed rapidly when it reaches the altitude, termed the stopping altitude, where the mean-free path equals one scale height (an altitude region over which the atmospheric density changes by a factor of e (approximately 2.7). Stopping altitudes for the principal radiations from a nuclear weapon are shown in Table 8-1.

Table 8-1 [redacted] Approximate Stopping Altitudes for Principal Weapon Outputs Causing Ionization [redacted]

Weapon Output	Stopping Altitude (km)
Prompt Radiation	
x-rays (1 kev radiator)	80
Neutrons	25
Gamma rays	25
Debris (kinetic energy)	115
Delayed Radiation	
Gamma rays	25
Beta particles (1 Mev)	60

[redacted] For detonations below the stopping altitude of a particular radiation, most of that radiation will be contained locally. When detonations occur above the stopping altitude of a particular radiation, that radiation can spread large distances before being deposited and causing ionization. About 3×10^4 ion pairs are produced for each 1 Mev of energy deposited in the atmosphere. Since about 3×10^{28} Mev are released per megaton of weapon yield, even a small fraction of the weapon output can cause large electron densities. The lifetime for many of the electrons produced is short, however, and it depends critically on the altitude at which they are produced.

[redacted] Electrons and ions produced by the ionization sources undergo various atmospheric reactions that change their number density. Four principal reactions must be considered:

1. Attachment. Electrons can attach to neutral air particles (primarily to oxygen molecules and/or atoms) to form negative ions.
2. Detachment. Once attached, electrons can be detached from negative ions by collisions, solar radiation, or radiation from the fireball.
3. Recombination. Electrons and positive ions can recombine to form neutral particles.
4. Mutual Neutralization. Positive ions can combine with negative ions formed by attachment, to produce neutral particles.

[redacted] The rate at which these reactions proceed is a strong function of altitude. Thus, the altitude distribution of electron density after a period of time generally will not coincide with the altitude distribution immediately after the deposition of weapon energy. Detailed solutions of the time history of electron density require consideration of a large number of atmospheric species. Many reaction-rate coefficients are not well known, even for the natural atmosphere. The uncertainties in these coefficients provide a significant source of uncertainty in the prediction of electron density time history. In the natural atmosphere above about 70 km, where neutral particle density is low, recombination accounts for the major electron loss. At lower altitudes, attachment becomes increasingly important in the removal of free electrons, particularly at night

[redacted]

when there is no photodetachment of electrons from negative ions by sunlight.

In heated or highly ionized regions, the air chemistry (interaction between species) is modified, and electron loss processes are changed. The expansion of heated regions also reduces the electron density.

In discussing electron density caused by nuclear weapons, it is convenient and useful to consider the electron density resulting from prompt radiation and delayed radiation separately. Also, since ionization and deionization processes are significantly different inside and outside the fireball, these regions will be discussed separately. Although electrons are the principal cause of effects on electromagnetic propagation, ions can affect propagation in the VLF and LF bands (frequencies below a few hundred kilohertz).

8-1 Electron Density Within the Fireball

Initially the incandescent region termed the fireball is highly ionized. For detonations below about 60 km, thermal ionization of air and debris from the weapon and carrier maintains high electron densities until the fireball cools below about 2500°K. For cooler fireballs, beta particles deposited within the fireball may be a significant ionization source. Predictions of electron density within the fireball require knowledge of the distribution of temperature and debris within the fireball, the shape of the fireball as a function of time, and the detailed chemistry of heated regions.

Detailed calculations, which have been performed for a few burst conditions, are imprecise, particularly with regard to inhomogeneities and gradients in fireball properties. However, for many cases, relatively simple fireball models in which the mass density and temperature are assumed uniform within the fireball can be used. Figures 8–2 and 8–3 show calculated values of average fireball electron density and temperature following 1-Mt detonations at altitudes of 25 and 50 km, respectively. The calculations contained the assumption that the fireball gas was in thermal equilibrium, as well as being homogeneous.

When detonations occur above about 60 km, losses of free electrons within the fireball are slower and the electron density does not decay rapidly enough to remain in equilibrium with the cooling fireball. Volume expansion controls the decline of electron density during the first few tens of seconds following detonation. Later, recombination of electrons with positive atomic ions predominates.

For detonations at altitudes above about 80 km, the geomagnetic field influences the fireball expansion and location. After a few tens of seconds, magnetic forces cause the expansion across the magnetic field to become slower, while expansion along the magnetic field continues. Thus, the fireball becomes elongated along the magnetic field in a roughly cylindrical or tube shape. Figures 8–4 and 8–5 show calculations of average fireball electron density and temperature following 1-Mt detonations at altitudes of 75 and 150 km, respectively.

Photographs of fireballs affected by the magnetic field show many field-aligned striations within the fireball (see Figure 1–4C). The optical striations also indicate large variations of electron density within the fireball. The size of the striations and the variation of electron density from the average value cannot be scaled accurately with burst parameters at present.

For detonations at altitudes above about 300 km, the mean-free path of both X-rays and debris particles is large, and localized fireballs may not form around the detonation point. However, debris particles initially directed downward may heat and ionize a region below the detonation point. This region, if sufficiently disturbed, is termed a fireball region. The formation of a fireball region depends on the detonation altitude, the weapon yield, and the atmospheric density

[redacted]

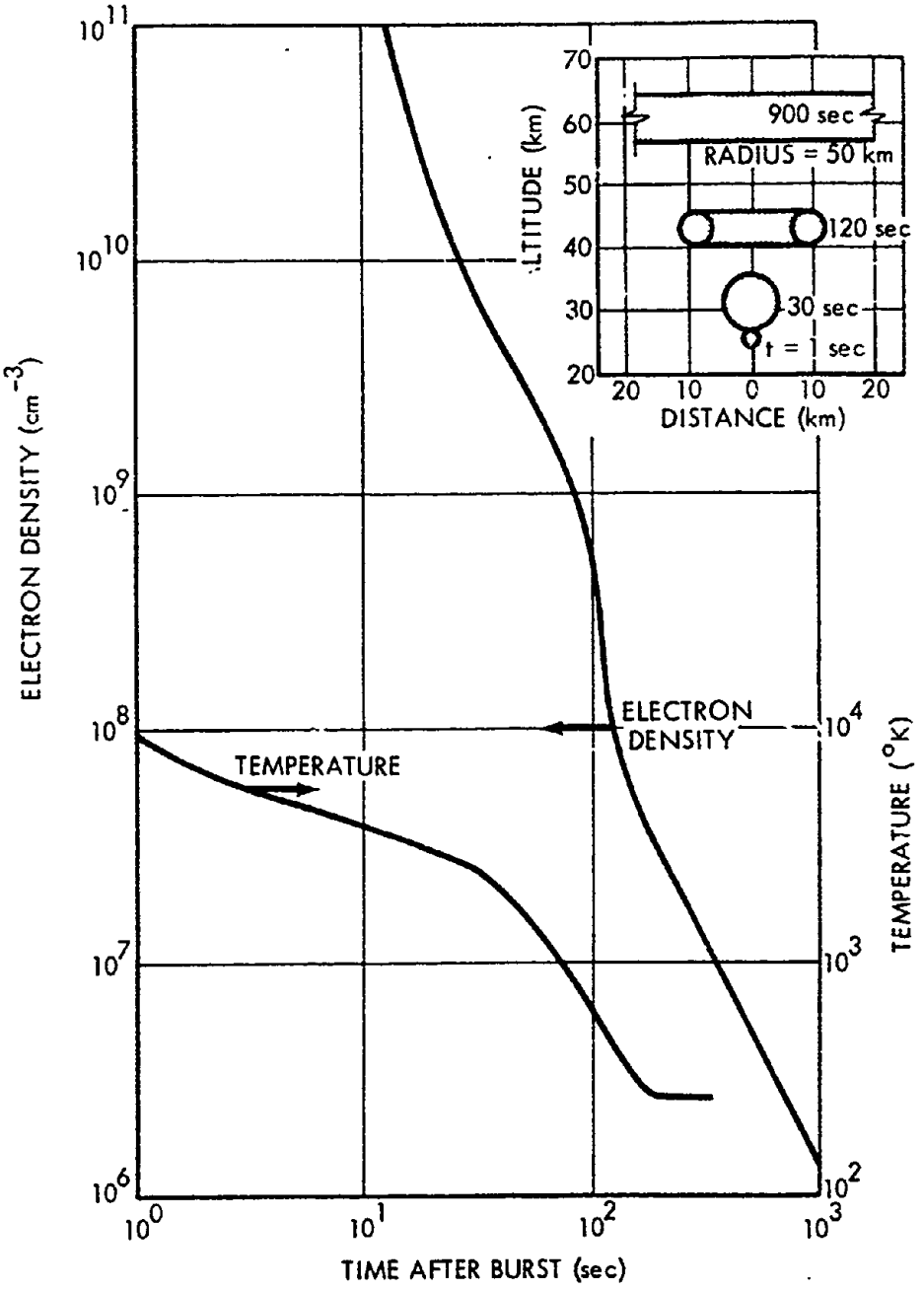

Figure 8-2. [redacted] Fireball Electron Density and Temperature, 1-Mt at 25 km [redacted]

[redacted]

[redacted]

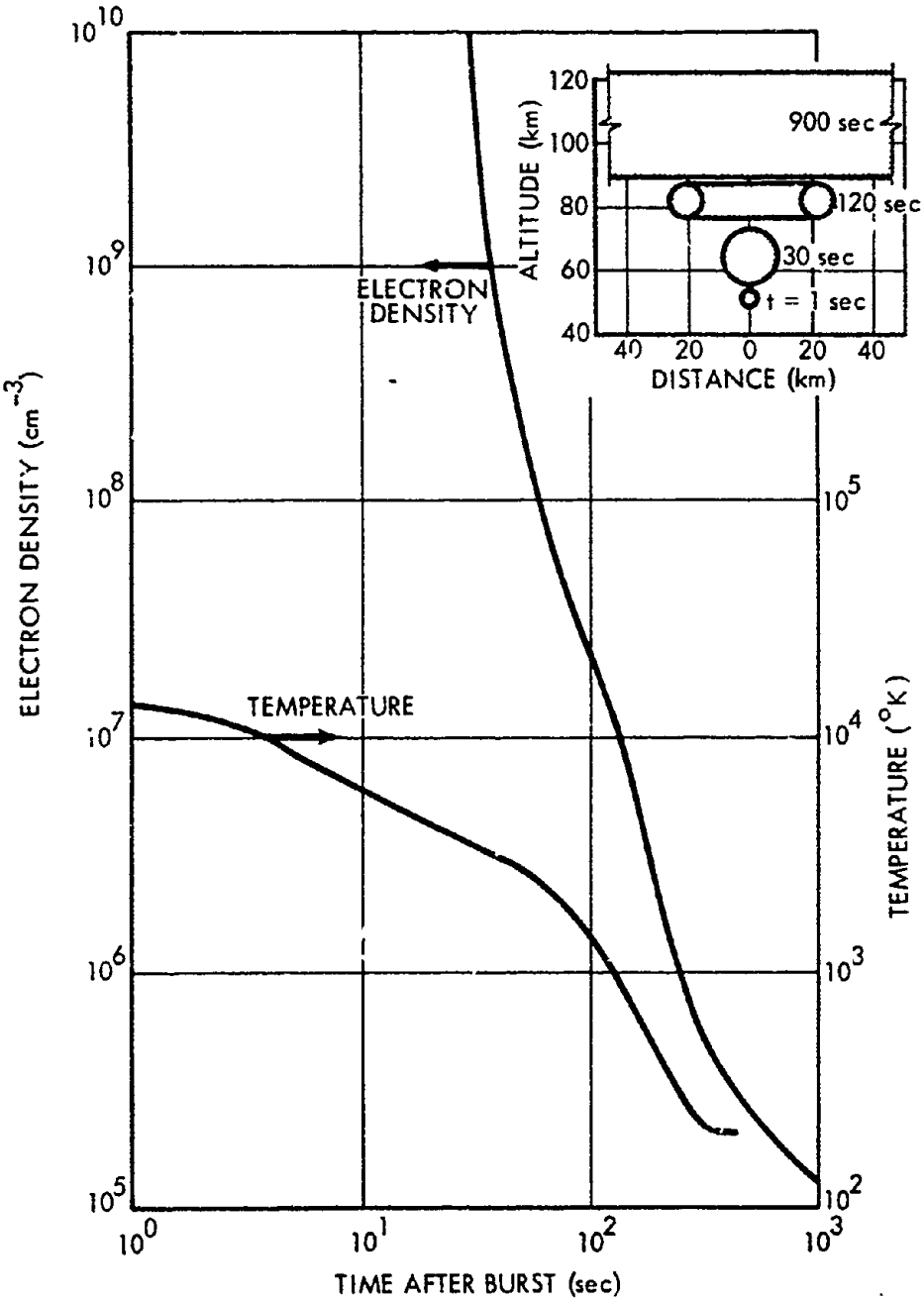

Figure 8-3. [redacted] Fireball Electron Density and Temperature, 1-Mt at 50 km [redacted]

[redacted]

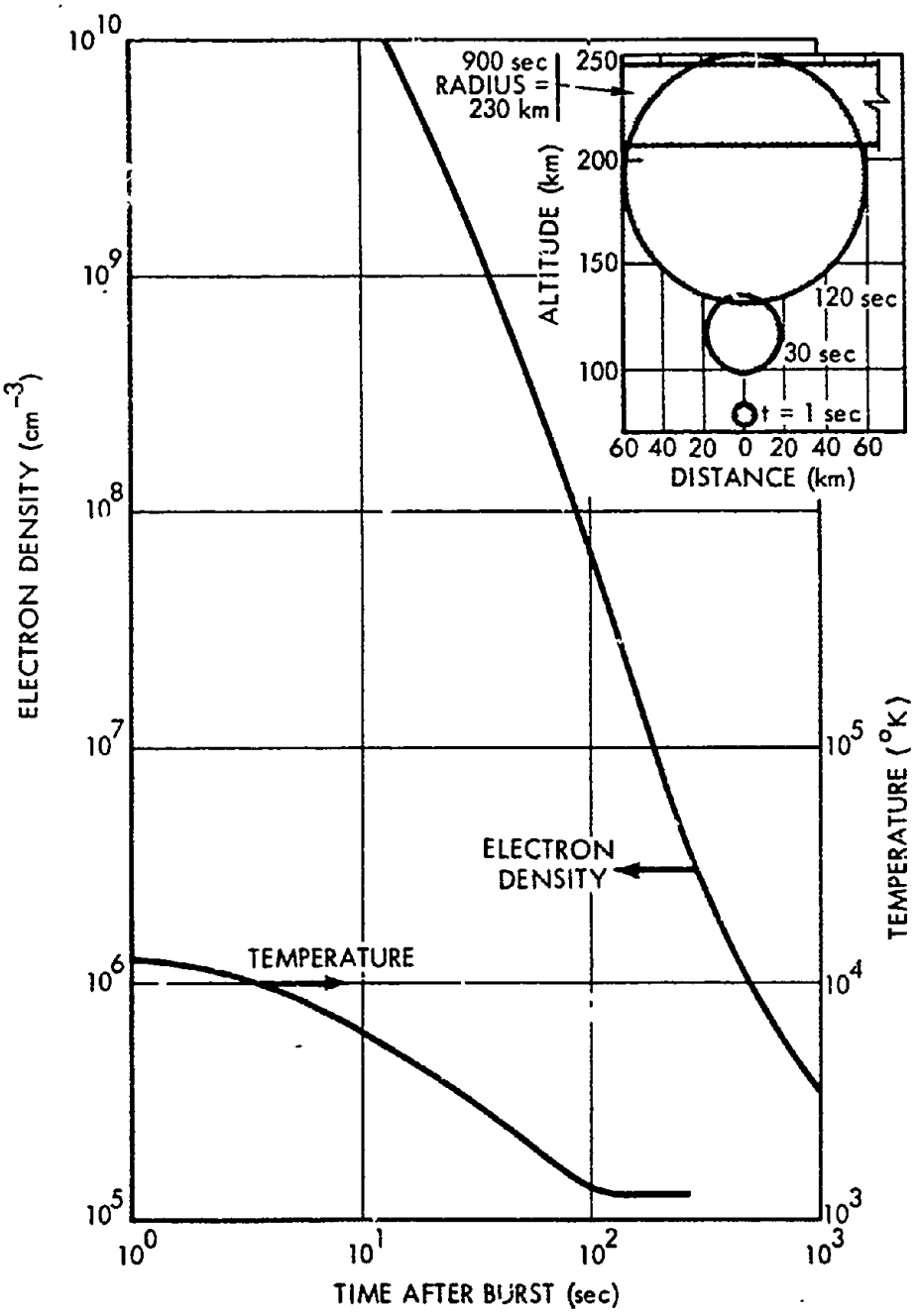

Figure 8-4. [redacted] Fireball Electron Density and Temperature, 1-Mt at 75 km [redacted]

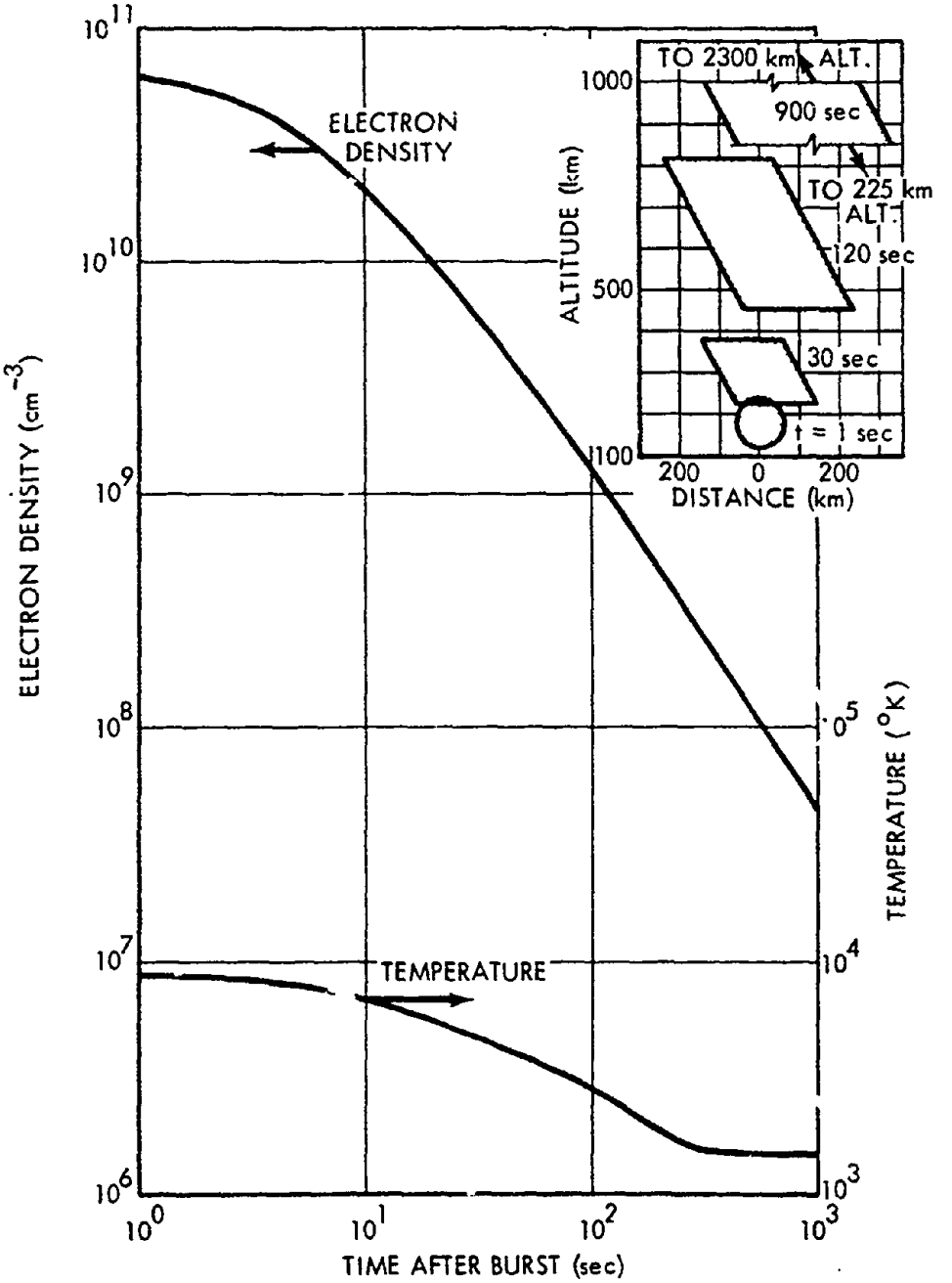

Figure 8-5. [redacted] Fireball Electron Density and Temperature, 1-Mt at 150 km [redacted]

[redacted]

[redacted]

[redacted]

at burst time. Figure 8–6 shows calculated values of electron density and temperature within the fireball following a 1-Mt detonation at an altitude of 400 km.

[redacted] Only a few nuclear tests have been carried out by the U.S. at detonation altitudes above 80 km; therefore, theoretical calculations of fireball formation, size, location, and properties are dependent on parameters that are poorly known. Calculations of fireball properties for detonations at altitudes above 80 km should be considered illustrative of the general order of magnitude rather than as detailed quantitative results.

8–2 Electron Density Caused by Prompt Radiation Outside the Fireball [redacted]

[redacted] Ionization produced outside the fireball by prompt gamma rays can be neglected insofar as effects on radio propagation are concerned. For detonations at altitudes below about 25 km, both neutrons and X-rays are deposited within or close to the fireball, and the effects of prompt radiation outside the fireball are minimal. For detonation altitudes between 25 and about 80 km, X-rays are largely confined, but neutrons produce ionization over distances of several hundred kilometers. For higher altitude detonations, both X-rays and neutrons cause widespread ionization. Figure 8–7 shows the initial ionization caused by prompt radiation from a nominal megaton weapon detonated at 120 km. Because of earth's curvature, radiation reaching a given altitude at large horizontal distances from the source must pass through lower altitudes where it is strongly attenuated by the denser air.

[redacted] The decay of electron and ion densities following the ionization impulse depends on electron and ion loss rates, which are functions of altitude and time of day. Below about 100 km, the electron and ion density after 1 second will be essentially independent of the initial ionization if the initial ion pair density is greater than 10^7 ion pairs cm^{-3}. This condition is termed saturation; larger initial ionization will not increase the electron or ion density remaining after 1 second. Figure 8–7 shows that the initial ion-pair density below 100 km exceeds 10^7 ion pairs cm^{-3} out to about 500 km from the burst.

[redacted] Figure 8–8 shows the altitude dependence of the electron density for several times after a saturation impulse. At night the electron concentration decays rapidly, particularly at low altitudes where attachment of electrons to neutral particles is the predominant reaction. During the day, electron densities greater than normal can persist for tens of minutes. The insert in Figure 8–8 illustrates the horizontal extent of the region that can be saturated by prompt radiation as a function of detonation altitude. The decay of electron and ion densities above 100 km depends on processes that may be affected by atmospheric chemistry changes caused by the deposition of prompt radiation. Because of the additional complications introduced at those altitudes, a simple representation of the decay is not possible.

[redacted] Many of the neutrons produced by the explosion will travel upward and will escape the atmosphere. Since neutrons are not affected by the geomagnetic field, they will spread isotropically over a large area. Each neutron eventually disintegrates spontaneously into a proton, a neutrino, and a beta particle (half-life for disintegration is about 12 minutes). Since the beta particle (a high-energy electron) is charged, it can move only in the direction of the geomagnetic field (motion normal to the magnetic field direction causes the beta particle to spiral around the magnetic field lines). The beta particles are guided by the geomagnetic field until reaching altitudes near the beta-particle stopping altitude (see paragraph 8–4 and Figure 8–10), where they deposit their energy to produce ionization. The amount of ionization caused by neutron-decay beta particles is small, but it has been noted at distances of many thousands of kilometers from the burst point.

[redacted]

[redacted]

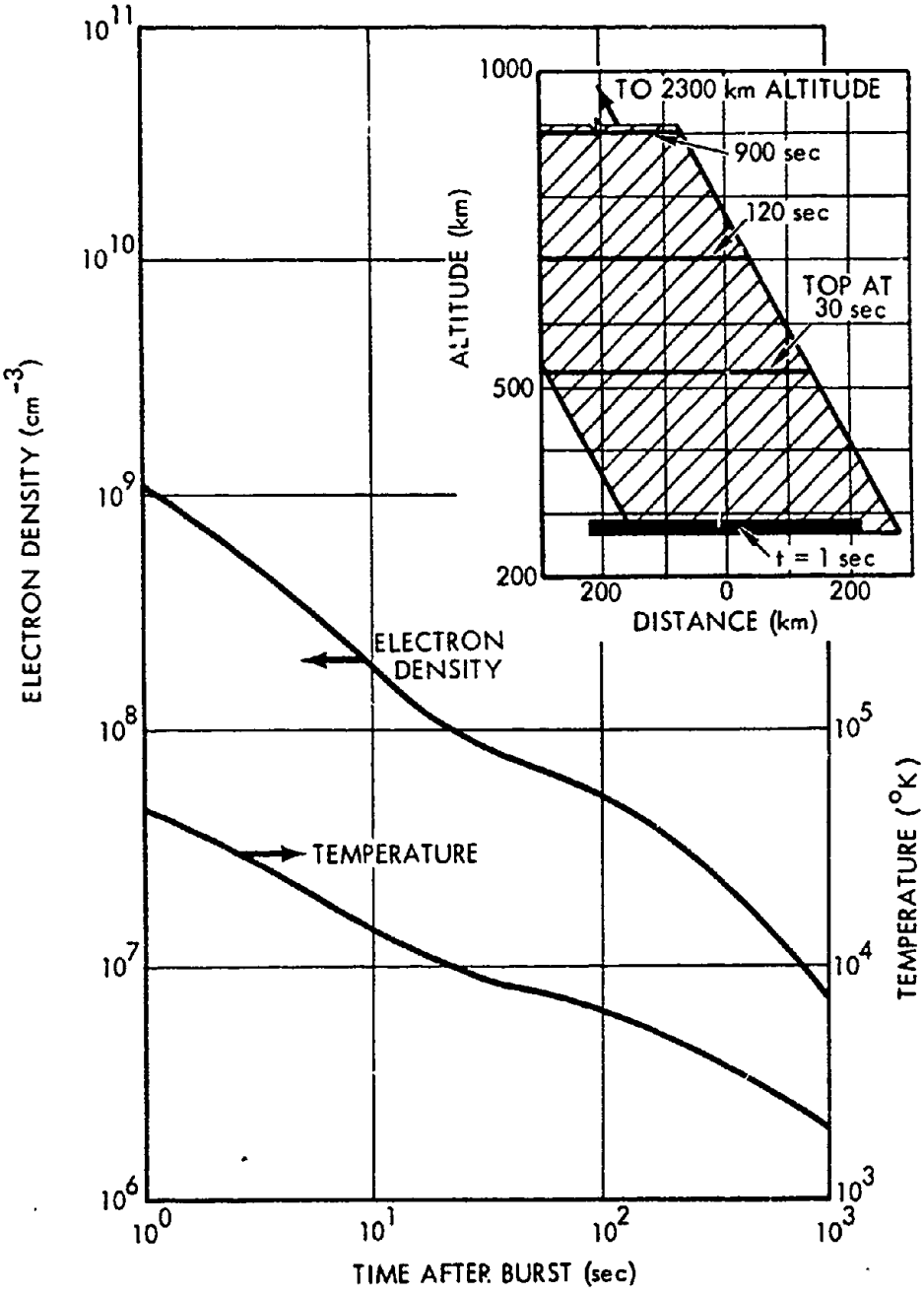

Figure 8-6. [redacted] Fireball Electron Density and Temperature, 1-Mt at 400 km [redacted]

[redacted]

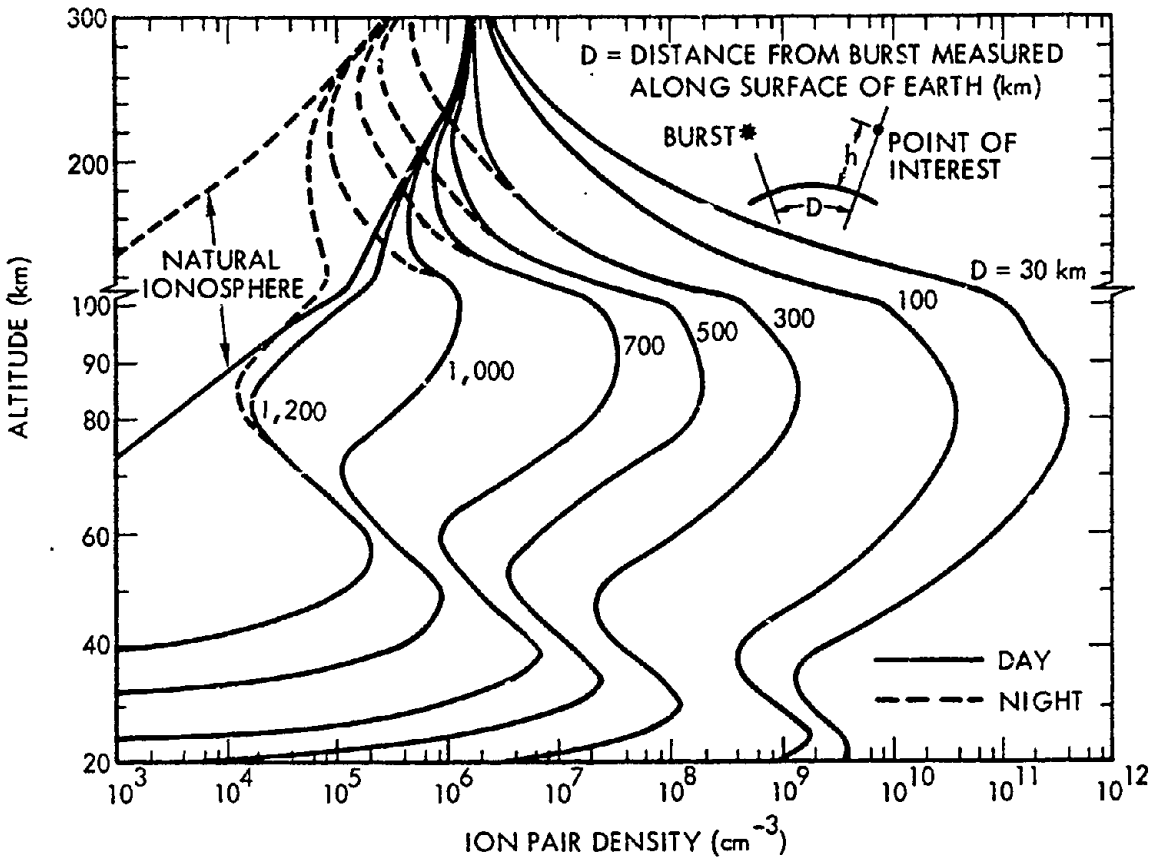

Figure 8-7. [redacted] Ion-Pair Density Due to Prompt Radiation from a 1-Mt Burst Detonated at 120 km, t = 0 [redacted]

8-3 Electron Density Caused by Delayed Gamma Radiation Outside the Fireball [redacted]

[redacted] In addition to prompt radiation, delayed gamma rays and beta particles (discussed in Section III, Chapter 5) are produced during the radioactive decay of the fission debris. This continuing radiation produces ionization characterized by a production rate of ion pairs per unit volume per unit time. For detonations below several hundred kilometers, the fission debris (assumed to be mixed with the total weapon debris) is initially within the fireball and is carried upward as the fireball rises and expands.

[redacted] When the debris is below the gamma-ray stopping altitude, gamma rays can only penetrate a short distance, and the ionized region that they produce around the fireball is small. If the debris rises above the gamma-ray stopping altitude, gamma rays produce ionization over larger distances. The resulting electron and ion densities are a function of both the ion-pair production rate and the electron and ion loss processes. Most of the gamma-ray energy is deposited near the stopping altitude, but the electrons produced below about 40 km are lost quickly by attachment. Maximum electron density usually occurs at higher altitudes where the electron lifetimes

[redacted]

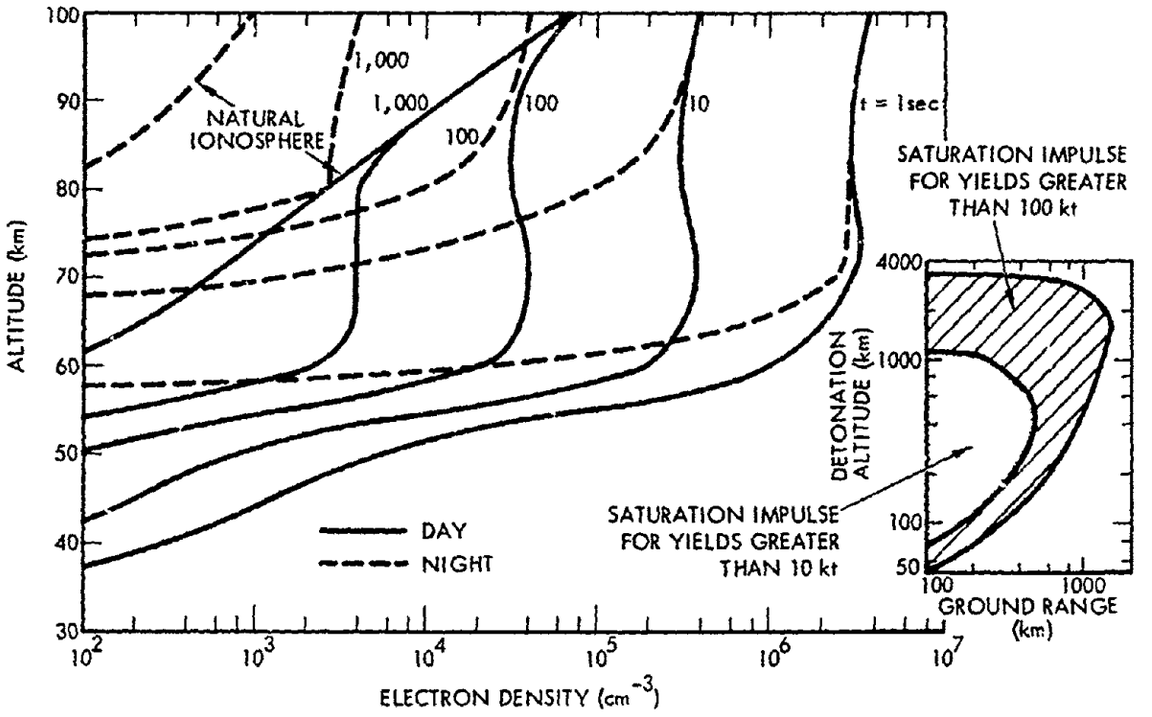

Figure 8-8. [redacted] D-Region Electron Density Caused by Prompt Radiation (Saturation) [redacted]

[redacted]

are longer. Near the debris region, where the gamma ray flux is large, substantial electron densities can be maintained even though the debris is at an altitude where free electrons are lost by attachment rapidly.

[redacted] When the fission debris and the point of interest are both well above the gamma-ray stopping altitude, the ion-pair production rate and electron and ion densities caused by gamma rays can be expressed conveniently in terms of a radiation intensity parameter, I_γ, defined by

$$I_\gamma = \frac{4 \times 10^{-7} W_F}{4\pi R^2 (1+t)^{1.2}} \text{ watts } m^{-2},$$

where

W_F = fission yield in megatons,

R = radial distance from debris center to point of interest in km,

t = time after detonation in seconds.

Figure 8-9 shows quasi-equilibrium electron densities for particular values of I_γ. The values are called quasi-equilibrium because they are the values that would be reached if the production rate remained constant and if sufficient time were allowed for equilibrium conditions to be reached. In an actual situation, the production rate changes with time because of the radioactive decay of the fission debris and the changing geometry as the debris moves. However, for most cases, the time to reach equilibrium is short, and the quasi-equilibrium values are close approximations to the electron densities. The insert in Figure 8-9 illustrates the horizontal extent as a function of

[redacted]

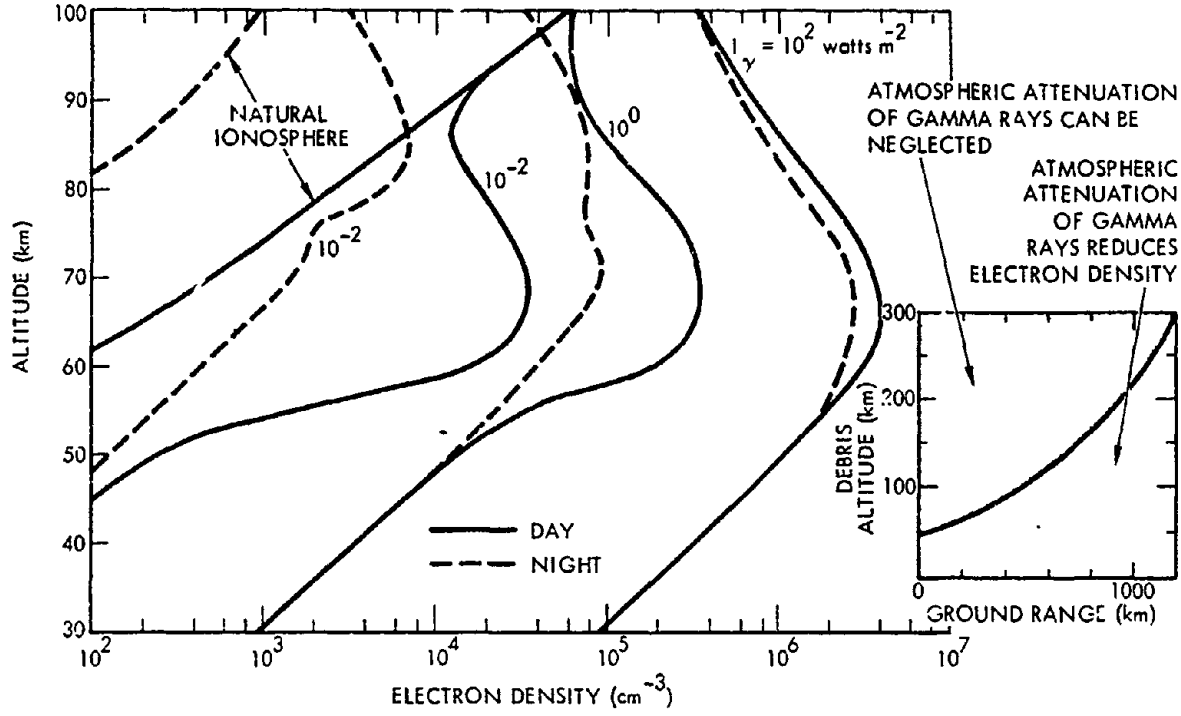

Figure 8-9. Quasi-Equilibrium Electron Density Due to Gamma Rays

debris altitude for which the electron densities are applicable.

Most delayed gamma rays deposit their energy in the atmosphere by first producing high-energy electrons (Compton electrons). Compton electrons travel very short distances in the lower atmosphere; however, some Compton electrons produced above about 60 km can escape to the conjugate region, as described for beta particles in paragraph 8-4. Ionization in the conjugate region caused by Compton electrons is of interest primarily for studies of propagation in and below the HF band (frequencies below 30 megahertz).

8-4 Electron Density Caused by Beta Particles Outside the Fireball

Since beta particles are electrically charged, their motion in the atmosphere is affected by the geomagnetic field. When the fission debris is above the beta-particle stopping altitude, about half of the betas will travel down the geomagnetic field lines, producing ionization (similar to auroral ionization at high latitudes) until they are deposited near the stopping altitude. The other half of the betas (those emitted upward) will follow the geomagnetic field lines across the geomagnetic equator and will produce ionization at the geomagnetic conjugate.[3]

Figure 8-10 illustrates the location of the beta-particle ionization regions. Because of the slope (dip angle) of the magnetic field lines, the beta-particle ionization region is offset from the debris. When the geomagnetic field is undisturbed by the detonation, the location of the

[3] As used herein, geomagnetic conjugate points are points at the north and south ends of a geomagnetic field line that are at corresponding altitudes.

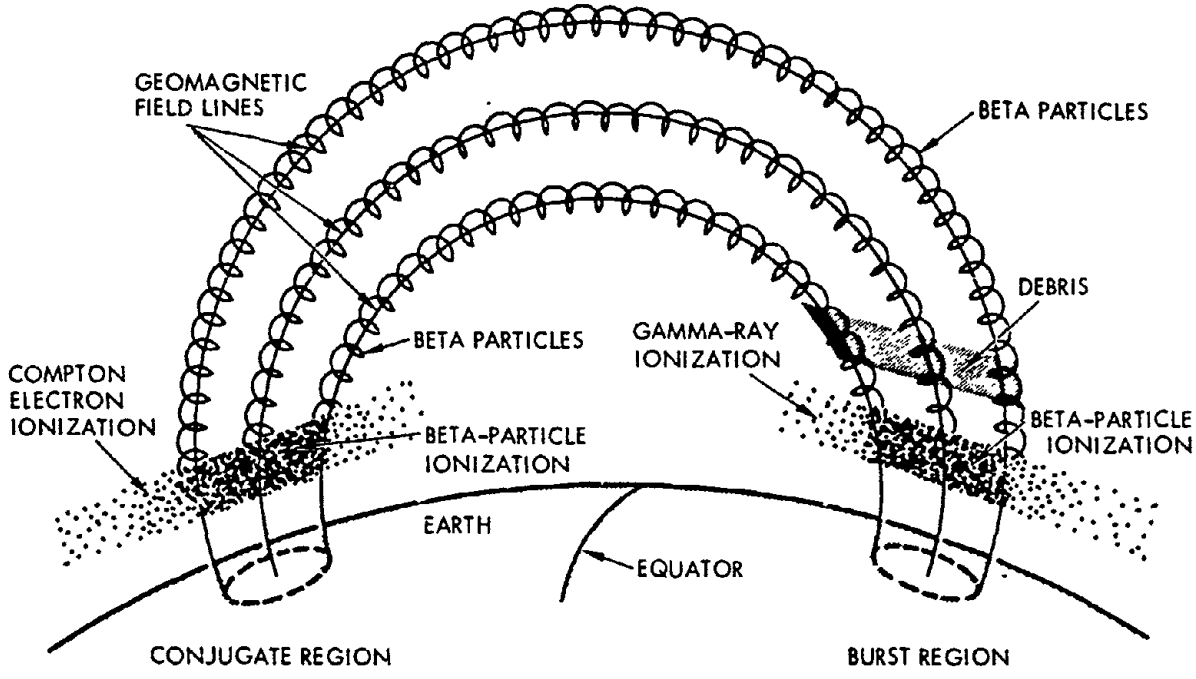

Figure 8-10. Location of Delayed Ionization Regions

beta-particle ionization region can be determined from a knowledge of the size and location of the debris region and the geomagnetic field lines. However, the geomagnetic field can be severely distorted for tens of seconds after a nuclear detonation. Determination of the magnetic dip angle and location of the conjugate point for undisturbed magnetic-field conditions are discussed in Problems 8-8 and 8-9.

The location of the gamma-ray ionization region and the region ionized by Compton electrons escaping to the conjugate region are also illustrated in Figure 8-10.

The ion-pair production rate and electron density caused by beta particles can be expressed conveniently in terms of a radiation intensity parameter, N_β, defined by:

$$N_\beta = \frac{8.8 \times 10^{15} W_F}{A(1+t)^{1.2}} \text{ betas } cm^{-2} sec^{-1}, \quad (8.1)$$

where

A = area covered by fission debris in square kilometers.

Figure 8-11 shows the quasi-equilibrium electron density caused by beta particles for particular values of N_β. These curves apply if the fission debris is well above the beta stopping altitude and if the debris is uniformly distributed over the area A.

8-5 Electromagnetic Propagation in Ionized Regions

An electromagnetic wave propagating through an ionized region does work on charged particles in the region and transfers a portion of the wave energy to charged-particle kinetic energy. The electric field exerts a force on all charged particles; however ions, because of their larger mass, absorb less energy than electrons and can usually be neglected (an exception is wave

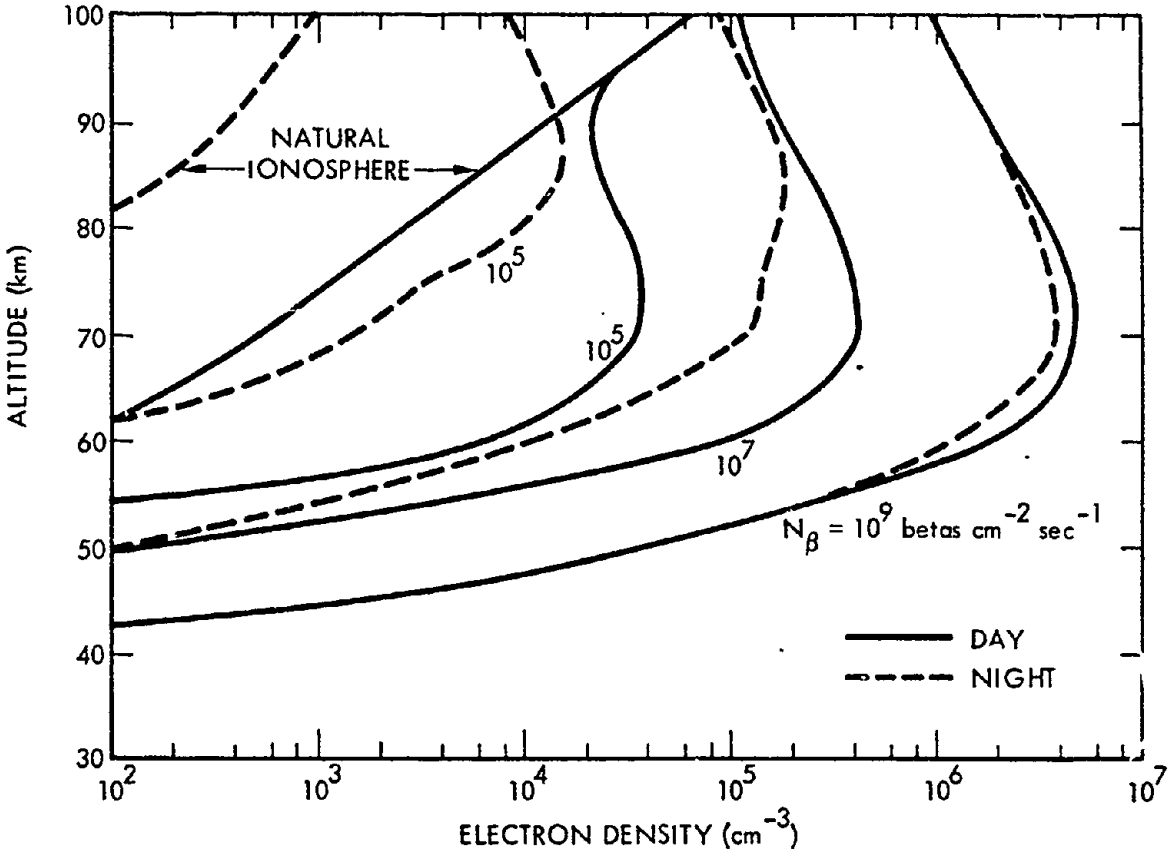

Figure 8-11. [redacted] Quasi-Equilibrium Electron Density Due to Beta Particles, Debris Altitude Greater than 60 km [redacted]

[redacted]

propagation at frequencies below a few hundred kilohertz). If the electrons do not collide with other particles, the energy is returned to the propagating wave without loss, but the phase of the wave is modified. Unless the geomagnetic field is parallel to the electric field of the propagating wave, some of the energy returned to the wave will have an electric field that is perpendicular to the incident electric field. The propagation wave then can be described as the sum of two plane waves termed the ordinary and the extraordinary waves—which have different phase velocities. One effect is to change the polarization of the propagation wave as it travels through the ionized medium. Electron collisions with other particles change the ordered motion of electrons into random motion (heat), and energy is absorbed from the wave. For many cases of interest, detonation-produced absorption is the overriding effect on electromagnetic propagation and it is the effect that is understood best.

[redacted] TRAVELING DISTURBANCES IN E AND F REGIONS OF IONOSPHERE [redacted]

[redacted] The preceding paragraphs discuss ionization sources from a nuclear explosion that add to the free electron content of the atmosphere. Following Teak and Orange (megaton

[redacted]

[redacted]

detonations at altitudes of 76 and 43 kilometers, respectively: 1958 test series) and again during Operation Fish Bowl (1962 test series), the normal E-region and F-region electron content appeared to be disturbed by hydrodynamic or hydromagnetic waves created by the detonation (the E-region includes the volume from 90 to 160 kilometers altitude, and the F-region begins at about 160 kilometers).

DNA (b)(3)

[redacted]

DNA (b)(3)

[redacted] ELECTROMAGNETIC RADIATIONS [redacted]

[redacted] A heated region emits thermal radiation according to its temperature and emissivity. The emissivity at a given frequency approaches unity as the absorption becomes large (10 decibels or more). The fireball may remain hotter than several thousand degrees Kelvin for about a hundred seconds. It may be sufficiently emissive for frequencies less than a few gigahertz that systems with antennas pointing at the fireball would register antenna temperatures equal to the fireball temperature if there were no intervening absorption outside the fireball. Generally, absorption caused by prompt and delayed radiation outside the fireball will reduce the escaping thermal radiation. The effective antenna noise temperature will depend on the size of the fireball relative to the antenna beam width, the location of the fireball relative to the antenna beam, and the absorption outside the fireball, as well as the temperature and emissivity of the fireball.

[redacted] A second source of electromagnetic radiation in the radio band is synchrotron radiation, which is caused by beta particles spiraling along geomagnetic field lines. A spiraling beta particle continually accelerates, and, therefore, it radiates electromagnetic energy. The radiation is maximum in the HF band, and it is approximately inversely proportional to frequency cubed for higher frequencies. The radiation is concentrated in the direction of the vector of electron motion. Because of its directivity, low intensity, and frequency dependence, synchrotron radiation does not appear to degrade present military systems seriously.

[redacted] ABSORPTION [redacted]

[redacted] Exact expressions for the absorption or energy loss involve components of the earth's magnetic field as well as electron density, collision frequency (number of collisions an electron makes per second), and wave frequency. For frequencies above about 10 megahertz and when bending of the wave is negligible, the incremental path absorption can be found from the following equation.

$$a = 4.6 \times 10^4 \frac{N_e \nu}{\omega^2 + \nu^2} \; dB/km, \qquad (8.2)$$

where

N_e = electron density (electrons/cm^3)

ν = collision frequency (collisions/sec)

ω = wave frequency (radians/sec).

[redacted]

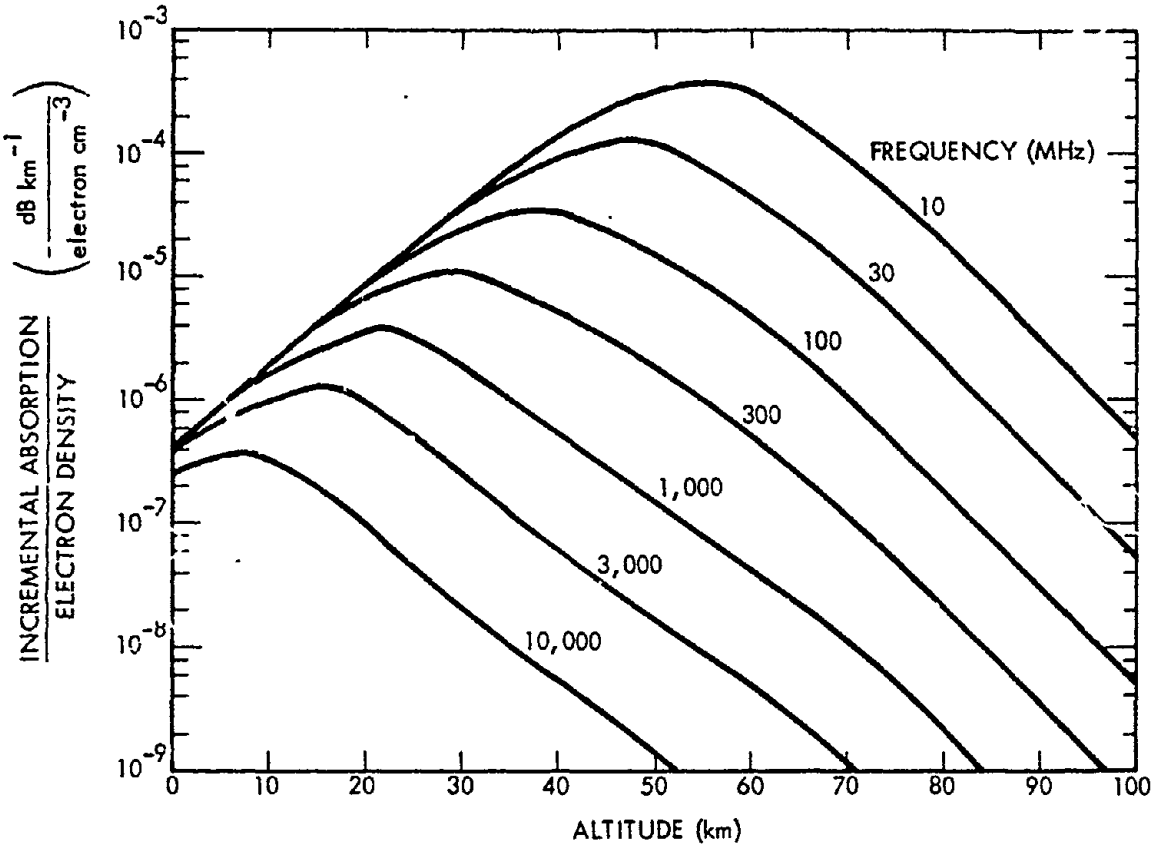

Figure 8-12. [redacted] Incremental Absorption Due to Electron-Neutral Collisions [redacted]

[redacted] Figure 8-12 shows incremental path absorption per electron per cubic centimeter as a function of altitude due to electron-neutral collisions. Above about 100 km, where the neutral particle density is low, absorption due to electron-neutral collisions is small; however, absorption due to electron-ion collisions may be important. Figure 8-13 shows incremental absorption due to electron-ion collisions for a temperature of 1000°K (approximate value of the atmospheric temperature above 200 km). The incremental absorption is proportional to $(1000/T)^{3/2}$ for other temperatures. The dotted portion of the curves indicates the volume where the electron density causes considerable bending of the wave, and a more detailed solution is required to obtain better values for the absorption. Figures 8-12 and 8-13 can be used with estimates of electron density (obtained from Figures 8-2 through 8-9 and 8-11) to determine incremental path absorption. The integral of the incremental path absorption along the propagation path gives the total path loss. Equation 8.1 and Figures 8-12 and 8-13 neglect ion-neutral collisions, which are important at low frequencies (VLF and LF bands). Problems 8-4 through 8-7 provide methods for estimating total one-way path absorption for various propagation paths.

[redacted] As was the case for electron density, it is convenient and useful to present absorption in-

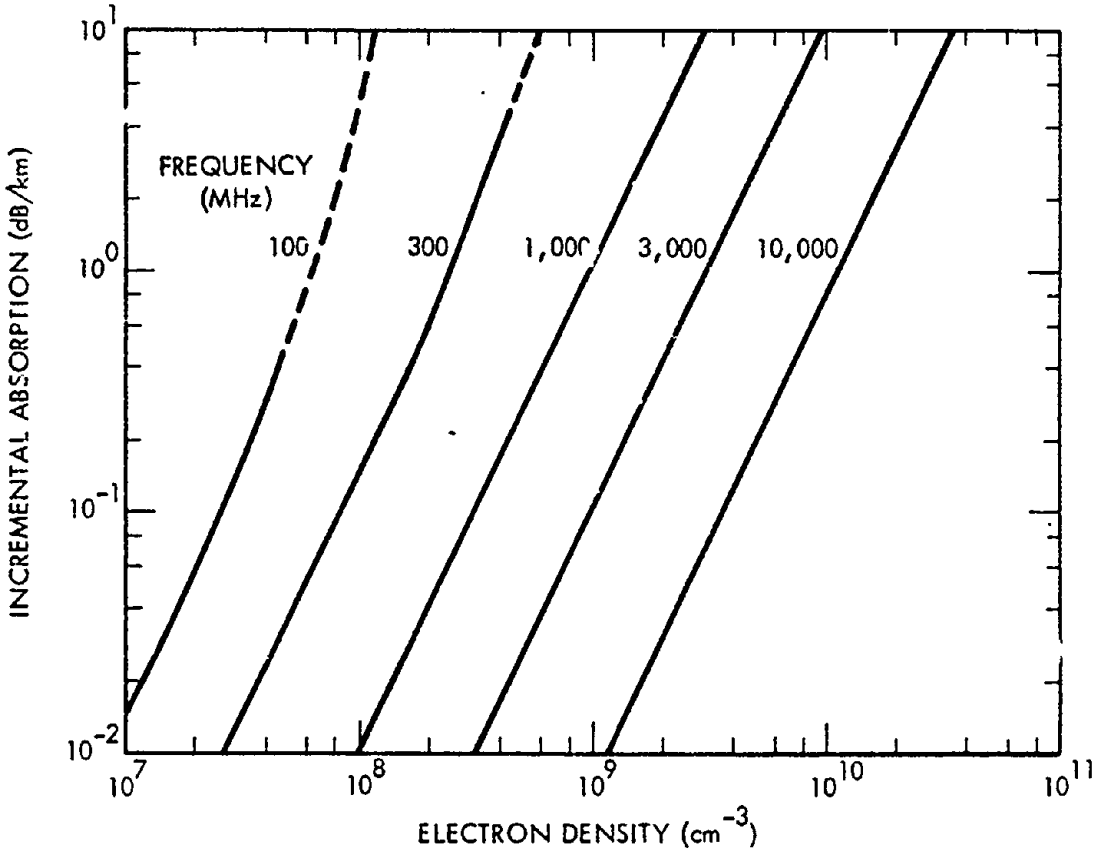

Figure 8-13. [redacted] Incremental Absorption Due to Electron-Ion Collisions, Electron Temperature = 1,000°K [redacted]

[redacted]

side the fireball and absorption caused by prompt and delayed radiation outside the fireball separately. With the exception of propagation paths that pass close to the fireball, absorption outside the fireball is maximum in the D-region (40 to 90 km). Generally it is sufficiently accurate to consider the largest of the separate absorptions as the total absorption along a particular propagation path.

[redacted] Scaling relations for the attenuation of low frequencies (VLF and LF bands) are difficult to present, because the amount of absorption for a particular propagation path depends in detail on the penetration of the wave into the atmosphere. A description of low-frequency propagation in nuclear environments is given in Chapter 17. Scaling relations for absorption of propagation at frequencies greater than a few megahertz are given in succeeding paragraphs; however detailed solutions of absorption for propagation paths associated with communication and radar systems usually require numerous calculations that cannot be obtained readily from simple hand-computation procedures. Figure 8-14 shows the burst conditions (detonation altitudes and yield) for which prompt and delayed radiation can cause absorption outside the fireball. The figure can be used in conjunction with the discussion in para-

[redacted]

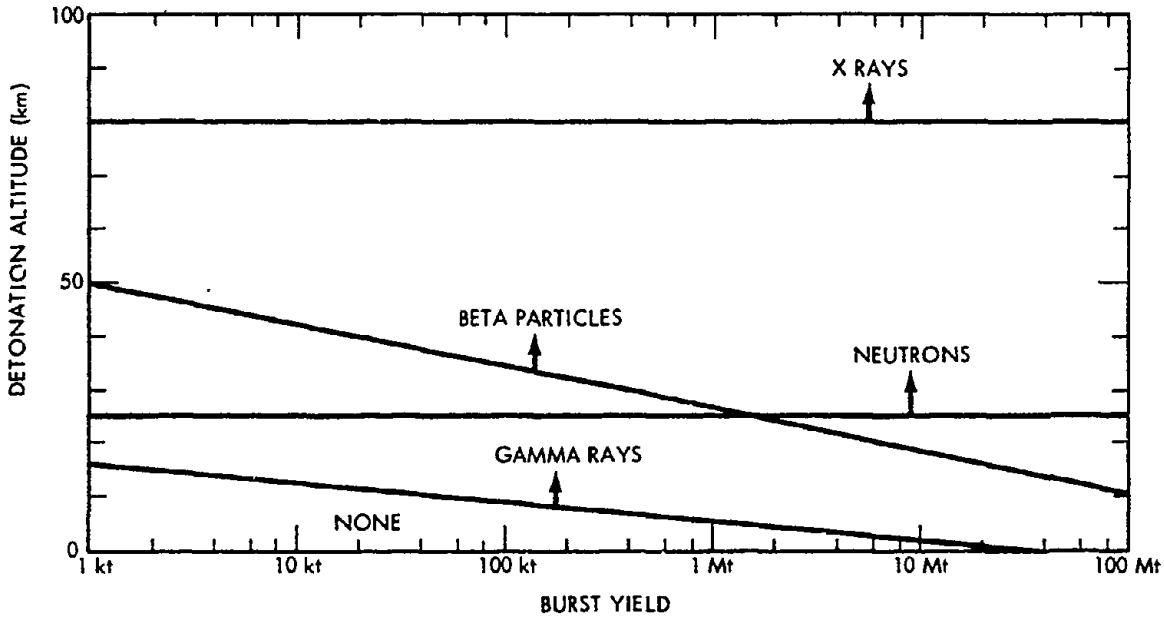

Figure 8-14. [redacted] Radiation Sources Causing Absorption Outside the Fireball [redacted]

[redacted] graphs 8-7 and 8-8 to determine whether absorption outside the fireball need be considered and which radiation sources are important.

8-6 Absorption Within the Fireball [redacted]

[redacted] Fireball ionization is localized and very intense: for most purposes, the fireball may be considered opaque at all radio frequencies for at least a few seconds. Calculations of the magnitude of absorption at a given time, or the duration of a given magnitude of absorption, are subject to considerable error because of uncertainties in predictions of the electron density within the fireball (see paragraph 8-1) and the fireball geometry. Methods for estimating fireball size and absorption through the fireball are given in Problems 8-1 through 8-4.

[redacted] For detonations below about 80 km and weapon yields greater than 100 kt, absorption through the fireball is expected to exceed 25 decibels for about 50 seconds at 10 gigahertz and for longer than 100 seconds at 1 gigahertz. Because the fireball rises a significant distance during these time periods, the duration of degradation due to absorption will generally be determined by the relative motion of fireball and propagation path.

[redacted]

[redacted]

[redacted]

[redacted]

[redacted]

DNA (b)(3)

8-7 Absorption Caused by Prompt Radiation Outside the Fireball [redacted]

[redacted] Absorption outside the fireball caused by prompt radiation may last from tens of seconds in the VHF band to tens of minutes in the HF band for daytime conditions. At night the absorption decreases more rapidly. For bursts below about 100 kilometers, the horizontal radius of the prompt absorption region only extends a few hundred kilometers from the burst point; for higher detonations the extent can be much longer.

8-8 Absorption Caused by Delayed Radiation Outside the Fireball [redacted]

[redacted] Absorption caused by delayed radiation (gamma rays and beta particles) is a function of the location and distribution of the fission debris. Estimates of debris rise and expansion for use in computing delayed-radiation effects are given in Problems 8-1 through 8-3.

[redacted] Delayed gamma rays can produce significant absorption when the debris is at altitudes above about 25 kilometers. Problem 8-6 describes methods that can be used to estimate one-way path absorption. The horizontal extent of the absorption region caused by gamma rays depends on weapon fission yield, debris altitude, time after burst, and wave frequency. The insert in Figure 8-9 shows the maximum possible extent of ionization and, thus the maximum extent of absorption; for most cases the region of significant absorption will be smaller.

[redacted] When the debris is above about 60 kilometers, beta particles produce D-region absorption at the burst locale and on the opposite side of the magnetic equator. Figures 8-49 through 8-51 can be used to obtain estimates of absorption caused by beta particles in terms of the beta-radiation intensity parameter that was defined in paragraph 8-4 for debris above the beta-particle stopping altitude (60 km). The location of the absorption region is offset from the debris region because of the effect of the geomagnetic field on the motion of beta particles, as illustrated in Figure 8-10. The horizontal radius of the absorption region is approximately equal to the debris radius. This radius can vary from a few kilometers to a few thousand kilometers depending on weapon yield, detonation altitude, and time after burst.

[redacted] PHASE CHANGES [redacted]

[redacted] Phase changes resulting from propagation through a region of uniform electron density affect propagation velocity and signal characteristics. Relative phase changes due to gradients in electron density change the direction of propagation and scatter energy from the propagating wave. Some phase effects become important only for electron densities that cause significant absorption. Evaluation of direction changes and scattering requires detailed information concerning the spatial distribution of electron density, which is difficult to predict theoretically and for which there is only limited experimental data.

8-9 Velocity of Propagation [redacted]

[redacted] Within an ionized region the phase velocity is increased over that in vacuum, but the group velocity, associated with the transmission of energy, is reduced. The increased time required to propagate energy through the region is proportional to the integral of electron density along the propagation path. Typical values of time delays associated with ionization caused by nuclear bursts range from a few nanoseconds to a few tens of microseconds. The larger time delays usually are accompanied by significant absorption when the ionized region occurs below 100 km.

[redacted] The phase velocity in an ionized region depends on the frequency. Therefore, the region

[redacted]

[redacted]

[redacted]

separates waves of different frequencies, i.e., the region is dispersive. The significance of dispersion depends critically on the type of signal being propagated and the type of signal processing being employed. For frequency-modulated signals, dispersion causes intermodulation and harmonic distortion. For digital systems, dispersion causes pulse-envelope distortion. Dispersion effects caused by electrons below 100 kilometers appear to be negligible when compared to absorption. At higher altitudes, electrons can only cause important dispersion effects for wide-band signals (bandwidths of the order of 1 percent or more of the carrier frequency), and these effects will probably only occur for propagation paths through fireball regions after the electron density has decreased sufficiently that absorption is not overriding.

8-10 Frequency of Propagation [redacted]

[redacted] A time-dependent phase change is equivalent to a frequency shift. The frequency shift is proportional to the time rate of change of the electron density integral along the propagation path. Frequency changes may be caused by changes in electron density with time along a fixed propagation path or by motion of the propagation path in a region of inhomogeneous electron density. For a fixed propagation path, frequency changes caused by nuclear-weapon-produced ionization are small (a few hertz for a 10 megahertz signal) by a few seconds after burst. Larger frequency changes may occur when the propagation path moves through regions of high electron density, such as the fireball; however, in those cases absorption generally will be overriding.

8-11 Direction of Propagation [redacted]

[redacted] Spatial gradients in electron-density can change the direction of propagation. When the electron density gradient is steep, part of the energy can be reflected. Reflection is important in the propagation of low frequencies (tens of kilohertz) over paths that are remote from the fireball. It also may be important in the propagation of much higher frequencies for paths that pass near the fireball, where high electron density gradients can exist.

[redacted] Smaller electron-density gradients cause ray bending (refraction). Refraction in the ambient ionosphere (E- and F-region) is important for beyond-the-horizon propagation in the HF band. For radar systems, refraction in the D-region caused by nuclear-burst-produced ionization normally is accompanied by significant absorption. Possible exceptions may occur if the propagation path passes close to the fireball or close to regions ionized by beta particles (particularly when the propagation path is nearly parallel to the geomagnetic field lines). Changes in the E- and F-region electron density caused by the fireball or by traveling disturbances may modify HF and VHF propagation significantly. E- and F-region electron densities sufficient to change the direction of propagation at higher frequencies by a few degrees can occur without causing significant absorption.

8-12 Scatter and Scintillation [redacted]

[redacted] Inhomogeneities in the propagation medium (variations in the dielectric constant of the medium) cause a small amount of incident energy to be scattered away from the original propagation direction. The direction of scatter depends on the shape of the inhomogeneities and their orientation relative to that of the incident beam. Energy that is forward scattered as the wave traverses inhomogeneous regions can cause fluctuations in the amplitude and the phase of the wave, called scintillation. The phase fluctuations are equivalent to fluctuations in the direction of propagation that result in random variations in the angle of arrival of received signals. Small amounts of backscattered energy can produce interference to radar systems called clutter.

[redacted] The analysis and quantitative description

[redacted]

[redacted]

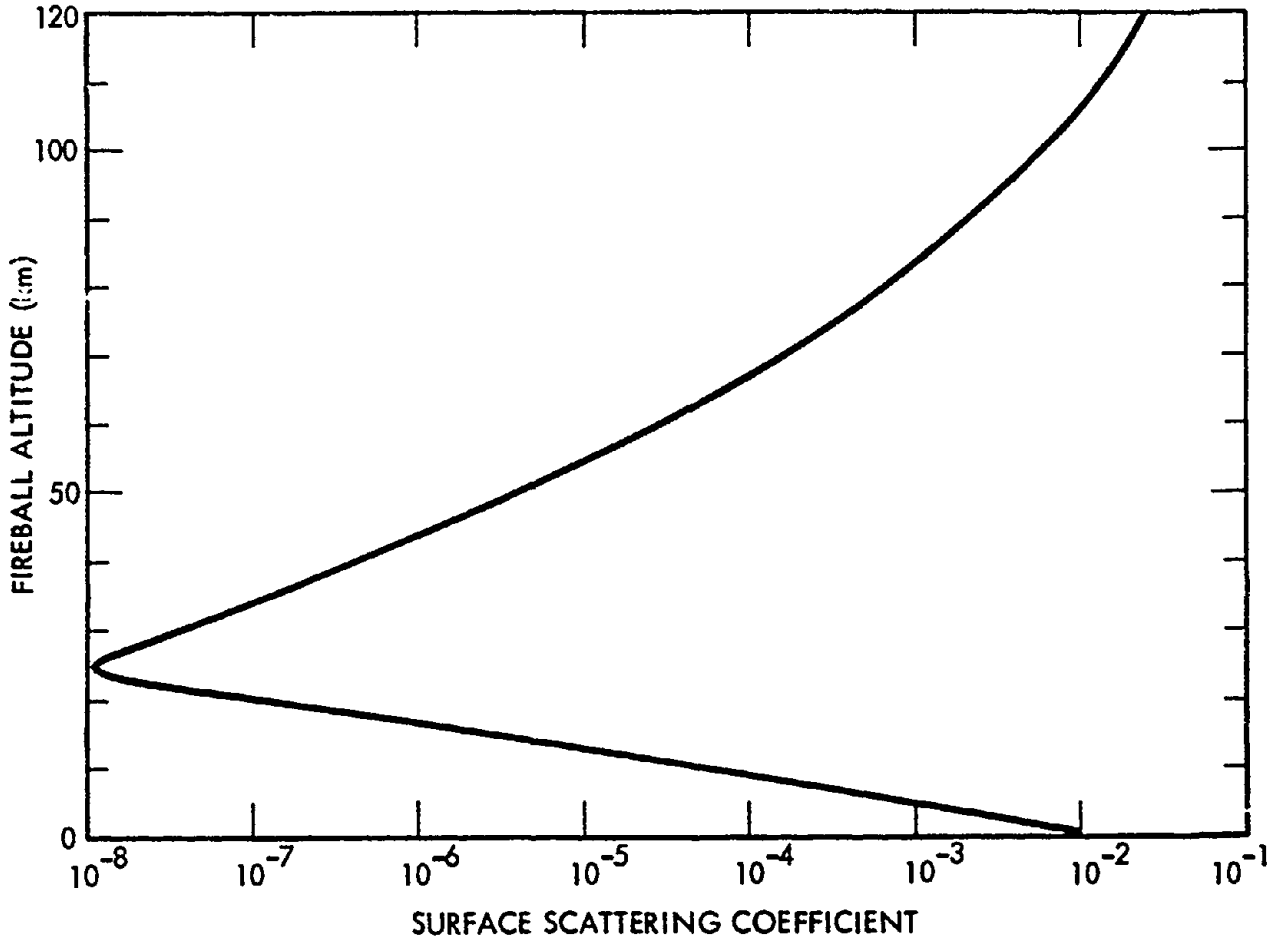

Figure 8-15. [redacted] Apparent Fireball Surface Scattering Coefficient at 400 MHz [redacted]

[redacted]

of scatter requires a statistical model of the spatial distribution of inhomogeneities in the propagating medium. Sufficient information from which such models could be constructed for nuclear-weapon-produced ionization is not available. There are limited experimental data from nuclear weapon tests concerning backscatter; however, interpretation of these data is difficult, and sufficient information for the construction of a complete empirical model is not available.

[redacted] Significant backscatter has been observed from fireball regions from a few tens of seconds to a few minutes after burst. Figure 8-15 shows the general order of magnitude of the surface scattering coefficient (multiply by the area of the scattering surface to obtain radar cross section) derived from experimental data. Below about 20 km, scattering is apparently due to variations in air density across fireball boundaries and across shock waves. For surface bursts, dust, dirt, and water vapor appear to cause backscatter

[redacted]

from the stem of the rising cloud. Backscatter from fireballs above 20 km can be explained in terms of partial reflection, or scatter from inhomogeneities in electron density in the fireball or in the shock fronts. The cross section appears to decrease with increasing frequency. The minimum in the apparent cross section near 20 km is due to several mechanisms, the prime of which is the absorption sheath caused by beta particles escaping from the fireball. The scattering coefficients shown in Figure 8-15 are only illustrative; observed values vary over an order of magnitude, depending on the relative geometry of propagation path and fireball, the characteristics of radars used in obtaining the data, and the time after burst.

Backscatter is also observed from regions of field-aligned ionization (ionized regions that are elongated along the geomagnetic field, often referred to as auroral ionization) which can be produced above about 80 km by beta particles. Field-aligned ionization can also occur within the fireball after a few tens of seconds for detonations above about 80 kilometers. The magnitude of backscatter is aspect sensitive; maximum backscatter occurs when the propagation path is normal to geomagnetic field lines. Backscatter from field-aligned ionization is thought to be a volume effect; volume scattering coefficients of about 10^{-13} m^2/m^3 at 400 MHz have been observed from beta-particle ionization regions. Significantly larger coefficients may occur from field-aligned ionization caused by the fireball. The cross section scales inversely as about the 4.5 power of frequency. Returns have been recorded for several hours after burst.

SECTION II
METHODS FOR CALCULATING ABSORPTION OF RADIO FREQUENCIES

As discussed previously, absorption frequently is the most important phenomena affecting propagation of radio frequencies; however, detailed solutions of absorption for propagation paths associated with communication and radar systems usually require numerous computations that cannot be obtained readily by hand calculations. The procedure for calculating absorption that are described below offer a means for obtaining reasonable estimates of radio frequency absorption for many situations of interest, however, the user should maintain awareness of the limitations defined for each of the calculations.

The calculation of the absorption of radio frequencies will be described separately for three conditions: absorption of propagation paths going through the fireball, absorption caused by prompt radiation outside of the fireball, and absorption caused by delayed radiation outside of the fireball (this last condition is divided further into absorption caused by delayed gamma rays and absorption caused by delayed beta particles).

Prior to the determination of the absorption along any of the paths discussed above, the size and location of the fireball region and/or the debris region must be determined. The spatial and temporal characteristics of the fireball and the debris regions created by nuclear bursts are complex. Idealized geometric models have been adopted for the purpose of analysis. The dimensions of three scaling models, based largely on interpolations of data from high-altitude nuclear tests, are used to represent detonations in three burst altitude regimes; below 80 kilometers, between 85 and 120 kilometers, and above 120 kilometers. The characteristics of the fireball and the debris are discussed separately for these three burst altitude regimes in succeeding paragraphs. Figure 8-16 illustrates the idealized geometric models referred to in the discussions. Dimensions shown in Figure 8-16 are defined in the discussions or in the illustrative problems that follow.

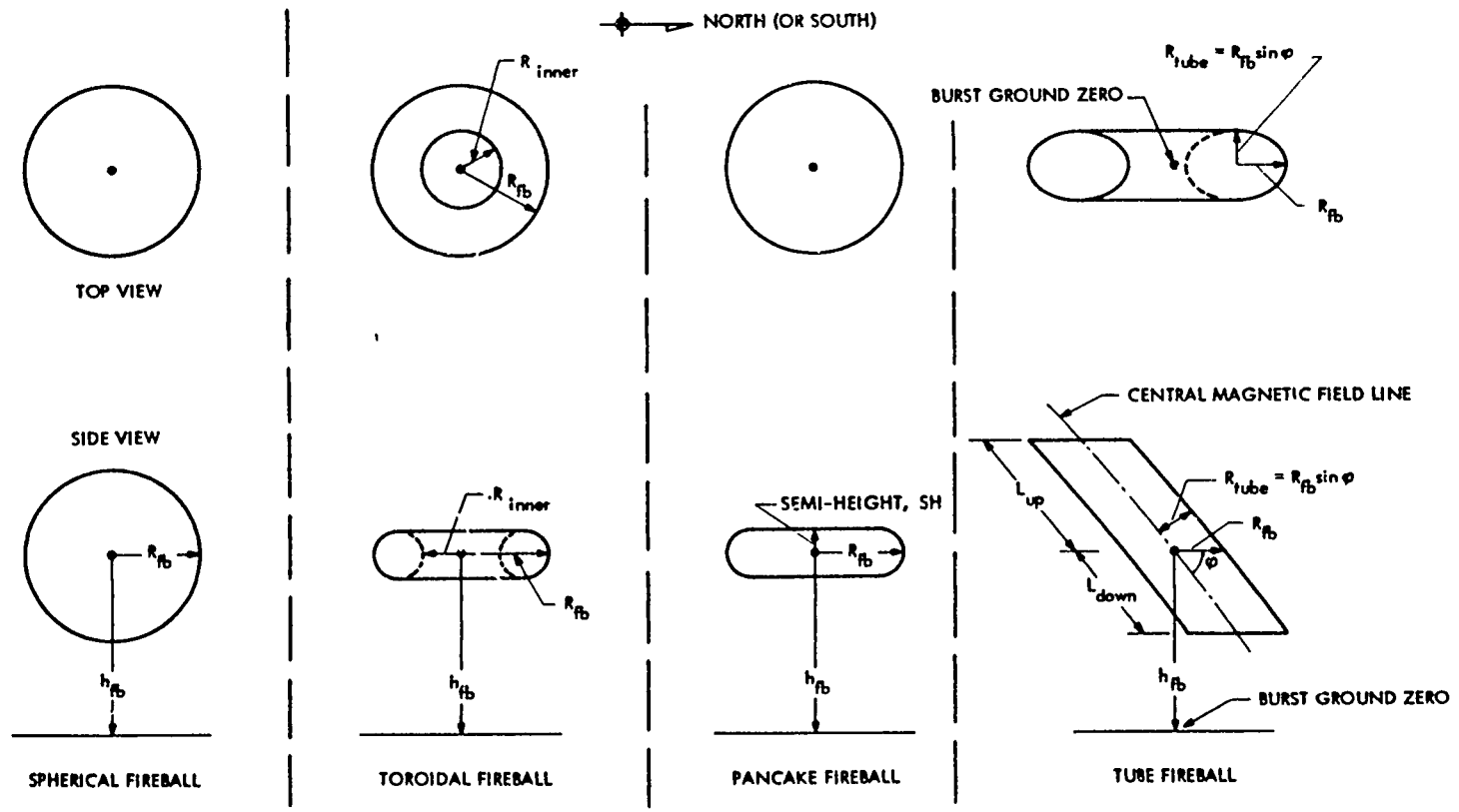

Figure 8-16. Examples of Fireball Geometry

[redacted]

8-13 Size and Location of Fireball and Debris Regions for Detonations Below 85 Kilometers [redacted]

[redacted] When a nuclear weapon is detonated at an altitude below about 85 kilometers, the fireball initially is a reasonably well defined and relatively small spherical region (see Chapter 1). After the fireball is formed, it expands and rises above the detonation point, carrying the fission debris with it. Depending on the weapon yield and the detonation altitude, the fireball may become toroidal in shape as it rises. After rising, the fireball will become stabilized in altitude and will diffuse into a pancake shape.

[redacted] If the fireball rises above 200 kilometers, it is assumed to fall back to 200 kilometers. If the peak altitude of the fireball is less than 200 kilometers, it is assumed to stabilize at its peak altitude.

[redacted] The initial fireball radius is the parameter used to determine whether the fireball will form a toroid. The toroid is assumed to transform into a pancake at 7 minutes after burst, with a vertical thickness equal to the vertical dimension of the toroid at 7 minutes. If the fireball does not form a toroid, the fireball is assumed to transform from a sphere to a pancake when the radius becomes 100 kilometers. The vertical thickness of the pancake is assumed to be 100 kilometers.

[redacted] The model provided for determining the location of the debris is intended for calculation of delayed-radiation (gamma rays and beta particles) effects. For times later than a few tens of minutes after burst, the size and location of the debris region will depend on atmospheric winds and diffusion, and the model may be considerably in error.

[redacted] Figures 8-19 through 8-25 are used to determine the spatial and temporal history of the fireball (and the debris), for bursts that occur below 85 kilometers.

8-14 Size and Location of Fireball and Debris Regions for Detonations Between 85 and 120 Kilometers [redacted]

[redacted] When a nuclear detonation occurs between 85 and 120 kilometers, the fireball transforms from a sphere to a cylinder or tube aligned along the geomagnetic field. The model used for the calculations described herein assumes that the fireball stabilizes at its maximum altitude above ground zero. The fireball radial dimension also is assumed to remain constant after 7 minutes. A fireball region is not defined for times longer than 2 hours after burst.

[redacted] Delayed radiation (gamma rays and beta particles) is assumed to be emitted from a single debris pancake, which is assumed to rise with the fireball and then to settle slowly along the geomagnetic field until it reaches 200 kilometers altitude at approximately 2 hours after burst. As the debris settles, the center is offset from ground zero toward the nearest magnetic pole, as illustrated in Figure 8-17. Figures 8-19 through 8-29 are used to determine the spatial and temporal history of the fireball (and the debris) for bursts that occur at altitudes between 85 and 120 kilometers.

8-15 Size and Location of Fireball and Debris Regions for Detonations Above 120 Kilometers [redacted]

[redacted] Theoretical and experimental data are incomplete for this altitude region; therefore, scaling relations are given only for a few parametric yields and detonation altitudes. Three shapes are used to model the fireball region: a sphere, a pancake, and a cylinder or tube aligned along the geomagnetic field. Figure 8-16 illustrates the fireball geometry.

[redacted] As the detonation altitude is increased above 120 kilometers, the debris is distributed over a larger region. Some debris can be transported across the magnetic equator. The single-pancake debris region used at lower altitudes to

[redacted]

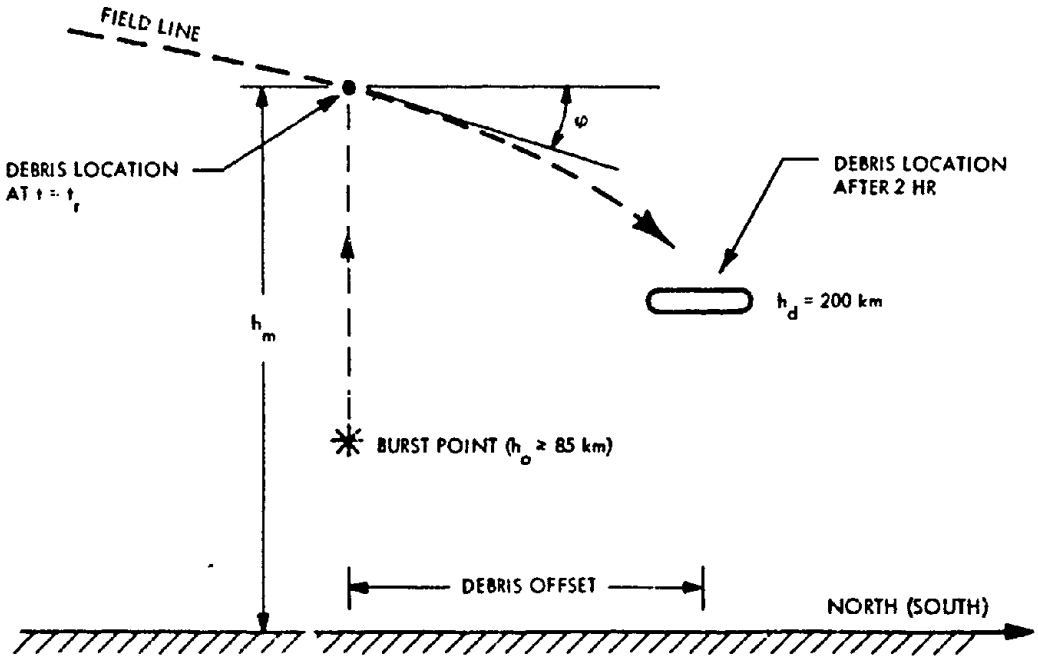

Figure 8-17. [redacted] Debris Behavior for Detonation Altitudes Greater Than 85 km [redacted]

[redacted]

model delayed radiation effects is not adequate, so multiple regions are used.

[redacted] Up to three debris regions are used to determine the delayed radiation resulting from detonations above 120 kilometers. Figure 8-18 illustrates the geometry. Two of these regions (Regions 1 and 2) model debris in the burst region, and the third (Region 3) models debris transported across the magnetic equator to the conjugate region. For convenience and because little is known about the debris location in the conjugate region, the beta-particle ionization in the burst and conjugate regions associated with Debris Region 3 is assumed to coincide with that associated with Debris Region 1. Debris Region 3 is used to compute gamma-ray ionization in the conjugate region. For weapons detonated above 250 kilometers, Region 2 is used to determine both gamma-ray and beta-particle ionization.

[redacted] in the model used herein, the fraction of debris transported across the magnetic equator is assumed to be independent of geomagnetic dip angle for detonations above 250 kilometers. A small amount of debris can reach the conjugate region for detonations below 250 kilometers and low dip angles. The time required for the debris to reach the conjugate region depends on detonation altitude and geomagnetic dip angle; however, for purposes of calculating delayed gamma radiation, the debris can be assumed to reach the conjugate region immediately after burst.

[redacted] About 20 percent of the debris for detonations above 120 kilometers is not accounted for in the model. This debris is assumed to escape to large distances; some may be carried into space and some may be spread world-wide. At least part of this debris will be trapped on the magnetic field lines above the burst. While this debris probably is not important for single bursts, it could cause significant delayed radiation after

[redacted]

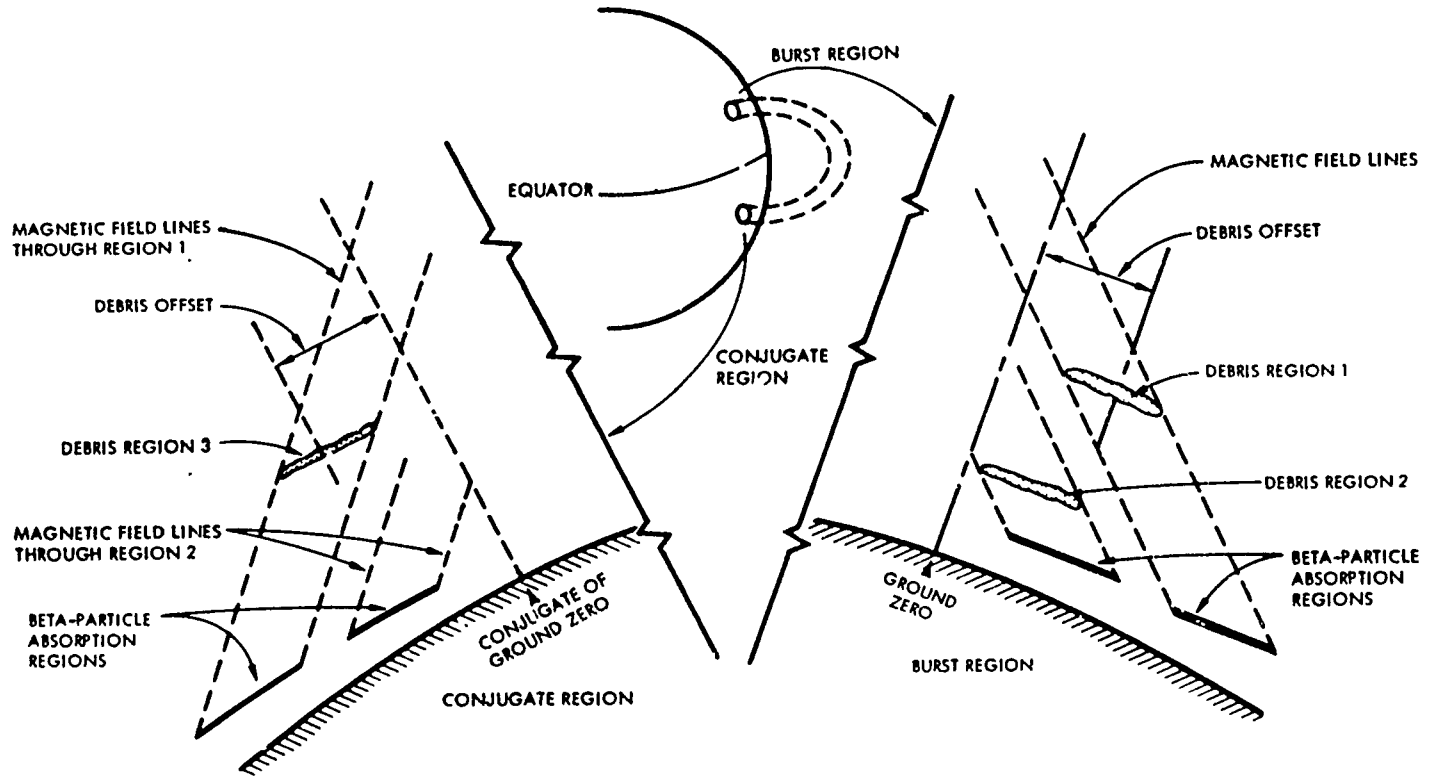

Figure 8-18. [redacted] Illustration of Debris and Beta-Particle Absorption Regions for Times Later Than 10 Minutes After Burst, H_0 Above 120 km [redacted]

[redacted]

[redacted]

multiple weapon detonations.

[redacted] After rising to peak altitude, the three debris regions are assumed to settle along the geomagnetic field lines until they reach 200 kilometers altitude at about 2 hours after burst. The debris regions are offset from ground zero or the conjugate of ground zero toward the magnetic pole.

[redacted]

[redacted]

Problem 8-1 Calculation of Fireball Size, Shape, and Location for a Burst Below 85 Kilometers

[redacted] Figures 8-19 through 8-25 contain families of curves with which the size, shape, and location of the fireball resulting from a nuclear detonation below 85 kilometers may be estimated. For bursts in this altitude regime, the debris altitude h_d is assumed to be the same as the fireball altitude h_{fb}. The debris is distributed non-uniformly within the fireball region. However, for simplified calculations of delayed radiation effects, the debris region can be assumed to be a thin pancake region with radius R_d equal to the fireball radius R_{fb}.

[redacted] The altitude of the fireball at a time t after burst is obtained from Figures 8-19 through 8-22 by a series of steps, as follows:

1. Enter Figure 8-19 with the weapon yield and detonation altitude h_o to obtain h_r, the distance the fireball will rise above the detonation point. The maximum fireball altitude, h_m, is

$$h_m = h_o + h_r \text{ km.}$$

Enter Figure 8-20 with h_r to obtain the time required to reach maximum altitude t_r. If $t \geq t_r$ and $h_m \leq 200$ km, go to 3; otherwise go to 2.

2. If $t < t_r$, enter Figure 8-21 with time after burst and h_r to obtain h_N, an altitude normalizing factor. If $h_m > 200$ km, enter Figure 8-22 with $\tau = t/t_r$ to obtain f_h, the fireball height factor.

3. Compute h_{fb}, the fireball altitude at time t:

$$h_{fb} = \begin{cases} (h_o + h_N h_r) \text{ km} \\ \quad \text{when } t < t_r \\ h_m \text{ km} \\ \quad \text{when } t \geq t_r,\ h_m < 200 \\ [200 + f_h (h_m - 200)] \text{ km} \\ \quad \text{when } t > t_r,\ h_m > 200 \end{cases}$$

[redacted] The radius and shape of the fireball at a time t after burst are obtained from Figures 8-23 through 8-25, as follows:

1. Enter Figure 8-23 with weapon yield and detonation altitude h_o to obtain the initial fireball radius R_o. If $R_o < 4$ km, go to 2; otherwise go to 3 when $t < 7$ minutes or go to 4 when ≥ 7 minutes.

2. Determine t_{toroid}, the time of toroid formation, from Figure 8-24 by selecting the fireball radius curve for the value of R_o determined above, by locating the intercept of this curve with the toroid formation time curve, and by reading t_{toroid} on the abscissa.

3. Enter Figure 8-24 with the time of interest t and the initial fireball radius R_o. Determine R_{fb}, the fireball radius at time t, then go to 5.

4. Enter Figure 8-24 with $t = 7$ minutes and the initial fireball radius R_o; obtain the fireball radius at 7 minutes after burst, $R_{fb}(7)$. Enter Figure 8-25 with t and h_m to obtain ΔR. Compute R_{fb}, as follows:

$$R_{fb} = R_{fb}(7) + \Delta R.$$

5. The fireball will be a

sphere if $R_o \leq 4$ km and $t < t_{toroid}$, or if

$$R_o > 4 \text{ km and } R_{fb} < 100 \text{ km;}$$

toroid if $R_o < 4$ km and $t_{toroid} \leq t < 7$ minutes;

pancake if $R_o \leq 4$ km and $t \geq 7$ minutes, or if

$$R_o > 4 \text{ km and } R_{fb} \leq 100 \text{ km.}$$

If the fireball shape is a toroid, compute the inner toroid radius:

$$R_{inner} = \frac{R_{fb}}{2}$$

[redacted]

[redacted]

If the fireball shape is a pancake, compute the pancake semithickness:

$$SH = \begin{cases} \frac{1}{4} R_{fb}(7) & R_o \leq 4 \text{ km} \\ 50 & R_o > 4 \text{ km.} \end{cases}$$

Example

Given: A 1 Mt weapon burst at an altitude of 50 km.

Find: The size, shape, and location of the fireball and debris region 2 minutes after the burst.

Solution:

a. From Figure 8-19 $h_r \approx 50$ km for a 1 Mt weapon burst at 50 km.

b. $h_m = h_o + h_r = 50 + 50 = 100$ km.

c. From Figure 8-20, $t_r = 10$ min for $h_r = 50$ km.

d. From Figure 8-21, $h_N = 0.6$ for $t = 2$ min and $h_r = 50$ km.

e. Since $t < t_r$,

$$h_{fb} = h_o + h_N h_r = 50 + (0.6)(50) = 80 \text{ km}$$

f. From Figure 8-23, $R_o = 2$ km for a 1 Mt weapon detonation at 50 km.

g. From Figure 8-24, $t_{toroid} = 1.7$ min for $R_o = 2$ km.

h. From Figure 8-24, $R_{fb} = 30$ km 2 min after a burst with $R_o = 2$ km.

i. Since $t_{toroid} < t < 7$ minutes, the fireball shape is a toroid, and

$$R_{inner} = \frac{R_{fb}}{2} = \frac{30}{2} = 15 \text{ km.}$$

Answer: The fireball is a toroid centered at 80 kilometers altitude. The outer radius is 30 kilometers and the inner radius is 15 kilometers (see Figure 8-16). The altitude and radius of the debris pancake are 80 kilometers and 30 kilometers, respectively.

Reliability The size and location of the debris region depend on atmospheric winds and diffusion. Since these effects are neglected in the model described herein, the results predicted by the model may be considerably in error.

Related Material See paragraph 8-13.

[redacted]

[redacted]

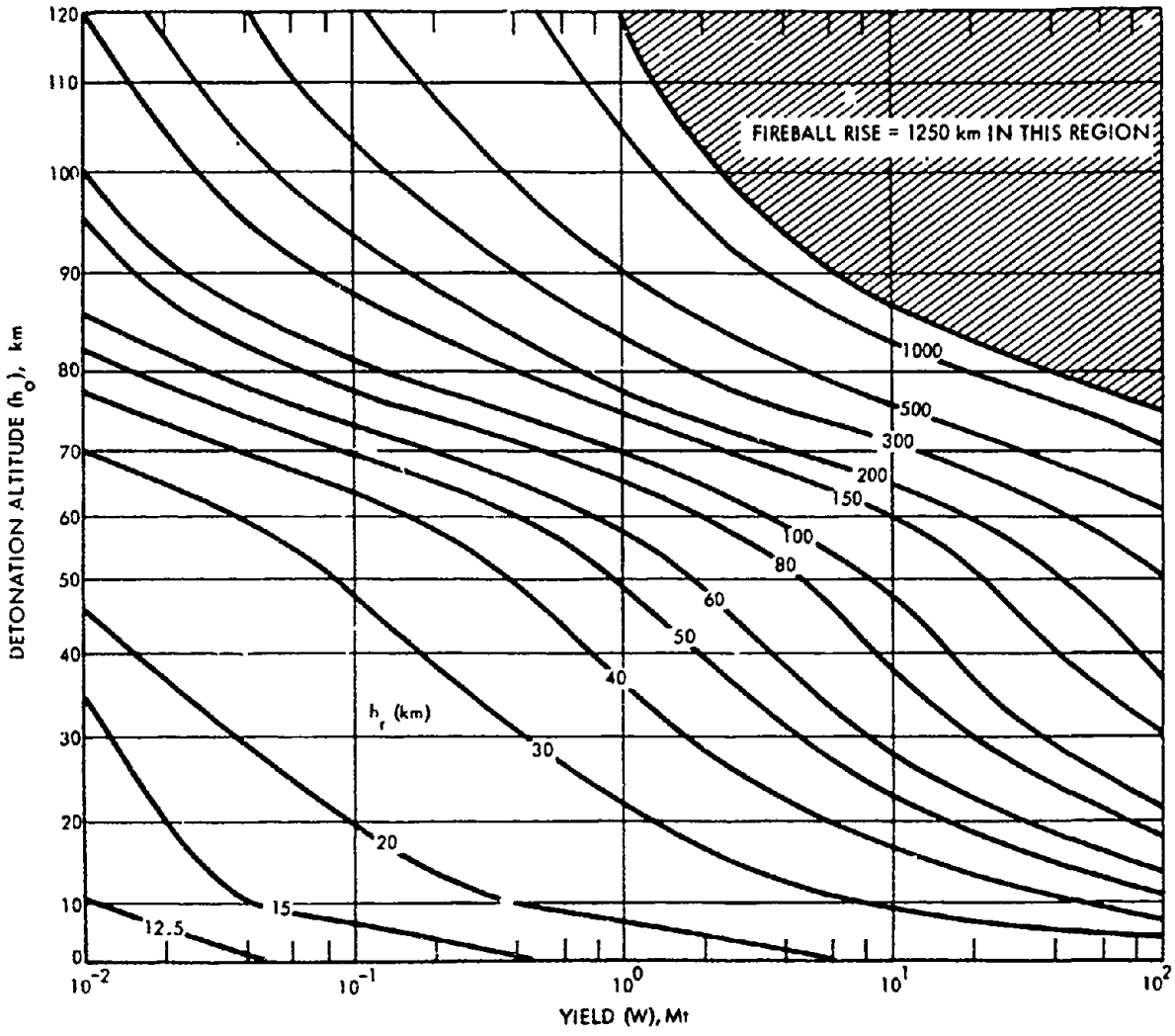

Figure 8-19. [redacted] Maximum Fireball Rise [redacted]

[redacted]

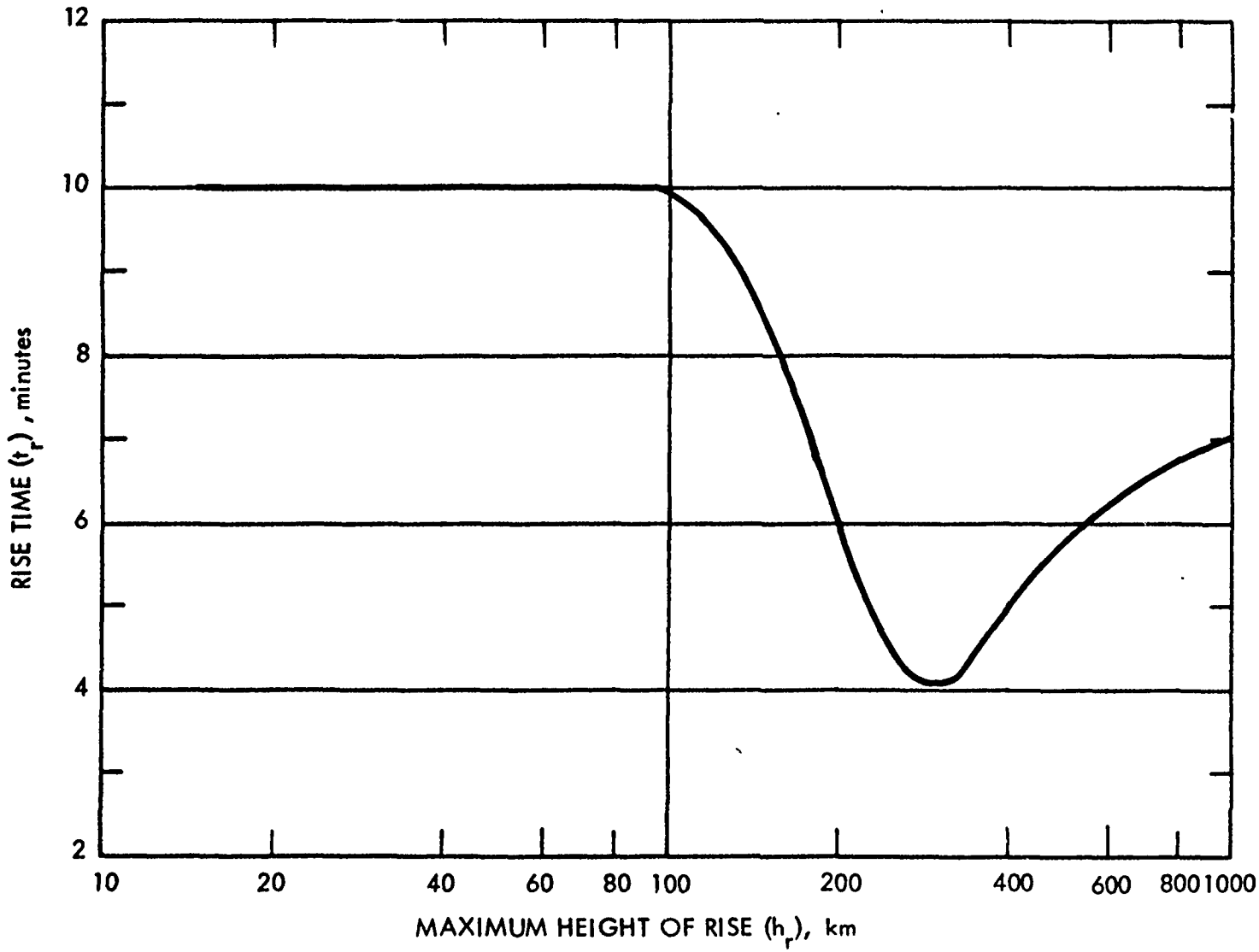

Figure 8-20. [redacted] Time for Fireball to Reach Its Maximum Altitude [redacted]

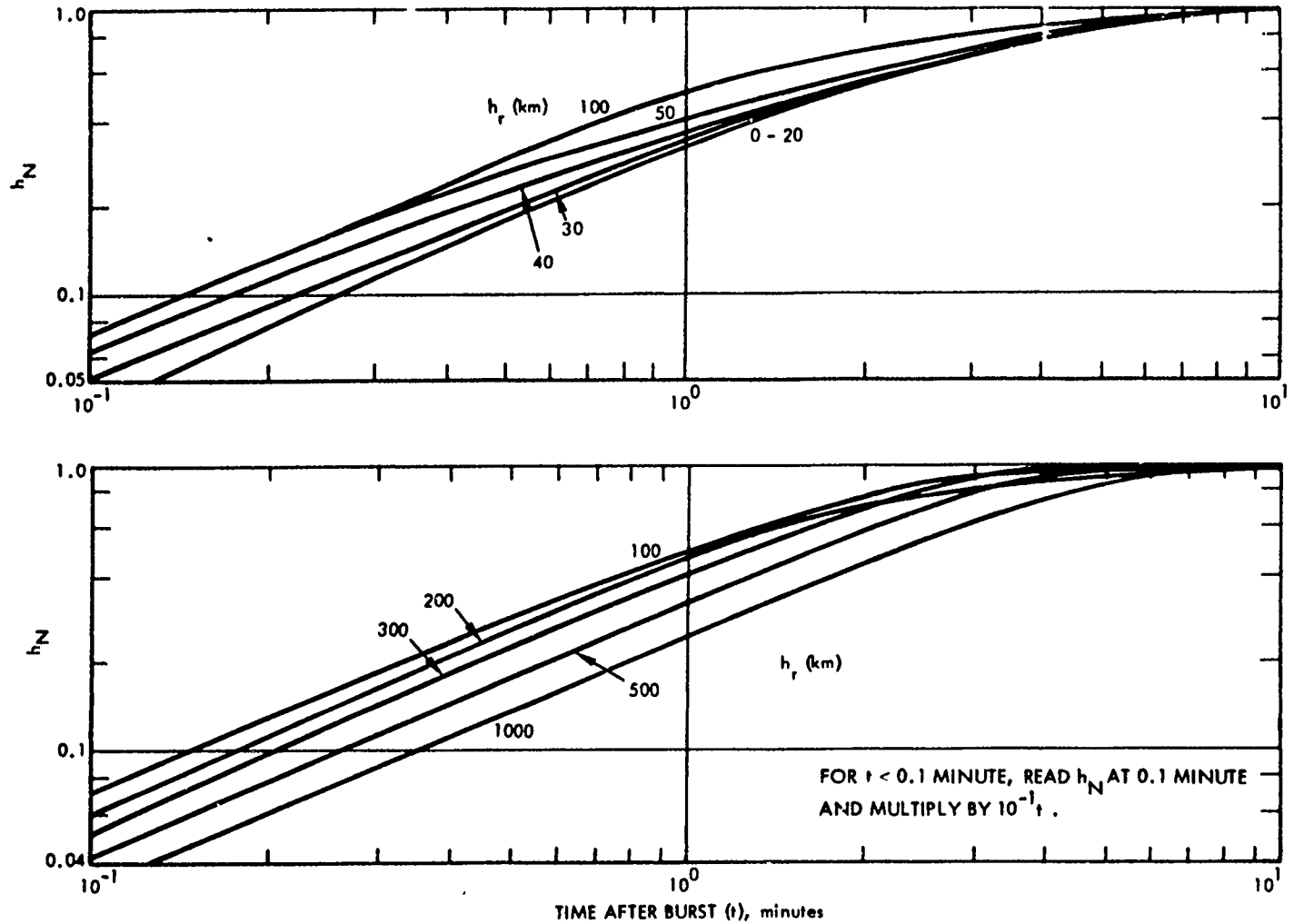

Figure 8-21. Altitude Normalizing Factor h_N

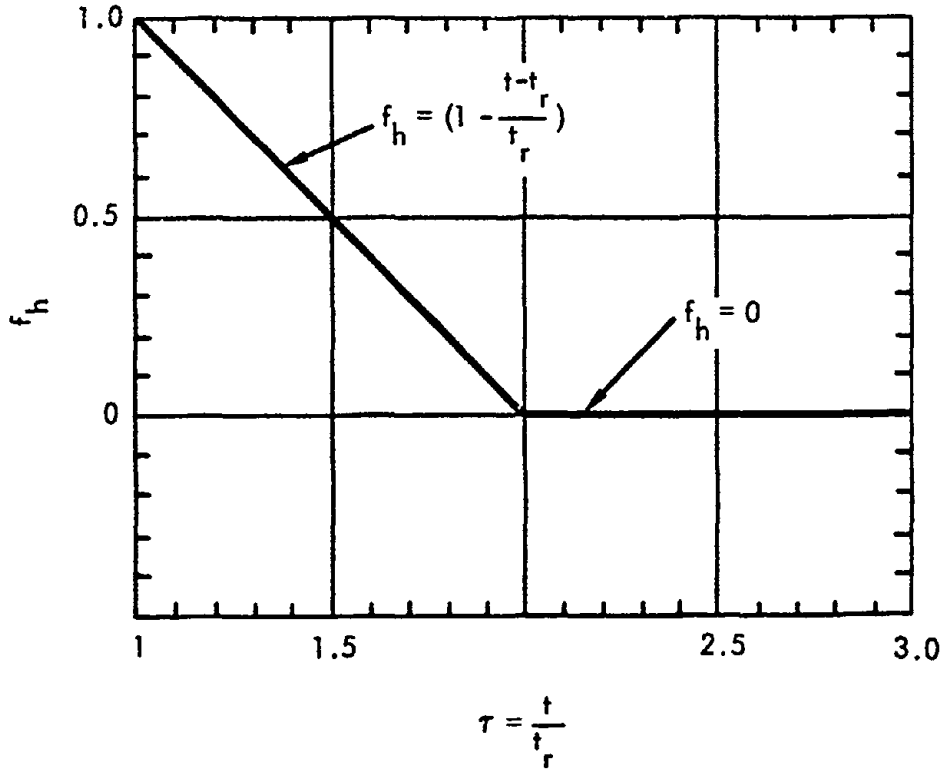

Figure 8-22. [redacted] Fireball Height Factor [redacted]

[redacted]

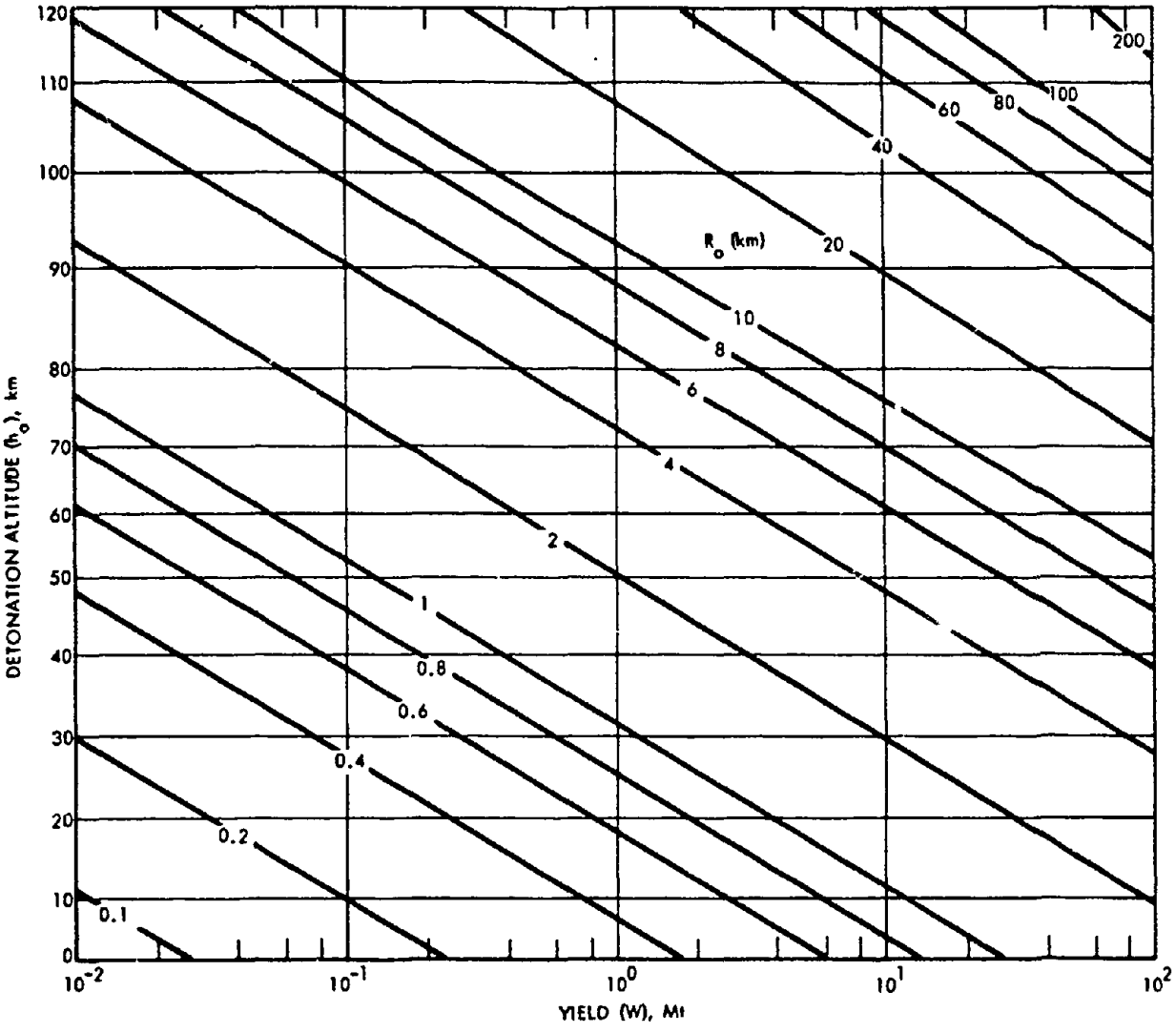

Figure 8-23. [redacted] Initial Fireball Radius [redacted]

[redacted]

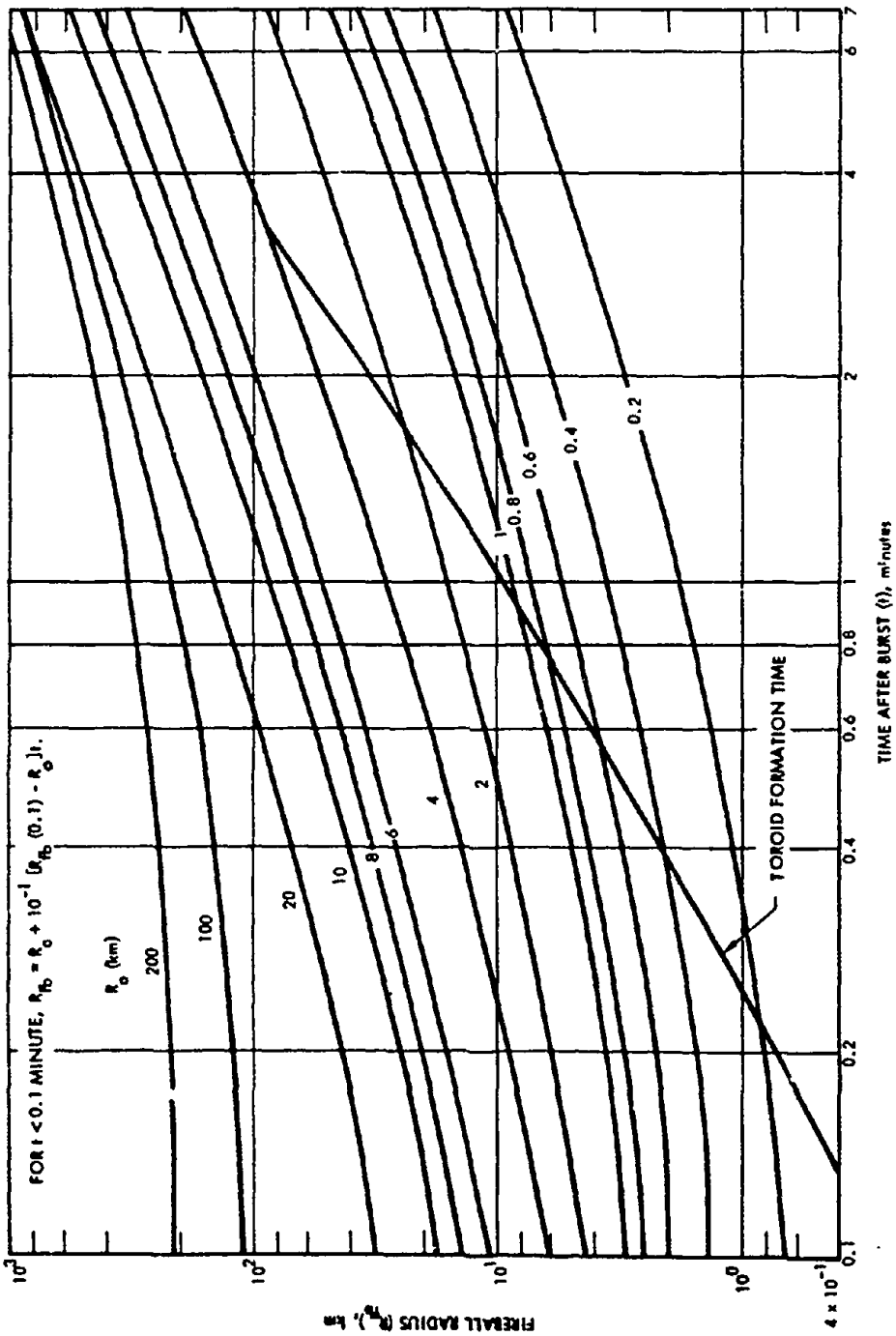

Figure 8-24. [redacted] Fireball Radius

[redacted]

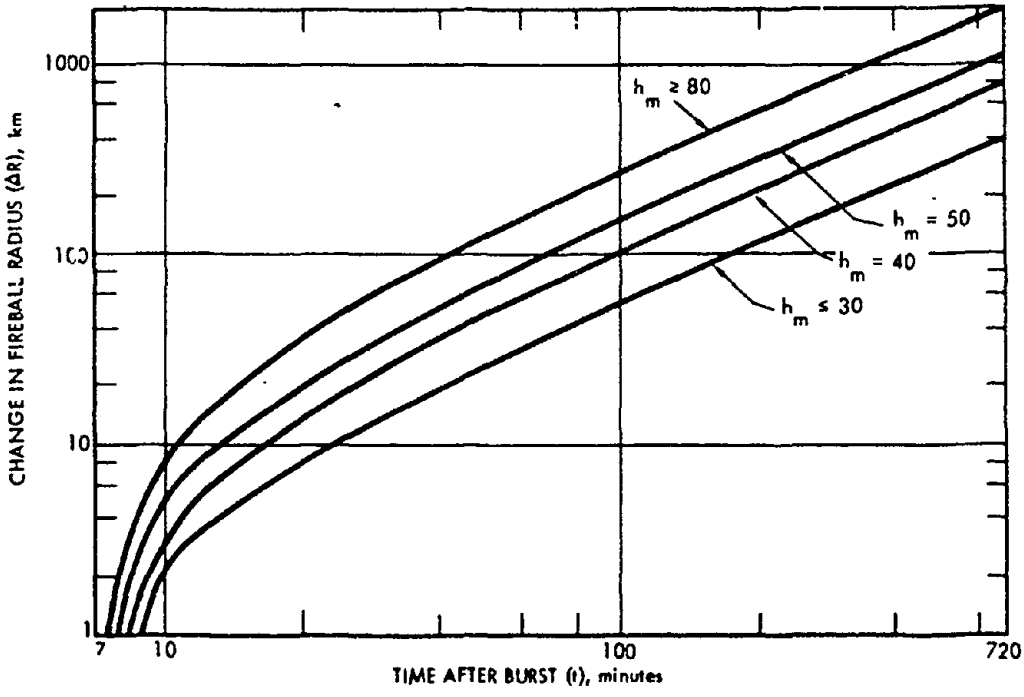

Figure 8-25. [redacted] Change in Fireball/Debris-Region Radius After Sever Minutes [redacted]

[redacted]

[redacted]

Problem 8-2 Calculation of Fireball Size, Shape, and Location for a Burst Between 85 and 120 kilometers

[redacted] Figures 8-19 through 8-29 contain families of curves with which the size, shape, and location of the fireball resulting from a nuclear detonation between 85 and 120 kilometers may be estimated. For bursts in this altitude regime, the fireball transforms from a sphere to a cylinder or tube aligned along the geomagnetic field line. A fireball region is not defined for times after burst greater than 2 hours.

[redacted] The altitude of the fireball at a time t after burst is obtained from Figures 8-19 through 8-21 by a series of steps, as follows:

1. Enter Figure 8-19 with weapon yield W and detonation altitude h_o to obtain h_r, the distance the fireball will rise above the detonation point. The maximum fireball altitude, h_m, is

$$h_m = h_r + h_o \quad km.$$

Enter Figure 8-20 with h_r to obtain the time to reach maximum altitude t_r. If $t \geq t_r$ go to 3; otherwise go to 2.

2. If $t < t_r$, enter Figure 8-21 with time after burst and h_r to obtain h_N, and altitude normalizing factor.

3. Compute h_{fb}, the fireball altitude at time t:

$$h_{fb} = \begin{cases} (h_o + h_N h_r) \quad km \\ \qquad t < t_r \text{ minutes} \\ h_m \quad km \\ \qquad t_r < t < 120 \text{ minutes} \end{cases}$$

[redacted] The radius and shape of the fireball at a time t after burst are obtained from Figures 8-23, 8-24, and 8-26, as follows:

1. Enter Figure 8-23 with weapon yield and detonation altitude h_o to obtain fireball radius R_o. Enter Figure 8-26 with weapon yield to obtain the magnetic equilibrium radius R_{eq}. Determine the time to reach R_{eq}, t', from Figure 8-24 by selecting the fireball radius curve for the value of R_o obtained from Figure 8-23 and by determining the time when the fireball radius (R_{fb}) is equal to R_{eq}. If $t > t'$, go to 3; otherwise go to 2.

2. Enter Figure 8-24 with t and R_o to obtain R_{fb}, the fireball radius at time t. Go to Step 4.

3. Compute R_{fb}:

$$R_{fb} = \begin{cases} (R_{eq} + (t - t')\, R_o \quad km \\ \qquad t < 7 \text{ minutes}, \\ (R_{eq} + (7 - t')\, R_o) \quad km \\ \qquad t \geq 7 \text{ minutes}. \end{cases}$$

4. The fireball shape will be a

sphere if $t < t'$

tube if $t \geq t'$.

[redacted] If the time of interest t is greater than t', the time to reach the magnetic equilibrium radius, the tube fireball dimensions are obtained as follows:

1. If $t' > t_r$ (obtained from Figure 8-20 above), go to 2; otherwise enter Figure 8-21 with $t = t'$ and h_r (from Figure 8-19) and obtain $h_N(t')$.

2. Compute $h_{fb}(t')$:

$$h_{fb}(t') = \begin{cases} (h_o + h_N(t')h_r) \quad km \\ \qquad t' \leq t_r \text{ minutes}, \\ h_m \quad km \\ \qquad t' > t_r \text{ minutes}. \end{cases}$$

Compute the altitude of the base of the

[redacted]

tube h_b (h_b is taken as the altitude of the base if $h_b > 200$ km):

$$h_b = h_{fb}(t') - R_{eq} \quad km.$$

Compute the length of the fireball up the tube in the direction of the magnetic field line, L_{up}:

$$L_{up} = 6\ (t - t')\ R_o + R_{fb} \quad km.$$

Compute the quantity L':

$$L' = \begin{cases} \dfrac{h_{fb} - h_b}{\sin \varphi} \ km & h_b \leqslant 200 \text{ km} \\ \dfrac{h_{fb} - 200}{\sin \varphi} \ km & h_b > 200 \text{ km}, \end{cases}$$

where φ is the magnetic dig angle at the burst location. If the magnetic dip angle is not known for the burst location, it can be determined from Figure 8-54. The length of the fireball down the tube will be the smaller of L_{up} and L'.

If the time of interest t is equal to or less than t_r, the time to reach maximum altitude, or if the maximum fireball altitude, h_m, is less than 200 kilometers, the debris altitude, h_d, is determined from the fireball altitude as described below. If the time of interest is equal to or greater than the time to reach maximum altitude ($t \geqslant t_r$), and the maximum fireball altitude is greater than 200 kilometers ($h_m > 200$), Figure 8-27 is entered with the quantity $(t - t_r)$ to obtain the debris height factor f_h. The debris altitude is then determined as follows:

$$h_d = \begin{cases} h_{fb} \quad km \\ \qquad t \leqslant t_r \text{ min} \\ h_m \quad km \\ \qquad t \geqslant t_r \text{ min}, \ h_m \leqslant 200 \text{ km} \\ [200 + f_h(h_m - 200)] \quad km \\ \qquad t \geqslant t_r \text{ min}, \ h_m \geqslant 200 \text{ km} \end{cases}$$

If the maximum fireball altitude, h_m, is equal to or less than 200 kilometers, the debris offset is zero (see Figure 8-17). If h_m is greater than 200 kilometers, enter Figure 8-28 with h_m and the magnetic dip angle, φ, to obtain the maximum debris offset D_d. Then enter Figure 8-29 with the quantity $(t - t_r)$ to obtain a value of the debris offset correction factor f_o. The debris offset, Δd, is:

$$\Delta d = f_o D_d \quad (h_m > 200 \text{ km}).$$

The radius of the debris is obtained from previously determined dimensions, as follows:

$$R_d = \begin{cases} R_{fb} \quad km \\ \qquad t \leqslant 120 \text{ minutes} \\ [R_{eq} + (7 - t')\ R_o \\ \qquad + 3\ (t - 120)] \quad km \\ \qquad t > 120 \text{ minutes} \end{cases}$$

Example

Given: A 1 Mt weapon burst at an altitude of 100 km, at a location where the magnetic dip angle, φ, is 60°.

Find: The shape, size, and location of the fireball, and the altitude, radius, and offset of the debris region 20 minutes after the burst.

Solution:

a. From Figure 8-19, h_r = 800 km for a 1 Mt weapon burst at 100 km.

b. $h_m = h_r + h_o = 800 + 100 = 900$ km.

c. From Figure 8-20, t_r = 7 minutes for h_r = 800 km.

d. Since $t_r < t$,

$$h_{fb} = h_m = 900 \text{ km}$$

e. From Figure 8-23, R_o = 15 km for a 1 Mt burst at 100 km altitude.

f. From Figure 8-26, R_{eq} = 100 km for a 1 Mt weapon.

g. From Figure 8-24, t' = 0.9 min for R_o = 15 km and $R_{fb} = R_{eq}$ = 100 km.

h. Since $t > 7$ min, the fireball shape is a tube, and

$$R_{fb} = R_{eq} + (7 - t')\, R_o$$
$$= 100 + (6.1)(15) = 192 \text{ km}$$

i. From Figure 8-21, $h_N(t) = 0.25$ for $t = t' = 0.9$ min and h_r = 800 km.

j. Since $t' < t_r$,

$$h_{fb}(t') = h_o + h_N(t')\, h_r$$
$$= 100 + (0.25)(800) = 300 \text{ km}.$$

k. The height of the fireball base is

$$h_b = h_{fb}(t') - R_{eq} = 300 - 100 = 200 \text{ km}$$

l. The length up the fireball tube is

$$L_{up} = 6(t - t')\, R_o + R_{fb}$$
$$= (6)(19.1)(15) + 192 = 1911 \text{ km}$$

m. Since h_b = 200 km, the quantity L' is

$$L' = \frac{h_{fb} - h_b}{\sin \varphi} = \frac{900 - 200}{0.87} = 810 \text{ km}$$

n. Since $L' < L_{up}$

$$L_{down} = L' = 810 \text{ km}.$$

o. Since $t > t_r$ and $h_m > 200$ km, the quantity f_h must be determined from Figure 8-27. Entering Figure 8-27 with $t - t_r = 13$, the quantity is determined to be

$$f_h = 0.9.$$

The altitude of the debris is, therefore,

$$h_d = 200 + f_h(h_m - 200)$$
$$= 200 + (0.9)(900 - 200) = 830 \text{ km}.$$

p. From Figure 8-28, the maximum debris offset D_d = 350 km for $\varphi = 60°$ and h_m = 900 km. From Figure 8-29, the debris offset correction factor is f_o = 0.1 for $(t - t_r)$ = 13 min. Therefore, the debris offset is

$$\Delta d = f_o D_d = (0.1)(350) = 35 \text{ km}.$$

q. Since $t < 120$ minutes,

$$R_d = R_{fb} = 192 \text{ km}.$$

Answer:

a. The fireball is a tube with dimensions as follows (refer to Figure 8-16):

$$h_{fb} = 900 \text{ km},$$
$$R_{fb} = 192 \text{ km},$$
$$L_{up} = 1911 \text{ km},$$
$$L_{down} = 810 \text{ km}.$$

b. The debris region is a pancake with a radius of 192 km centered at an altitude of 830 km. It is offset 35 km towards the north pole from the burst point (refer to Figure 8-17).

[redacted] *Reliability* [redacted] The size and location of the fireball and debris, particularly late time debris expansion, are affected by atmospheric winds and diffusion. Since these effects are neglected in the model described herein, the results predicted by the model may be considerably in error.

[redacted] *Related Material* [redacted] See paragraph 8-14.

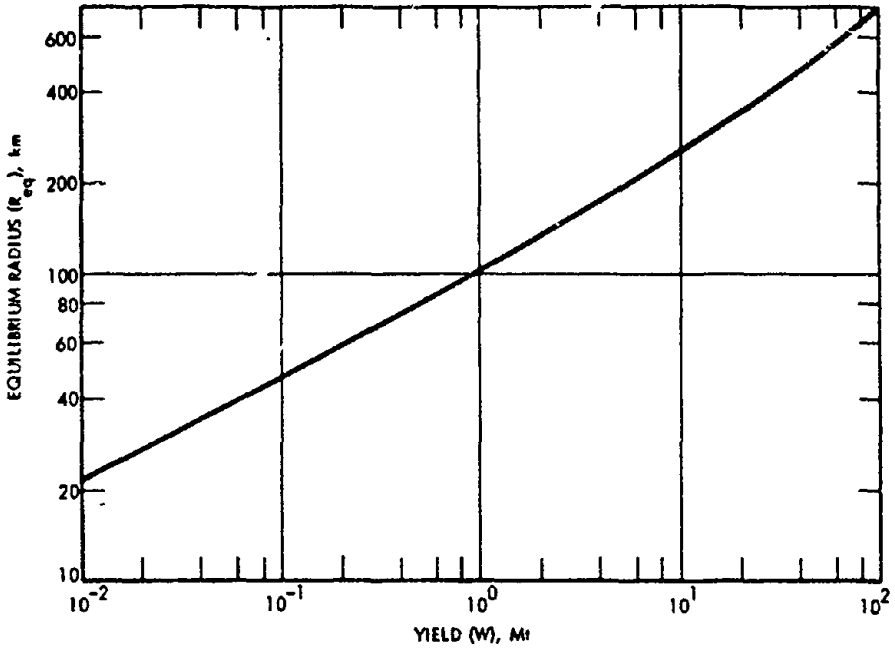

Figure 8-26. [redacted] Magnetic Equilibrium Radius [redacted]

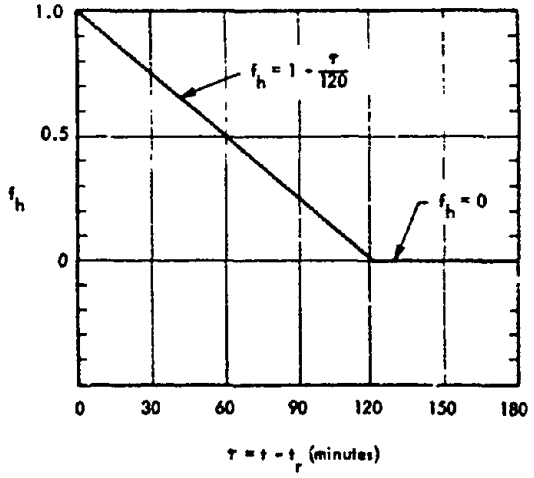

Figure 8-27. [redacted] Debris Height Factor [redacted]

[redacted]

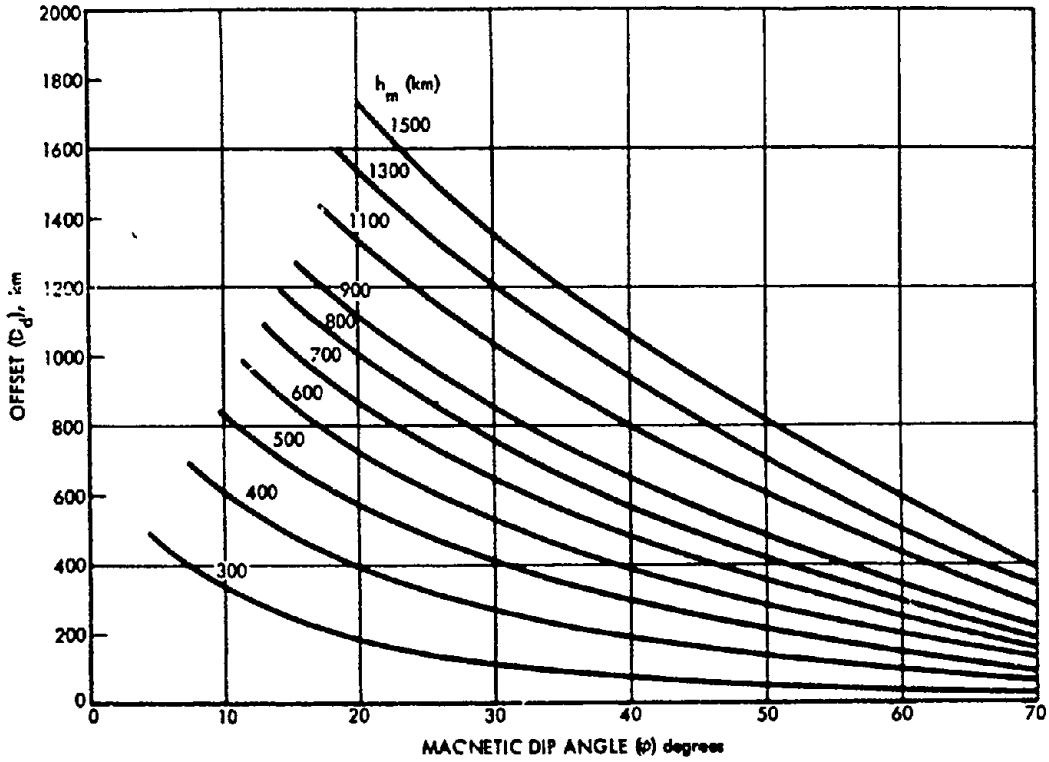

Figure 8-28. [redacted] Maximum Debris Offset [redacted]

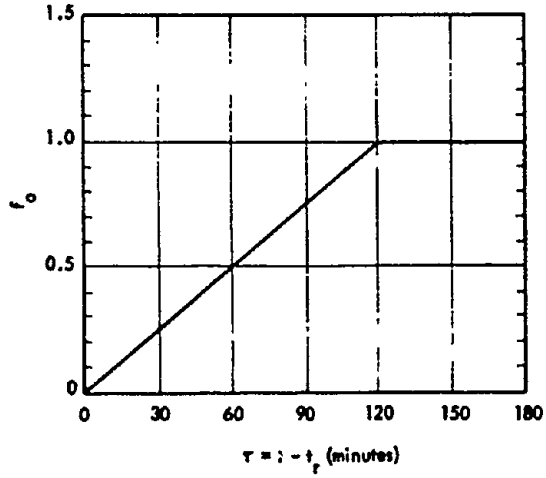

Figure 8-29. [redacted] Debris Offset Correction Factor [redacted]

[redacted]

[redacted]

Problem 8-3 Calculation of Size, Shape, and Location of Fireball and Debris Regions for a Burst Above 120 kilometers

[redacted] Table 8-2 and Figures 8-27 through 8-38 contain data with which estimates may be made of the size, shape, and location of the fireball and the debris regions for nuclear detonations above 120 kilometers. As discussed in paragraph 8-15 and shown in Figure 8-18, three separate debris regions are considered. Three shapes are used to model the fireball region: a sphere, a pancake, and a tube (cylinder) along the geomagnetic field. The shapes are illustrated in Figure 8-16.

[redacted] Table 8-2 is used to determine the fireball size, shape, and location (note that time after burst is given in *seconds* in Table 8-2). The table provides relations for a few parametric yields and detonation altitudes. In view of the uncertainties in both theoretical and experimental data in this burst altitude regime, interpolation between sections of Table 8-2 is not warranted. Data provided in the table for the yield and altitude combination nearest to those desired should be used. If either the desired yield or the desired detonation altitude is midway between values given in the table, values for the next higher yield and/or detonation altitude should be used. The phenomenology is very uncertain for yields greater than 10 Mt. If estimates are required for yields greater than 10 Mt, the dimensions and location given for a 10 Mt burst should be used. Table 8-2 indicates the shape of the fireball for the various yields and burst altitudes as a function of time (in seconds) after burst. The size and location of the fireball are determined as described below.

1. If the fireball is a sphere, the fireball altitude, h_{fb}, and fireball radius. R_{fb}, are read directly from Table 8-2 for the time of interest.

2. If the fireball is a pancake, the fireball altitude, h_{fb}, and the fireball radius, R_{fb}, are read directly from Table 8-2 for the time of interest. The semithickness of the pancake in kilometers (see Figure 8-16) is equal to the value shown in the column headed "x" in Table 8-2. Together, these values provide the size and location of the fireball at the desired time.

3. If the fireball is a tube, the fireball altitude, h_{fb}, and fireball radius, R_{fb}, are once again read directly from Table 8-2. The fireball lengths up and down the tube (see Figure 8-16) are determined from the values in the columns headed "x" and "y" in Table 8-2, as follows:

$$L_{down} = \frac{h_{fb} - 200}{|\sin \varphi|} \text{ km, or}$$

$$L_{down} = \frac{x}{2|\sin \varphi|} \text{ whichever is smaller,}$$

$$L_{up} = \frac{y}{2|\sin \varphi|} \text{ km,}$$

where φ is the magnetic dip angle at the burst point. If the magnetic dip angle is not known, it can be obtained from Figure 8-54. A negative value for y in Table 8-2 means that both x and y are dimensions down the geomagnetic field and the fireball is below h_{fb}.

[redacted] Figures 8-30 through 8-38 contain families of curves with which the size and location of the three debris regions may be estimated. Once again, the uncertainties in the data are such that interpolation between figures is not warranted. Data on the figure for the yield nearest to that desired should be used. If the desired yield is midway between values provided, data for the next higher value should be used.

[redacted] The fraction of the total weapon debris in each of the debris regions is obtained by use of Figure 8-30 and the calculations described below. Enter Figure 8-30 with the magnetic dip angle φ and the altitude of detonation h_o to obtain the fraction of debris going to debris region

[redacted]

[redacted]

3, X (see Figure 8-18). Compute the fraction of the debris in each of the three regions as follows:

$$FF1 = \begin{cases} 0.8 - X & h_o \leq 250 \text{ km}, \\ 0.6 - X & h_o > 250 \text{ km}, \end{cases}$$

$$FF2 = \begin{cases} 0 & h_o \leq 250 \text{ km}, \\ 0.2 & h_o > 250 \text{ km}, \end{cases}$$

$$FF3 = X,$$

where FF1, FF2, and FF3 are the fractions of total weapon debris in regions 1, 2, and 3, respectively. The sum of the three fractions is always less than 1.0, since some debris is assumed to escape to long distances (see paragraph 8-15).

[redacted] The altitude, h_d, for debris region 1 is obtained from Figures 8-31 through 8-34 by selecting the figure with the yield closest to that desired, and by determining h_{d1} for the time and burst altitude of interest. The maximum altitude to which the debris rises in region 1, h_{m1} should also be obtained for use in determining the debris offset as described later.

[redacted] The debris radius, R_{d1}, for debris region 1 is obtained from Figures 8-35 through 8-38 by selecting the figure with the yield closest to that desired, and by determining R_{d1} for the time and burst altitude of interest.

[redacted] If $t \leq 10$ minutes, the offset for debris region 1, Δd, is zero. If $t > 10$ minutes, the offset of debris region 1 is determined as follows.

1. Obtain the maximum debris offset D_d from Figure 8-28 for $h_m = h_{m1}$, as determined above, and the magnetic dip angle, φ, of interest.
2. Calculate τ:

$$\tau = t - 10 \text{ min}.$$

Enter Figure 8-29 with τ to obtain the debris offset correction factor f_o.

3. The offset of debris region 1 is

$$\Delta d_1 = f_o D_d \text{ km}.$$

[redacted] Debris region 2 is only defined for bursts above 250 km. The size and location are determined by a series of steps, as follows. If $t \leq 10$ minutes, go to 2; otherwise go to 1.

1. Enter Figure 8-27 with $\tau = t - 10$ min to obtain the debris height correction factor f_h.
2. Compute the maximum altitude, h_{m2}, for debris region 2:

$$h_{m2} = h_o + 500\ W^{1/3} \text{ km}$$

Compute the altitude for debris region 2 at time t:

$$h_{d2} = \begin{cases} h_{m2} \text{ km} \\ \quad t \leq 10 \text{ min}, \\ 200 + f_h(h_o + 500\ W^{1/3} - 200) \text{ km} \\ \quad t > 10 \text{ min}, \end{cases}$$

where W is the weapon yield in megatons.

3. Compute the radius for debris region 2, R_{d2}:

$$R_{d2} = \begin{cases} 500\ W^{1/3} \text{ km} \\ \quad t \leq 120 \text{ min}, \\ 500\ W^{1/3} + 3\ (t - 120) \text{ km} \\ \quad t > 120 \text{ min}, \end{cases}$$

4. If $t \leq 10$ minutes, the debris offset, Δd_2, equals zero. If $t > 10$ minutes, Δd_2 is determined from Figures 8-28 and 8-29. Enter Figure 8-28 with magnetic dip angle, φ, and $h_m = h_{m2}$ to obtain D_d. Calculate τ:

$$\tau = t - 10 \text{ min}.$$

Enter Figure 8-29 to obtain the debris offset

[redacted]

correction factor, f_o. Calculate Δd_2, the debris offset for region 2:

$$\Delta d_2 = D_d f_o.$$

The debris altitude, radius, and offset for debris region 3 are assumed to be the same as those determined for debris region 1, but they are located in the magnetic conjugate area (see Figure 8-18).

Example

Given: A 1 Mt weapon detonated at 250 km altitude at a location where the magnetic dip angle is 60°.

Find: The shape, size, and location of the fireball, and the altitude, radius, and offset of the debris regions 2 minutes after the burst.

Solution:

a. Since the altitude of interest is midway between the altitudes provided in Table 8-2, the larger (300 km) is used. From the data provided in Table 8-2 for 1 Mt at a burst altitude of 300 km, the following values are obtained for t = 120 sec:

Fireball shape is a tube.

$$h_{fb} = 290 \text{ km}$$

$$R_{fb} = 150 \text{ km}$$

$$x = 160$$

$$y = 300$$

b.

(1) $$\frac{h_{fb} - 200}{|\sin \varphi|} = \frac{290 - 200}{0.87} = 103 \text{ km.}$$

(2) $$\frac{x}{2|\sin \varphi|} = \frac{160}{(2)(0.87)} = 92 \text{ km.}$$

Since the result obtained in (2) is less than that obtained in (1),

$$L_{down} = 92 \text{ km.}$$

$$L_{up} = \frac{y}{2|\sin \varphi|} = \frac{300}{(2)(0.87)} = 172 \text{ km.}$$

c. From Figure 8-30, the fraction of debris transported to debris region 3, X, is 0.2 for a burst altitude of 250 km. Therefore,

$$FF1 = 0.6$$

$$FF2 = 0$$

$$FF3 = 0.2$$

d. From Figure 8-33,

$$h_{d1} = 625 \text{ km, and}$$

$$h_{m1} = 800 \text{ km.}$$

e. From Figure 8-37,

$$R_{d1} = 150 \text{ km.}$$

f. Since $t < 10$ min, $\Delta d_1 = 0$.

g. Since the burst altitude is not greater than 250 km, no debris region 2 is defined.

h. The size and altitude of debris region 3 are the same as those of debris region 1, but debris region 3 is centered over the magnetic conjugate of the burst point.

Answer:

a. The fireball is a tube with the following dimensions (see Figure 8-16 for illustration of the meaning of the dimensions):

$$h_{fb} = 290 \text{ km}$$

$$R_{fb} = 150 \text{ km}$$

$$L_{down} = 92 \text{ km}$$

$$L_{up} = 172 \text{ km}$$

b. There are two debris pancake regions for use in determining delayed radiation effects. Debris region 1 is a pancake centered over the burst point with an altitude and radius of 625 km and 150 km, respectively. Debris region 3 is a pancake directly over the conjugate of the burst

[redacted]

point, and it has the same altitude and radius as debris region 1. Sixty percent of the fission debris is in debris region 1, and twenty percent is in debris region 3. (Twenty percent is assumed to escape to large distances.)

[redacted] *Reliabilit*[redacted] Because of the theoretical and experimental uncertainties concerning bursts above 120 km, together with the uncertainties introduced by using fixed parametric yield/detonation altitude combinations, results predicted by the model described above may be considerably in error.

[redacted] *Related Materia*[redacted] See paragraph 8-15.

[redacted]

Table 8-2 [redacted] Fireball Location and Dimensions for Detonations Above 80 km [redacted]

Time is in seconds, distances are in kilometers. E refers to the power of 10, e.g., 1.5E4 = 1.5×10^4.

10 kt, 150 km

t	Shape	h_{fb}	R_{fb}	x	y
1	Sphere	1.5E2	1.2E1		
3	"	1.6E2	1.3E1		
10	"	1.6E2	1.7E1		
30	Tube	1.9E2	2.2E1	3.0E1	3.0E1
60	"	2.1E2	2.6E1	6.0E1	6.0E1
120	"	2.4E2	3.2E1	1.0E2	1.0E2
300	"	2.6E2	5.1E1	1.4E2	2.2E2
600	"	2.7E2	6.3E1	1.6E2	4.4E2
900	"	"	"		6.4E2
1800	"	"	"		1.4E3

10 kt, 200 km

t	Shape	h_{fb}	R_{fb}	x	y
1	Sphere	2.0E2	1.8E1		
3	"	2.1E2	1.9E1		
10	Tube	"	2.2E1	4.0E1	4.0E1
30	"	2.3E2	2.3E2	5.0E1	5.0E1
60	"	2.6E	2.6E1	6.0E1	6.0E1
120	"	2.8E2	3.2E1	1.0E2	1.0E2
300	"	3.0E2	4.9E1	1.4E2	2.0E2
600	"	"	6.1E1	"	4.2E2
900	"	"	"	"	6.0E2
1800	"	"	"	"	1.3E3

10 kt, 300 km

t	Shape	h_{fb}	R_{fb}	x	y
1	Tube	3.1E2	3.2E1	4.0E1	4.0E1
3	"	"	"	"	"
10	"	3.2E2	3.3E1	5.0E1	5.0E1
30	"	3.4E2	3.5E1	6.0E1	6.0E1
60	"	3.7E2	3.8E1	8.0E1	8.0E1
120	"	4.0E2	4.5E1	1.4E2	1.4E2
300	"	4.2E2	6.5E1	2.6E2	2.6E2
600	"	4.3E2	7.8E1	4.0E2	4.8E2
900	"	"	"	"	7.0E2
1800	"	"	"	"	1.5E3

10 kt, 400 km

t	Shape	h_{fb}	R_{fb}	x	y
1	Tube	4.1E2	4.7E1	6 0E1	6.0E1
3	"	"	4.8E1	"	"
10	"	4.2E2	4.9E1	8.0E1	8.0E1
30	"	4. 32	5.1E1	1.0E2	1.0E2
60	"	_2	5.5E1	1.2E2	1.2E2
120	"	5.2E2	6.3E1	1.6E2	1.6E2
300	"	5.4E2	8.4E1	3.0E2	3.0E2
600	"	5.5E2	1.0E2	5.6E2	5.6E2
900	"	"	"	"	8.0E2
1800	"	"	"	"	1.9E3

Table 8-2 [redacted] Fireball Location and Dimensions for Detonations Above 80 km (Continued) [redacted]

Time is in seconds, distances are in kilometers. E refers to the power of 10, e.g., 1.5E4 = 1.5×10^4.

10 kt, 500 km

t	Shape	h_{fb}	R_{fb}	x	y
1	Tube	5.1E2	6.5E1	8.0E1	8.0E1
3	"	5.2E2	6.5E1	"	"
10	"	"	6.6E1	1.0E2	1.0E2
30	"	5.6E2	6.9E1	1.2E2	1.2E2
60	"	5.9E2	7.3E1	1.4E2	1.4E2
120	"	6.4E2	8.2E1	2.0E2	2.0E2
300	"	6.6E2	1.0E2	3.4E2	3.4E2
600	"	6.7E2	1.2E2	6.2E2	6.2E2
900	"	"	"	8.8E2	8.6E2
1800	"	"	"	"	1.9E3

100 kt, 150 km

t	Shape	h_{fb}	R_{fb}	x	y
1	Sphere	1.6E2	2.7E1		
3	"	"	2.9E1		
10	"	1.8E2	3.6E1		
30	Tube	2.3E2	4.8E1	8.0E1	8.0E1
60	"	2.9E2	5.5E1	1.2E2	1.2E2
120	"	3.9E2	6.8E1	2.0E2	2.0E2
300	"	4.8E2	1.0E2	4.4E2	4.4E2
600	"	"	1.3E2	5.2E2	8.4E2
900	"	"	"	"	1.2E3
1800	"	"	"	"	2.6E3

100 kt, 200 km

t	Shape	h_{fb}	R_{fb}	x	y
1	Sphere	2.1E2	4.0E1		
3	"	2.2E2	4.2E1		
10	Tube	2.3E2	4.7E1	6.0E1	6.0E1
30	"	2.7E2	5.1E1	8.0E1	8.0E1
60	"	3.3E2	5.6E1	1.2E2	1.2E2
120	"	4.2E2	6.8E1	2.0E2	2.0E2
300	"	4.8E2	1.0E2	4.2E2	4.2E2
600	"	"	1.2E2	5.2E2	7.8E2
900	"	"	"	"	1.2E3
1800	"	"	"	"	2.4E3

100 kt, 300 km

t	Shape	h_{fb}	R_{fb}	x	y
1	Tube	3.2E2	7.0E1	1.0E2	1.0E2
3	"	3.3E2	7.1E1	8.0E1	8.0E1
10	"	3.4E2	7.2E1	1.2E2	1.2E2
30	"	3.9E2	7.6E1	1.4E2	1.4E2
60	"	4.6E2	8.3E1	1.8E2	1.8E2
120	"	5.7E2	9 6E1	2.6E2	2.6E2
300	"	6.7E2	1 3E2	5.2E2	5.2E2
600	"	"	1.6E2	9.0E2	8 6E2
900	"	"	"	"	1.3E3
1800	"	"	"	"	2.9E3

Table 8-2 [redacted] Fireball Location and Dimensions for Detonations Above 80 km (Continued) [redacted]

Time is in seconds, distances are in kilometers. E refers to the power of 10, e.g., 1.5E4 = 1.5 x 10^4.

100 kt, 400 km

t	Shape	h_{fb}	R_{fb}	x	y
1	Tube	4.3E2	1.1E2	1.4E2	1.4E2
3	"	4.4E2	"	"	"
10	"	4.6E2	"	1.6E2	1.6E2
30	"	5.1E2	"	1.8E2	1.8E2
60	"	5.8E2	1.2E2	2.2E2	2.2E2
120	"	7.1E2	1.3E2	3.4E2	3.4E2
300	"	8.5E2	1.7E2	7.0E2	7.0E2
600	"	"	2.0E2	1.1E3	1.1E3
900	"	"	"	1.3E3	1.5E3
1800	"	"	"	"	3.3E3

100 kt, 500 km

t	Shape	h_{fb}	R_{fb}	x	y
1	Tube	5.5E2	1.4E2	2.0E2	2.0E2
3	"	"	1.5E2	"	"
10	"	5.7E2	"	"	2.2E2
30	"	6.3E2	"	2.4E2	2.4E2
60	"	7.1E2	1.6E2	3.0E2	3.0E2
120	"	8.5E2	1.8E2	5.0E2	5.0E2
300	"	1.0E3	2.2E2	6.4E2	8.0E2
600	"	"	2.5E2	1.1E2	1.2E3
900	"	"	"	1.6E2	1.8E3
1800	"	"	"	"	3.6E3

1 Mt, 150 km

t	Shape	h_{fb}	R_{fb}	x	y
1	Sphere	1.8E2	6.1E1		
3	"	1.9E2	6.4E1		
10	"	2.2E2	7.7E1		
30	Tube	3.0E2	1.1E2	1.4E2	1.4E2
60	"	4.2E2	1.2E2	2.2E2	2.2E2
120	"	6.5E2	1.4E2	3.6E2	3.6E2
300	"	1.1E3	2.0E2	8.0E2	8.0E2
600	"	1.2E3	2.5E2	1.4E3	1.4E3
900	"	"	"	2.0E3	2.0E3
1800	"	"	"	"	4.8E3

1 Mt, 200 km

t	Shape	h_{fb}	R_{fb}	x	y
1	Sphere	2.4E2	9.1E1		
3	"	2.5E2	9.5E1		
10	Tube	2.8E2	1.1E2	1.4E2	1.4E2
30	"	3.5E2	1.1E2	2.0E2	2.0E2
60	"	4.6E2	1.2E2	2.4E2	2.4E2
120	"	6.7E2	1.4E2	4.0E2	4.0E2
300	"	1.0E3	2.0E2	8.0E2	8.0E2
600	"	1.1E3	2.4E2	1.4E3	1.4E3
900	"	"	"	1.8E3	2.0E3
1800	"	"	"	"	4 6E3

Table 8-2 [redacted] Fireball Location and Dimensions for Detonations Above 80 km (Continued) [redacted]

Time is in seconds, distances are in kilometers. E refers to the power of 10, e.g., 1.5E4 = 1.5×10^4.

1 Mt, 300 km

t	Shape	h_{fb}	R_{fb}	x	y
1	Pancake	2.2E2	1.5E2	9.1E0	
3	"	"	"	1.7E1	
10	"	2.5E2	"	4.6E1	
30	Tube	2.9E2	"	1.1E2	1.1E2
60	"	"	"	1.6E2	1.6E2
120	"	"	"	"	3.0E2
300	"	"	"	"	6.5E2
600	"	"	"	"	2.4E3
900	"	"	"	"	3.6E3
1800	"	"	"	"	8.0E3

Mt, 400 km

t	Shape	h_{fb}	R_{fb}	x	y
1	Pancake	2.8E2	2.2E2	1.1E1	
3	"	2.9E2	"	2.2E2	
10	"	3.3E2	"	6.2E2	
30	Tube	3.9E2	"	2. E2	2.8E2
60	"	"	"	"	4.0E2
120	"	"	"	"	6.6E2
300	"	"	"	"	1.4E3
600	"	"	"	"	2.6E3
900	"	"	"	"	3.8E3
1800	"	"	"	"	8.2E3

1 Mt, 500 km

t	Shape	h_{fb}	R_{fb}	x	y
1	Pancake	3.4E2	3.0E2	1.2E1	
3	"	3.5E2	"	2.7E1	
10	"	4.0E2	"	8.0E1	
30	Tube	4.8E2	"	3.2E2	3.4E2
60	"	"	"	"	4.6E2
120	"	"	"	"	7.2E2
300	"	"	"	"	1.4E3
600	"	"	"	"	2.6E3
900	"	"	"	"	3.8E2
1800	"	"	"	"	8.2E3

10 Mt, 150 km

t	Shape	h_{fb}	R_{fb}	x	y
1	Sphere	2.5E2	1.5E2		
3	"	2.6E2	1.5E2		
10	"	2.9E2	1.7E2		
30	"	3.9E2	2.1E2		
60	"	5.2E2	2.7E2		
120	Tube	7.9E2	3.0E2	5.2E2	5.2E2
300	"	1.3E3	3.7E2	1.0E3	1.0E3
600	"	1.5E3	4.1E2	1.8E3	1.8E3
900	"	"	"	2.6E3	2.6E3
1800	"	"	"	"	5.6E3

Table 8-2 [redacted] Fireball Location and Dimensions for Detonations Above 80 km (Concluded) [redacted]

Time is in seconds, distances are in kilometers. E refers to the power of 10, e.g., 1.5E4 = 1.5×10^4.

10 Mt, 200 km

t	Shape	h_{fb}	R_{fb}	x	y
1	Sphere	3.4E2	2.2E2		
3	"	3.5E2	2.3E2		
10	"	3.8E2	2.4E2		
30	Tube	4.8E2	2.7E2	3.8E2	3.8E2
60	"	6.1E2	2.8E2	4.4E2	4.4E2
120	"	8.8E2	3.0E2	5.2E2	6.2E2
300	"	1.4E3	3.7E2	7.0E3	1.0E3
600	"	1.6E3	4.2E2	2.0E3	2.0E3
900	"	"	"	2.8E3	2.8E3
1800	"	"	"	"	5.6E3

10 Mt, 300 km

t	Shape	h_{fb}	R_{fb}	x	y
1	Pancake	1.6E2	3.1E2	7.6E0	
3	"	1.7E2	"	1.3E1	
10	"	1.8E2	"	3.1E1	
30	Tube	2.1E2	"	1.2E2	1.6E2
60	"	"	"	"	2.8E2
120	"	"	"	"	5.4E2
300	"	"	"	"	1.2E3
600	"	"	"	"	2.4E3
900	"	"	"	"	3.6E3
1800	"	"	"	"	8.0E3

10 Mt, 400 km

t	Shape	h_{fb}	R_{fb}	x	y
1	Pancake	2.0E2	4.7E2	8.6E0	
3	"	2.1E2	"	1.6E1	
10	"	2.3E2	"	4.1E1	
30	Tube	2.7E2	"	1.6E2	2.0E2
60	"	"	"	"	3.2E2
120	"	"	"	"	5.8E2
300	"	"	"	"	1.3E3
600	"	"	"	"	2.5E3
900	"	"	"	"	3.7E3
1800	"	"	"	"	8.1E3

10 Mt, 500 km

t	Shape	h_{fb}	R_{fb}	x	y
1	Pancake	2.4E2	6.4E2	9.6E0	
3	"	2.5E2	"	1.9E1	
10	"	2.8E2	"	5.1E1	
30	Tube	3.2E2	"	1.8E2	2.4E2
60	"	"	"	"	3.6E2
120	"	"	"	"	6.2E2
300	"	"	"	"	1.3E3
600	"	"	"	"	2.6E3
900	"	"	"	"	3.8E3
1800	"	"	"	"	8.2E3

[redacted]

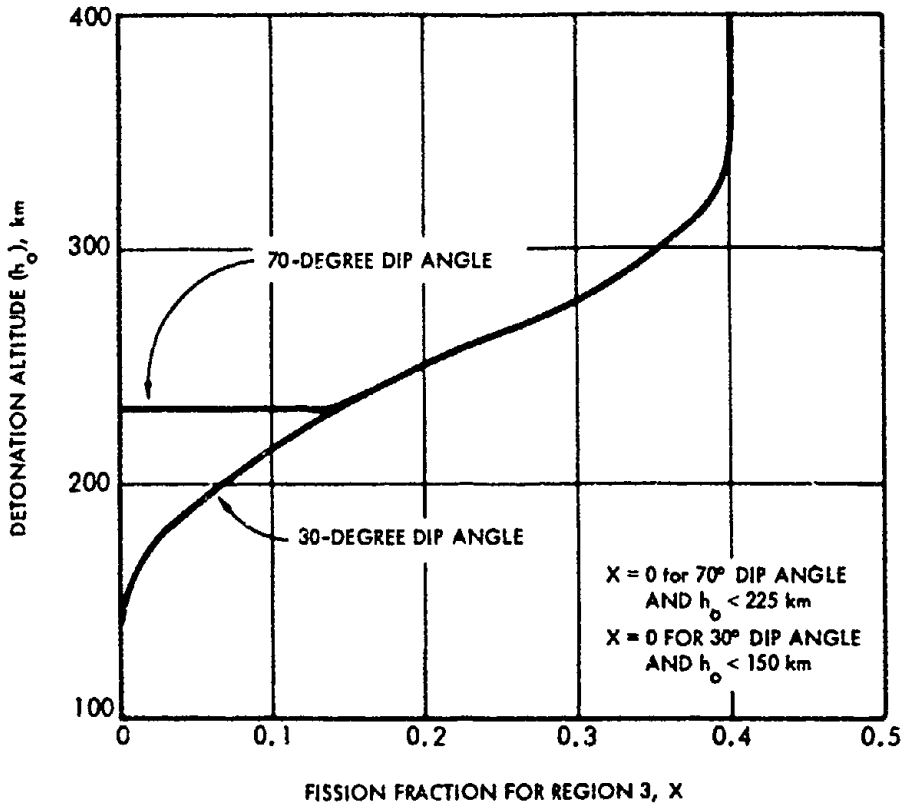

Figure 8-30. [redacted] Fraction of Total Debris Transported to Conjugate Region (Region 3) [redacted]

[redacted]

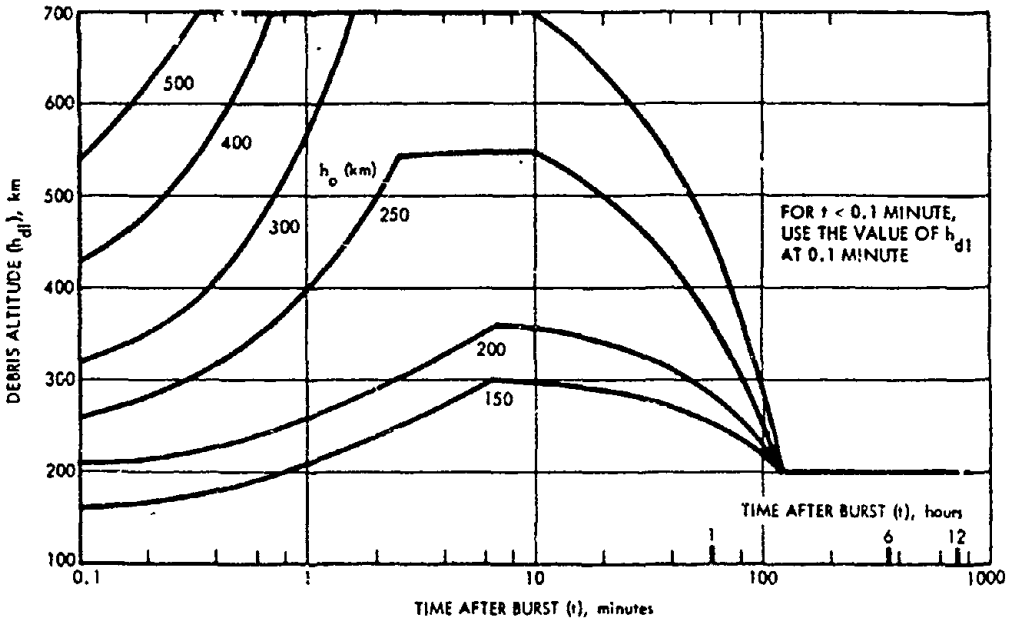

Figure 8-31. [redacted] Altitude of Debris Region 1, 10-kt Burst [redacted]

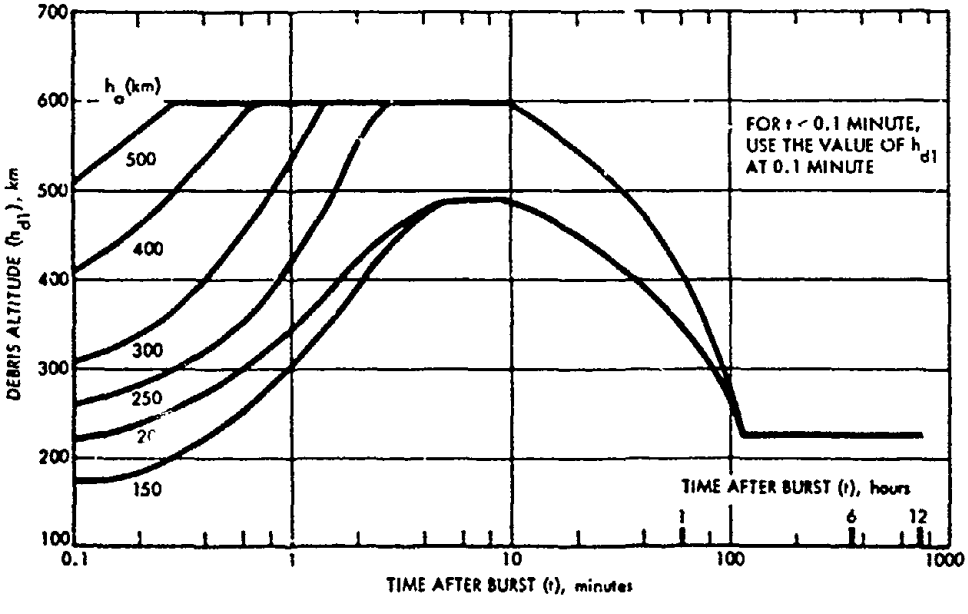

Figure 8-32. [redacted] Altitude of Debris Region 1, 100-kt Burst [redacted]

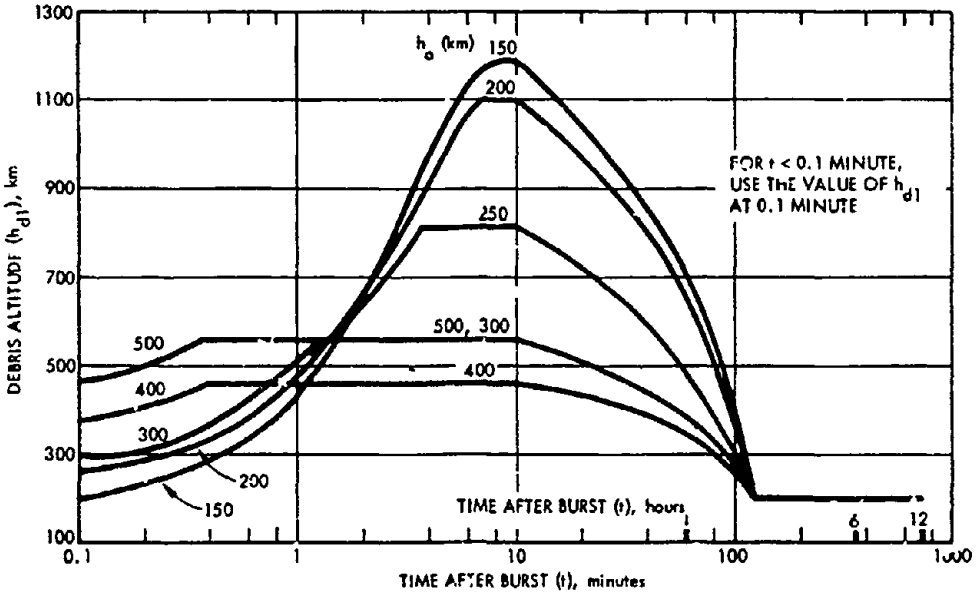

Figure 8-33. [redacted] Altitude of Debris Region 1, 1-Mt Burst [redacted]

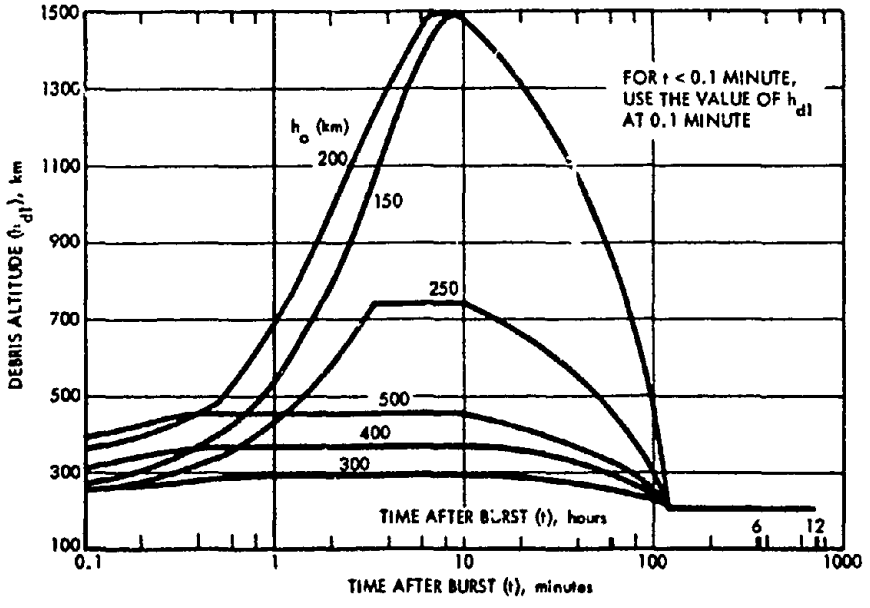

Figure 8-34. [redacted] Altitude of Debris Region 1, 10-Mt Burst [redacted]

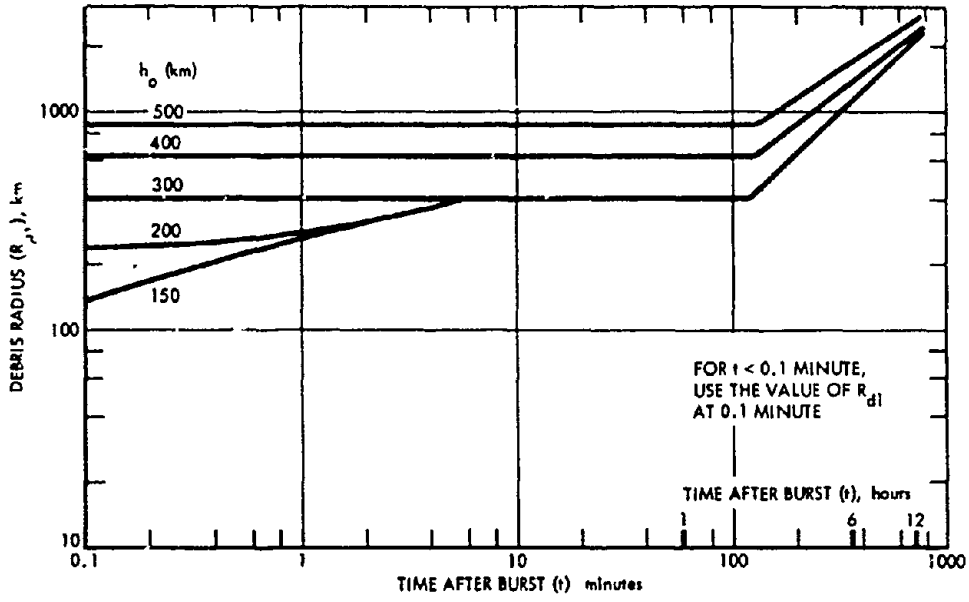

Figure 8-35. [redacted] Radius of Debris Region 1, 10-kt Burst [redacted]

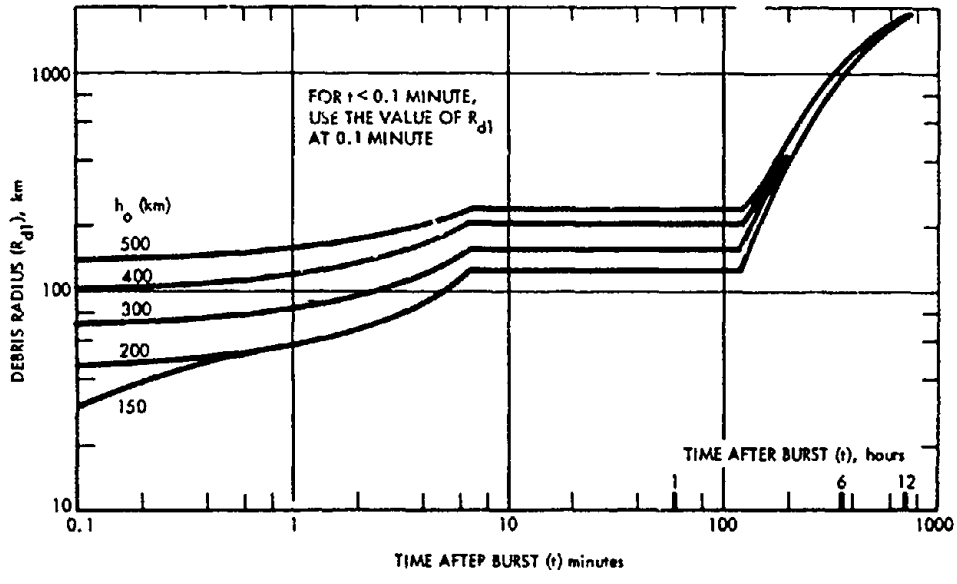

Figure 8-36. [redacted] Radius of Debris Region 1, 100-kt Burst [redacted]

[redacted]

[redacted]

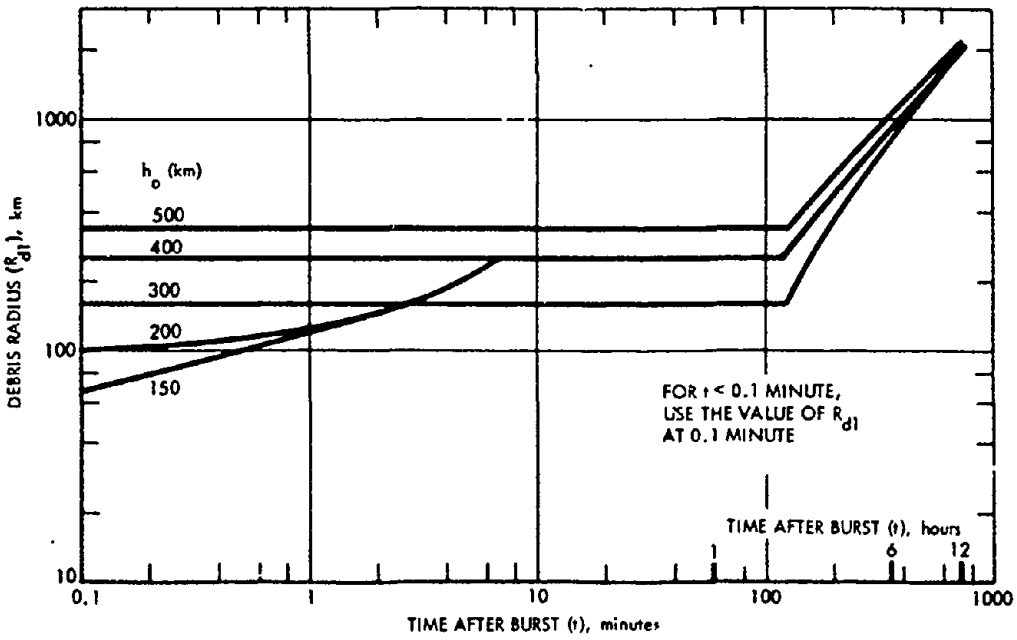

Figure 8-37. [redacted] Radius of Debris Region 1, 1-Mt Burst [redacted]

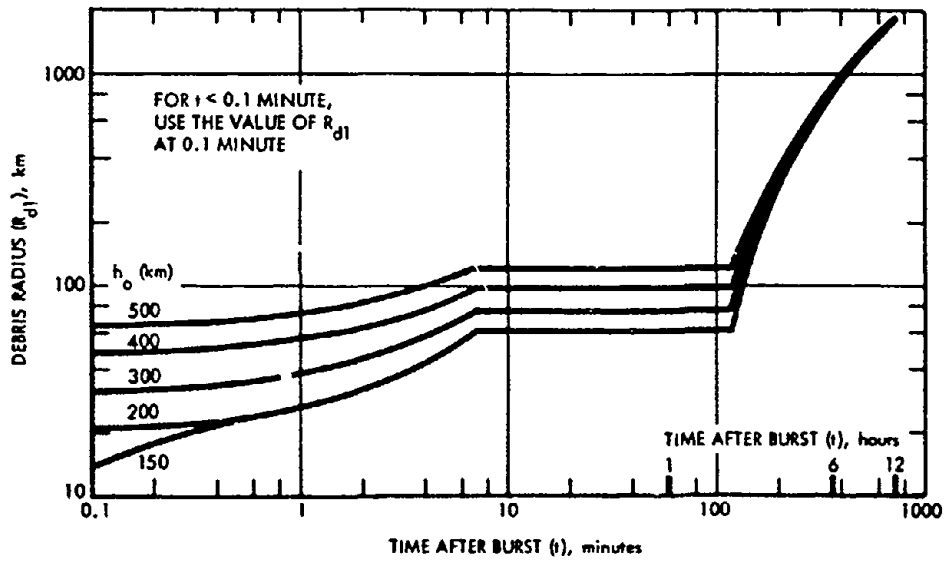

Figure 8-38. [redacted] Radius of Debris Region 1, 10-Mt Burst [redacted]

[redacted]

[redacted]

Problem 8-4 Absorption through the Fireball [redacted]

[redacted] Tables 8-3 through 8-7 and Figure 8-39 are used to obtain estimates of the absorption of signals propagating through the fireball for parametric burst yields and detonation altitudes. The temperature and electron density within the fireball are assumed to be uniformly distributed; thus, the absorption through the fireball is linearly dependent upon the distance the propagation path travels through the fireball. The fireball location and size can be determined from Table 8-2 and Figures 8-16 through 8-38, as described in Problems 8-1 through 8-3.

[redacted] The absorption data are given for a path length through the fireball equal to the fireball diameter if the fireball is a sphere, equal to the diameter of the toroid arm if the fireball is a toroid, equal to the vertical thickness of a pancake if the fireball is a pancake, or equal to the diameter of the tube if the fireball is a tube. For detonations that occur above about 50 km, the fireball absorption scales inversely with the square of the frequency.

[redacted] When the fireball is below an altitude of about 60 km, beta particles deposit their energy within the fireball, and they are the major source of ionization and absorption after the fireball has cooled to the atmospheric temperature. When the altitude of the fireball is greater than 60 km, absorption caused by beta-particle ionization should be determined by the methods described in Problem 8-7.

[redacted] Tables 8-3 through 8-6 provide data to determine absorption of signals propagating through the fireball of bursts that occur below 80 km at times after burst less than 300 seconds and fireball altitudes greater than 60 km (the fireball altitude at the time of interest may be obtained by the methods described in Problem 8-1). If the detonation altitude is below 50 km, the absorption A_{fb} is read directly from the table with the weapon yield closest to the desired yield at the closest detonation altitude, time after burst, and frequency given in the table. If the detonation altitude is 50 km or greater (but not greater than 80 km), the absorption for 1000 MHz, A'_{fb} is read from the appropriate table at the closest detonation altitude and time after burst. The absorption is then calculated as follows:

$$A_{fb} = A'_{fb} \frac{10^6}{f^2} ,$$

where f is the desired frequency in MHz.

[redacted] If the time after burst is greater than 300 seconds and the fireball altitude is less than 60 kilometers, the absorption of signals propagating through the fireball may be estimated from Figure 8-39. The quantity L'_a is obtained from Figure 8-39 for the appropriate fireball altitude and frequency. The absorption is then calculated as follows:

$$A_{fb} = L'_a \frac{N_\beta}{10^9} ,$$

where N_β is the beta particle radiation intensity parameter defined by equation 8.1 in paragraph 8-4.

[redacted] Table 8-7 provides data to determine absorption of signals propagating through the fireball of bursts that occur at altitudes above 80 km. The absorption of a 1000 MHz signal (A'_{fb}) is read from Table 8-7 for the weapon yield and altitude closest to those desired. The absorption at the desired frequency (A_{fb}) is then calculated as follows:

$$A_{fb} = A'_{fb} \frac{10^6}{f^2} ,$$

where f is the frequency in MHz.

[redacted]

[redacted]

[redacted] *Example 1*

Given: A 1 Mt weapon burst at an altitude 50 km.

Find: The absorption of a 400 MHz signal propagating through the fireball 2 min after burst.

Solution: From Table 8-5, the absorption of a 1000 MHz signal 2 min after a burst at 50 km is

$$A'_{fb} = 0.2 \text{ dB};$$

therefore,

$$A_{fb} = (0.2)\frac{10^6}{(400)^2} = 1.25 \text{ dB}.$$

Answer: The absorption of a 400 MHz signal propagating through the fireball of a 1 Mt weapon 2 min after the weapon was detonated at an altitude of 50 km is 1.25 dB.

[redacted] *Example 2*

Given: A 4 Mt weapon burst at an altitude of 150 km.

Find: The absorption of a 400 MHz signal propagating through the fireball 15 min after burst.

Solution: The yield and time nearest to those desired that are tabulated in Table 8-7 are 1 Mt and 10 min (600 sec). The absorption for a 1000 MHz signal 10 min after a 1 Mt burst at 150 km is

$$A'_{fb} = 3.2 \text{ dB};$$

therefore,

$$A_{fb} = (3.2)\frac{10^6}{(400)^2} = 20 \text{ dB}.$$

Answer: The absorption of a 400 MHz signal propagating through the fireball of a 4 Mt weapon 15 min after the weapon was detonated at an altitude of 150 km is approximately 20 dB.

[redacted] *Reliability* [redacted] The uncertainties in predicting fireball dimensions and electron density are such that estimates of the duration of a given level of absorption are uncertain by at least a factor of two. In general, the duration of absorption caused by the rising fireball will be determined by how long the fireball interdicts the propagation path, rather than the time period that the fireball remains absorbing at a given frequency.

[redacted] *Related Material* [redacted] See paragraph 8-6 and Problems 8-1 through 8-3.

[redacted]

[redacted]

Table 8-3 [redacted] Absorption (dB) Through Fireball for Detonations Below 80 km, W = 10 kt [redacted]

Time (sec)	Freq. (MHz)	Detonation Altitude (km)								
		0	10	20	30	40	50	60	70	80
10	100	8.5E3	2.0E4	2.7E5	9.1E6	1.7E7				
	400	8.5E3	1.9E4	2.4E5	2.5E6	1.4E6				
	1,000	8.5E3	1.9E4	1.4E5	5.0E5	2.2E5	1.4E5	1.1E3	3.8E2	1.7E2
	4,000	8.2E3	1.2E4	1.7E4	3.3E4	1.4E4				
	10,000	6.7E3	3.7E3	2.8E3	5.3E3	2.2E3				
20	100	3.1E3	1.2E4	2.9E4	5.2E4	3.0E5				
	400	3.2E3	1.2E4	2.4E4	1.2E4	2.2E4				
	1,000	3.1E3	1.2E4	1.3E4	2.3E3	3.6E3	1.3E4	3.7E2	1.0E2	2.7E1
	4,000	3.0E3	6.7E3	1.4E3	1.5E2	2.3E2				
	10,000	2.4E3	2.0E3	2.3E2	2.3E1	3.6E1				
30	100	7.4E2	8.5E3	2.2E4	3.8E4	1.5E4				
	400	7.4E2	8.4E3	1.8E4	7.5E3	1.1E3				
	1,000	7.3E2	8.0E3	8.7E3	1.4E3	1.7E2	7.5E1	2.7E2	4.2E2	8.8E0
	4,000	7.0E2	4.1E3	8.5E2	8.7E1	1.1E1				
	10,000	5.4E2	1.1E3	1.4E2	1.4E1	1.7E0				
40	100	7.3E1	3.2E3	1.7E4	2.9E4	9.9E3				
	400	7.3E1	3.1E3	1.4E4	5.0E3	6.9E2				
	1,000	7.3E1	3.0E3	6.0E3	8.9E2	1.0E2	1.7E1	1.8E1	2.0E1	3.8E0
	4,000	6.9E1	1.4E3	5.5E2	5.7E1	7.0E0				
	10,000	5.2E1	3.5E2	9.0E1	9.3E0	1.1E0				
50	100	4.6E0	4.7E2	1.2E4	2.3E4	7.0E3				
	400	4.6E0	4.7E2	8.6E3	3.5E3	4.8E2				
	1,000	4.6E0	4.3E2	3.5E3	6.1E2	7.6E1	1.1E1	1.1E1	2.2E0	1.9E0
	4,000	4.3E0	1.8E2	3.0E2	3.9E1	4.9E0				
	10,000	3.2E0	4.4E1	4.9E1	6.2E0	7.7E-1				
60	100	2.6E-1	3.9E1	3.8E3	1.8E4	5.1E3				
	400	2.6E-1	3.9E1	2.7E3	2.4E3	3.4E2				
	1,000	2.6E-1	3.5E1	1.0E3	4.1E2	5.5E1	8.0E0	6.6E0	1.3E0	1.1E0
	4,000	2.3E-1	1.4E1	8.3E1	2.6E1	3.4E0				
	10,000	1.7E-1	3.1E0	1.4E1	4.2E0	5.5E-1				
90	100	5.6E-3	4.8E-1	3.3E1	6.5E2	1.5E3				
	400	5.6E-3	4.6E-1	2.0E1	6.9E1	9.9E1				
	1,000	5.6E-3	4.0E-1	6.1E0	1.2E1	1.6E1	3.3E0	2.1E0	3.4E-1	7.7E-2
	4,000	5.0E-3	1.2E-1	4.5E-1	7.2E-1	9.9E-1				
	10,000	3.2E-3	2.4E-2	7.3E-2	1.2E-1	1.6E-1				
120	100		3.1E-1	1.7E1	2.2E-2					
	400		2.9E-1	8.4E0	1.9E-1					
	1,000		2.3E-1	2.2E0	3.2E0	1.7E0	9.0E-1	7.8E-1	1.1E-1	3.5E-2
	4,000		5.8E-2	1.7E-1	2.1E-1					
	10,000		1.0E-2	2.4E-2	3.2E-2					
150	100		2.7E-1	1.5E1	1.7E2					
	400		2.6E-1	6.4E0	1.4E1					
	1,000		2.0E-1	1.5E0	2.3E0	1.2E0	5.5E-1	4.3E-1	6.0E-2	2.3E-2
	4,000		3.8E-2	1.0E-1	1.4E-1					
	10,000		6.9E-3	1.7E-2	2.3E-2					
180	100		2.4E-1	1.3E1	1.3E2					
	400		2.2E-1	4.9E0	1.0E1					
	1,000		1.6E-1	1.1E0	1.7E0	8.8E-1	4.0E-1	2.6E-1	3.6E-2	1.6E-2
	4,000		2.6E-2	6.9E-2	1.0E-1					
	10,000		4.9E-3	1.2E-2	1.7E-2					
300	100		1.3E-1	5.7E0	5.0E1					
	400		1.2E-1	1.7E0	3.5E0					
	1,000		6.9E-2	3.2E-1	5.6E-1	3.4E-1	1.7E-1	6.4E-2	4.9E-3	1.2E-3
	4,000		8.2E-3	2.1E-2	3.5E-2					
	10,000		1.4E-3	3.3E-3	5.6E-3					

Notes: E refers to the power of 10, e.g., $1.5E4 = 1.5 \times 10^4$. If f^{-2} scaling applies, only 1,000 MHz values are given.

[redacted]

[redacted]

Table 8-4 [redacted] Absorption (dB) Through Fireball for Detonations Below 80 km, W = 100 kt [redacted]

Time (sec)	Freq. (MHz)	Detonation Altitude (km)								
		0	10	20	30	40	50	60	70	80
10	100	1.3E5	6.5E5	4.3E6	2.5E7	4.8E7				
	400	1.3E5	6.4E5	3.7E6	6.5E6	3.8E6				
	1,000	1.3E5	6.2E5	2.1E6	1.3E6	6.1E5	4.8E5	2.1E3	9.5E2	9.2E2
	4,000	1.2E5	3.7E5	2.3E5	8.2E4	3.8E4				
	10,000	1.0E5	1.1E5	3.9E4	1.3E4	6.1E3				
20	100	9.0E3	4.3E4	1.0E5	3.5E6	4.7E6				
	400	9.0E3	4.3E4	8.3E4	6.9E5	3.3E5				
	1,000	3.3E3	2.4E4	2.5E4	3.4E3	3.7E3	4.0E3	2.3E2	3.1E1	2.5E1
	4,000	8.6E3	2.2E4	3.9E3	8.0E3	3.4E3				
	10,000	6.8E3	6.0E3	6.5E2	1.2E3	5.4E2				
30	100	3.3E3	2.6E4	8.1E4	1.3E5	3.3E5				
	400	3.3E3	2.6E4	6.1E4	2.0E4	2.3E4				
	1,000	5.8E2	1.4E4	1.7E4	2.1E3	5.5E2	1.2E2	1.1E2	1.2E1	1.1E0
	4,000	3.1E3	1.1E4	2.2E3	2.2E2	2.3E2				
	10,000	2.3E3	2.8E3	3.7E2	3.5E1	3.7E1				
40	100	5.8E2	1.5E4	6.7E4	9.4E4	2.3E4				
	400	5.8E2	1.5E4	4.7E4	1.2E4	1.6E3				
	1,000	5.8E2	1.4E4	1.7E4	2.1E3	2.5E2	1.7E2	1.1E2	1.2E1	9.1E0
	4,000	5.4E2	5.5E3	1.4E3	1.3E2	1.6E1				
	10,000	4.0E2	1.3E3	2.3E2	2.1E1	2.5E0				
50	100	5.5E1	5.5E3	5.7E4	7.1E4					
	400	5.5E1	5.4E3	3.6E4	8.0E3					
	1,000	5.5E1	4.8E3	1.2E4	1.3E3	1.6E2	9.2E1	6.0E1	5.7E0	4.2E0
	4,000	5.0E1	1.7E3	8.8E2	8.5E1					
	10,000	3.5E1	3.6E2	1.4E2	1.4E1					
60	100	4.0E0	8.9E2	4.2E4	5.5E4					
	400	4.0E0	8.7E2	2.4E4	5.5E3					
	1,000	4.0E0	7.5E2	6.9E3	9.1E2	1.1E2	1.4E1	3.3E1	3.0E0	2.2E0
	4,000	3.6E0	2.2E2	5.0E2	5.7E1					
	10,000	2.4E0	4.5E1	8.1E1	9.1E0					
90	100	2.3E-2	3.6E0	7.0E2	1.5E4					
	400	2.3E-2	3.5E0	2.8E2	1.2E3					
	1,000	2.2E-2	2.7E0	6.3E1	2.0E2	3.9E1	4.5E0	1.7E0	1.3E-1	5.4E-1
	4,000	2.0E-2	5.4E-1	4.3E0	1.2E1					
	10,000	1.1E-2	1.0E-1	6.9E-1	2.0E0					
120	100	1.4E-2	2.2E0	1.7E2	1.1E3					
	400	1.4E-2	2.0E0	4.7E1	8.0E1					
	1,000	1.4E-2	1.3E0	9.2E0	1.3E1	7.7E0	1.6E0	4.6E-1	4.8E-2	3.5E-2
	4,000	1.2E-2	2.1E-1	6.7E-1	9.1E-1					
	10,000	5.4E-3	3.3E-2	9.6E-2	1.3E-1					
150	100	1.2E-2	2.2E0	1.6E2	8.2E2					
	400	1.2E-2	2.0E0	3.4E1	5.6E1					
	1,000	1.2E-2	1.1E0	6.2E0	9.1E0	3.6E0	7.8E-1	2.2E-1	2.9E-2	1.7E-2
	4,000	9.0E-3	1.4E-1	4.0E-1	5.7E-1					
	10,000	4.0E-3	2.4E-2	6.4E-2	9.1E-2					
180	100	1.0E-2	2.2E0	1.5E2	6.1E2					
	400	1.0E-2	1.8E0	2.6E1	4.1E1					
	1,000	1.0E-2	9.8E-1	4.7E0	6.6E0	2.5E0	4.5E-1	1.2E-1	1.9E-2	7.9E-3
	4,000	7.2E-3	1.0E-1	2.9E-1	3.9E-1					
	10,000	3.0E-2	1.7E-2	4.8E-2	6.6E-2					
300	100	6.1E-3	1.7E0	8.5E1						
	400	6.1E-3	1.2E0	9.3E0						
	1,000	5.8E-3	4.2E-1	1.6E0	2.2E0	9.3E-1	8.6E-2	1.5E-2	2.6E-3	5.7E-4
	4,000	3.4E-3	3.4E-2	9.8E-2						
	10,000	1.0E-3	5.5E-3	1.6E-2						

Notes: E refers to the power of 10, e.g., 1.5E4 = 10^4. If f^{-2} scaling applies, only 1,000 MHz values are given.

[redacted]

[redacted]

Table 8-5 [redacted] Absorption (dB) Through Fireball for Detonations Below 80 km, W = 1 Mt [redacted]

Time (sec)	Freq. (MHz)	Detonation Altitude (km)								
		0	10	20	30	40	50	60	70	80
10	100	3.4E5	1.8E6	1.4E7	9.7E7	1.8E8				
	400	3.4E5	1.8E6	1.2E7	1.9E7	1.3E7				
	1,000	3.4E5	1.8E6	3.4E7	2.2E6	7.5E6	7.5E6	1.6E4	1.4E4	3.2E3
	4,000	3.3E5	1.0E6	6.2E5	2.2E5	1.4E5				
	10,000	2.7E5	3.0E5	1.0E5	3.5E4	2.2E4				
20	100	5.2E4	2.4E5	1.5E6	1.1E7	9.2E6				
	400	5.2E4	2.3E5	1.1E6	1.4E6	6.0E5				
	1,000	5.2E4	2.2E5	4.5E5	2.4E5	9.7E4	6.8E4	1.2E3	9.2E2	2.3E2
	4,000	5.0E4	1.0E5	3.8E4	1.5E4	6.0E3				
	10,000	3.8E4	2.6E4	6.3E3	2.4E3	1.0E3				
30	100	1.4E4	8.8E4	9.0E5	1.4E6	9.5E5				
	400	1.4E4	8.6E4	5.7E5	1.2E5	6.1E4				
	1,000	1.4E4	7.8E4	1.9E5	2.4E4	9.7E3	4.2E3	2.4E2	1.7E2	4.7E1
	4,000	1.3E4	3.0E4	1.4E4	1.5E3	6.0E2				
	10,000	1.0E4	6.8E3	2.3E3	2.5E2	9.7E1				
40	100	5.8E3	6.3E4	2.7E5	1.0E6	1.1E5				
	400	5.8E3	6.1E4	1.4E5	8.4E4	6.7E3				
	1,000	5.7E3	5.4E4	4.0E4	1.4E4	1.1E3	4.0E2	7.0E1	4.6E1	1.6E1
	4,000	5.3E3	1.7E4	2.9E3	8.6E2	1.7E1				
	10,000	3.7E3	3.4E3	4.6E2	1.4E2	1.1E1				
50	100	1.3E3	4.5E4	2.4E5	6.5E5	6.2E4				
	400	1.3E3	4.3E4	1.0E5	5.1E4	3.9E3				
	1,000	1.3E3	3.6E3	2.5E4	8.3E3	6.2E2	4.0E1	2.6E1	1.7E1	6.8E0
	4,000	1.1E3	8.9E3	1.7E3	5.2E2					
	10,000	7.4E2	1.7E3	2.7E2	8.3E1					
60	100	1.6E2	2.5E4	2.2E5	1.0E5					
	400	1.6E2	2.4E4	7.4E4	7.4E3					
	1,000	1.6E3	1.9E4	1.6E4	1.2E3	3.8E2	2.2E1	1.1E1	7.4E0	3.5E0
	4,000	1.4E2	3.8E3	1.1E3	7.5E1					
	10,000	8.7E1	6.9E2	1.7E2	1.2E1					
90	100	2.4E-1	2.2E2	7.8E4	3.4E4					
	400	2.4E-1	1.9E2	1.5E4	2.3E3					
	1,000	2.4E-1	1.2E2	2.6E3	3.6E2	2.4E1	4.5E0	1.6E0	1.3E0	6.4E-1
	4,000	1.9E-1	1.5E1	1.7E2	2.3E1					
	10,000	9.4E-2	2.6E0	2.7E1	3.6E0					
120	100	7.0E-2	2.7E1	3.1E3	7.6E3					
	400	7.0E-2	2.1E1	3.6E2	4.8E2					
	1,000	6.9E-2	9.3E0	6.1E1	7.8E1	6.8E0	2.0E-1	3.5E-1	3.2E-1	1.3E-1
	4,000	5.2E-2	9.6E-1	4.9E0	6.6E0					
	10,000	1.9E-2	1.4E-1	6.2E-1	7.8E-1					
150	100	6.9E-2	2.8E1	2.1E3						
	400	6.8E-2	1.9E1	2.0E2						
	1,000	6.6E-2	7.1E0	3.3E1	2.5E1	3.1E0	7.5E-2	3.2E-2	1.6E-1	9.5E-3
	4,000	4.3E-2	5.8E-1	2.1E0						
	10,000	1.4E-2	9.4E-2	3.4E-1						
180	100	6.8E-2	3.2E1	1.8E3						
	400	6.7E-2	1.9E1	1.5E2						
	1,000	6.5E-2	6.0E0	2.5E1	1.6E1	1.5E0	3.2E-2	1.8E-2	7.4E-2	3.9E-3
	4,000	3.6E-2	4.3E-1	1.5E0						
	10,000	1.1E-2	7.3E-2	2.5E-1						
300	100	5.2E-2	3.6E1	8.5E2						
	400	5.1E-2	1.2E1	5.8E1						
	1,000	4.6E-2	2.5E0	9.3E0	4.7E0	4.7E0	2.4E-3	3.3E-3	1.0E-3	1.8E-4
	4,000	1.7E-2	1.7E-1	5.8E-1						
	10,000	3.8E-3	2.7E-2	9.3E-2						

Notes: E refers to the power of 10, e.g., 1.5E4 = 1.5×10^4. If f^{-2} scaling applies, only 1,000 MHz values are given.

[redacted]

[redacted]

Table 8-6 [redacted] Absorption (dB) Through Fireball for Detonations Below 80 km, W = 10 Mt [redacted]

Time (sec)	Freq. (MHz)	Detonation Altitude (km)								
		0	10	20	30	40	50	60	70	80
10	100	1.2E6	7.4E6	8.4E7	8.8E8	1.0E10				
	400	1.1E6	7.4E6	6.2E7	2.9E8	5.2E9				
	1,000	1.1E6	7.0E6	2.5E7	6.0E7	1.4E9	1.2E10	7.8E4	2.5E4	8.2E3
	4,000	1.1E6	3.7E6	2.1E6	4.0E6	1,0E8				
	10,000	8.8E5	1.0E6	3.4E5	6.4E5	1.6E7				
20	100	1.3E5	6.6E5	1.2E7	5.0E7	1.8E8				
	400	1.3E5	6.4E5	4.9E6	4.5E6	1.2E7				
	1,000	1.3E5	5.9E5	1.1E6	7.3E5	2.0E6	8.8E6	4.8E3	1.6E3	5.9E2
	4,000	1.2E5	2.3E5	7.8E4	4.6E4	1.2E5				
	10,000	9.1E4	5.3E4	1.3E4	7.4E3	2.0E4				
30	100	9.0E4	5.3E5	4.3E6	2.4E6					
	400	8.9E4	5.1E5	1.1E6	1.6E5					
	1,000	8.9E4	4.4E5	2.2E5	2.6E4	4.5E4	7.1E4	7.4E2	2.5E2	1.2E2
	4,000	8.2E4	1.3E5	1.4E4	1.6E3					
	10,000	5.7E4	2.5E4	2.3E3	2.6E2					
40	100	6.8E4	4.7E5	3.4E6						
	400	6.8E4	4.4E5	6.1E5						
	1,000	6.7E4	3.5E5	1.1E5	4.0E3	1.8E3	2.3E3	1.8E2	6.7E1	3.9E1
	4,000	6.1E4	7.4E4	6.9E3						
	10,000	3.9E4	1.4E4	1.1E3						
50	100	2.1E4	4.3E5	2.7E6						
	400	2.1E4	4.0E5	3.4E5						
	1,000	2.1E4	2.8E5	5.9E4	1.4E3	2.5E2	5.9E1	6.0E1	2.4E1	1.7E1
	4,000	1.8E4	4.5E4	3.7E3						
	10,000	1.1E4	7.9E3	5.9E2						
60	100	9.2E3	2.0E5	2.0E6						
	400	9.2E3	1.7E5	2.1E5						
	1,000	9.1E3	1.1E5	3.4E4	6.9E2	9.2E1	1.6E1	2.4E1	1.1E1	1.7E0
	4,000	7.6E3	1.3E4	2.2E3						
	10,000	4.0E3	2.3E3	3.4E2						
90	100	7.4E1	7.7E4	2.3E5						
	400	7.3E1	5.4E4	1.7E4						
	1,000	7.2E1	2.1E4	2.7E3	1.4E2	8.9E2	1.3E0	3.1E0	1.8E0	2.0E-1
	4,000	5.1E1	1.7E3	1.7E2						
	10,000	2.0E1	2.8E2	2.7E1						
120	100	6.6E-1	1.3E3	6.2E4						
	400	6.5E-1	6.3E2	4.1E3						
	1,000	6.2E-1	1.6E2	6.5E2	6.8E0	1.2E0	1.7E-1	6.4E-1	6.1E-2	3.1E-2
	4,000	4.3E-1	2.0E1	5.2E1						
	10,000	1.0E-1	1.8E0	6.5E0						
150	100	5.5E-1	7.6E2							
	400	5.4E-1	2.5E2							
	1,000	5.1E-1	5.3E1	1.8E2	2.5E0	9.1E-2	5.3E-2	2.2E-2	1.1E-2	1.4E-2
	4,000	2.3E-1	3.5E0							
	10,000	5.6E-2	5.6E-1							
180	100	5.9E-1	8.2E2							
	400	5.7E-1	2.0E2							
	1,000	5.2E-1	3.8E1	9.6E1	1.0E0	2.7E-2	2.0E-2	2.2E-2	8.9E-3	4.5E-3
	4,000	1.9E-1	2.3E0							
	10,000	4.3E-2	3.9E-1							
300	100	6.5E-1	9.3E2							
	400	6.1E-1	9.8E1							
	1,000	4.6E-1	1.6E1	2.1E1	5.3E-2	5.8E-4	9.8E-4	4.0E-4	2.0E-4	2.7E-4
	4,000	8.7E-2	1.0E0							
	10,000	1.6E-2	1.6E-1							

Notes: E refers to the power of 10, e.g., 1.5E4 = 1.5×10^4. If f^{-2} scaling applies, only 1,000 MHz values are given.

[redacted]

[redacted]

Table 8-7 [redacted] Absorption (dB) Through Fireball at 1000 MHz for Detonations Above 80 km [redacted]

Time (sec)	Yield (Mt)	Detonation Altitude (km)								
		100	150	200	250	300	350	400	450	500
10	0.01	5.2E2	7.9E2	1.7E2	1.4E1	6.1E0	2.1E0	6.1E-1	2.0E-1	7.3E-2
	0.1	1.1E3	2.0E3	3.8E2	3.1E1	1.4E1	4.8E0	1.4E0	4.5E-1	1.6E-1
	1	3.2E3	5.4E3	9.0E2	5.0E1	5.5E0	7.9E-1	1.5E-1	3.3E-2	8.7E-3
	10	1.4E4	2.0E4	3.3E3	2.6E3	3.5E2	6.9E1	1.7E1	4.9E0	1.6E0
20	0.01	7.2E1	2.1E2	1.2E2	1.2E1	5.4E0	1.9E0	5.5E-1	1.8E-1	6.8E-2
	0.1	1.4E2	5.8E2	2.8E2	2.6E1	1.2E1	4.3E0	1.3E0	4.2E-1	1.5E-1
	1	4.1E2	1.8E3	6.7E2	4.3E1	5.1E0	7.6E-1	1.4E-1	3.2E-2	8.4E-3
	10	2.2E3	8.0E3	1.9E3	1.4E3	2.7E2	5.9E1	1.5E1	4.5E0	1.5E0
30	0.01	2.2E1	1.3E2	9.6E1	1.0E1	4.8E0	1.7E1	5.1E-1	1.7E-1	6.4E-2
	0.1	3.8E1	3.0E2	2.2E1	2.3E1	1.1E1	4.0E0	1.2E0	3.9E-1	1.5E-1
	1	1.2E2	7.2E2	5.3E2	4.6E1	6.2E0	1.0E0	2.0E-1	4.8E-2	1.30-2
	10	6.6E2	4.0E3	1.5E3	3.2E3	8.4E2	2.2E2	6.5E1	2.1E1	7.4E0
40	0.01	9.2E0	8.8E1	7.7E0	9.1E0	4.4E0	1.6E0	4.7E-1	1.6E-1	6.0E-2
	0.1	1.5E1	2.0E2	1.8E2	2.1E1	1.0E1	3.7E0	1.1E0	3.7E-1	1.4E-1
	1	4.6E1	4.9E2	4.3E2	3.6E1	5.3E0	9.1E-1	1.8E-1	4.4E-2	1.2E-2
	10	2.7E2	2.3E3	1.2E3	1.0E3	5.9E2	1.7E2	5.4E1	1.8E1	6.5E0
50	0.01	4.6E0	6.4E1	6.4E1	8.2E0	4.0E0	1.5E0	4.4E-1	1.5E-1	5.7E-0
	0.1	7.1E0	1.5E2	1.5E2	1.9E1	9.2E0	3.4E0	1.0E0	3.5E-1	1.3E-1
	1	2.2E1	3.6E2	3.5E2	3.0E1	4.6E0	8.2E-1	1.7E-1	4.1E-2	1.1E-2
	10	1.4E2	1.4E3	1.0E3	1.3E3	4.4E2	1.4E2	4.5E1	1.6E1	5.8E0
60	0.01	2.3E0	4.9E1	5.4E1	7.5E0	3.7E0	1.4E0	4.2E-1	1.4E-1	5.4E-2
	0.1	4.8E0	1.1E2	1.2E2	1.7E1	8.6E0	3.2E0	9.7E-1	3.3E-1	1.3E-1
	1	1.1E1	2.7E2	3.0E2	2.4E1	4.1E0	7.4E-1	1.6E-1	3.9E-2	1.1E-2
	10	7.5E1	9.3E2	8.7E2	9.3E2	3.4E2	1.1E2	3.9E1	1.4E1	5.2E0
90	0.01	9.9E-1	2.7E1	3.6E1	6.0E0	3.1E0	1.8E0	3.6E-1	1.2E-1	4.7E-2
	0.1	1.5E0	6.0E1	8.2E1	1.4E1	7.1E0	2.7E0	8.4E-1	2.9E-1	1.1E-1
	1	3.7E0	1.4E2	2.0E2	1.5E1	2.9E0	5.7E-1	1.3E-1	3.2E-2	9.2E-3
	10	2.0E1	4.1E2	5.8E2	4.2E2	1.8E2	6.8E1	2.5E1	9.9E0	3.9E0
125	0.01	4.7E-1	1.6E-1	2.5E1	5.0E1	2.6E0	1.0E0	3.1E-1	1.1E-1	4.2E-2
	0.1	5.5E-1	3.5E1	5.7E1	1.1E1	6.0E0	2.4E0	7.4E-1	2.6E-1	9.9E-2
	1	1.5E0	8.3E1	1.4E2	9.7E0	2.1E0	4.4E-1	1.0E-1	2.7E-2	7.8E-3
	10	6.8E0	2.3E2	3.9E2	1.8E2	1.0E2	4.2E1	1.8E1	7.1E0	3.0E0
180	0.01	2.8E1	9.9E0	1.8E1	4.0E0	2.1E0	8.6E-1	2.7E-1	9.4E-2	3.7E-2
	0.1	2.1E-1	2.1E1	3.8E1	9.2E0	5.0E0	2.0E0	6.4E1	2.2E1	8.7E0
	1	5.6E-1	4.8E1	9.0E1	5.9E0	1.4E0	3.3E-1	8.0E-2	2.1E-2	6.4E-3
	10	2.6E1	1.3E2	2.5E2	6.8E1	5.0E1	2.5E1	1.1E1	4.9E0	2.1E0
300	0.01	4.5E-2	4.6E0	1.0E1	2.8E0	1.6E0	6.5E-1	2.1E-1	7.5E-2	2.9E-2
	0.1	5.9E-2	7.7E0	2.0E1	6.4E0	3.6E0	1.5E0	4.9E-1	1.8E-1	6.9E-2
	1	1.3E-1	2.0E1	4.5E1	2.4E0	7.0E-1	1.8E-1	4.9E-2	1.4E-2	4.4E-3
	10	5.6E-1	4.9E1	1.2E2	1.4E1	1.2E1	9.1E0	5.0E0	2.4E0	1.2E0
600	0.01	7.3E-3	9.3E-1	3.3E0	1.3E0	7.1E-1	3.1E-1	1.2E-1	4.6E-2	1.8E-2
	0.1	1.1E-2	1.6E0	5.8E0	2.6E0	1.6E0	8.1E-1	3.0E-1	1.1E-1	4.4E-2
	1	1.7E-2	3.2E0	1.2E1	4.1E-1	2.4E-1	7.6E-2	2.3E-2	7.2E-3	2.4E-3
	10	7.0E-2	1.2E1	3.6E1	1.6E0	1.5E0	1.4E0	1.1E0	8.5E-1	4.5E-1
2000	0.01	2.2E-4	2.7E-2	1.2E-1	1.1E-1	8.5E-2	5.1E-2	2.2E-2	9.1E-3	4.0E-3
	0.1	2.8E-4	5.3E-2	2.5E-1	2.4E-1	2.1E-1	1.3E-1	5.9E-2	2.6E-2	1.2E-2
	1	5.7E-4	1.2E-1	5.7E-1	1.2E-2	10.0E-3	7.0E-3	4.1E-3	1.7E-3	6.4E-4
	10	2.2E-3	5.2E-1	2.3E0	3.5E-2	3.7E-2	3.9E-2	3.8E-2	3.5E-2	3.0E-2

Note: E refers to the power of 10, e.g., 1.5E4 = 1.5×10^4.

[redacted]

[redacted]

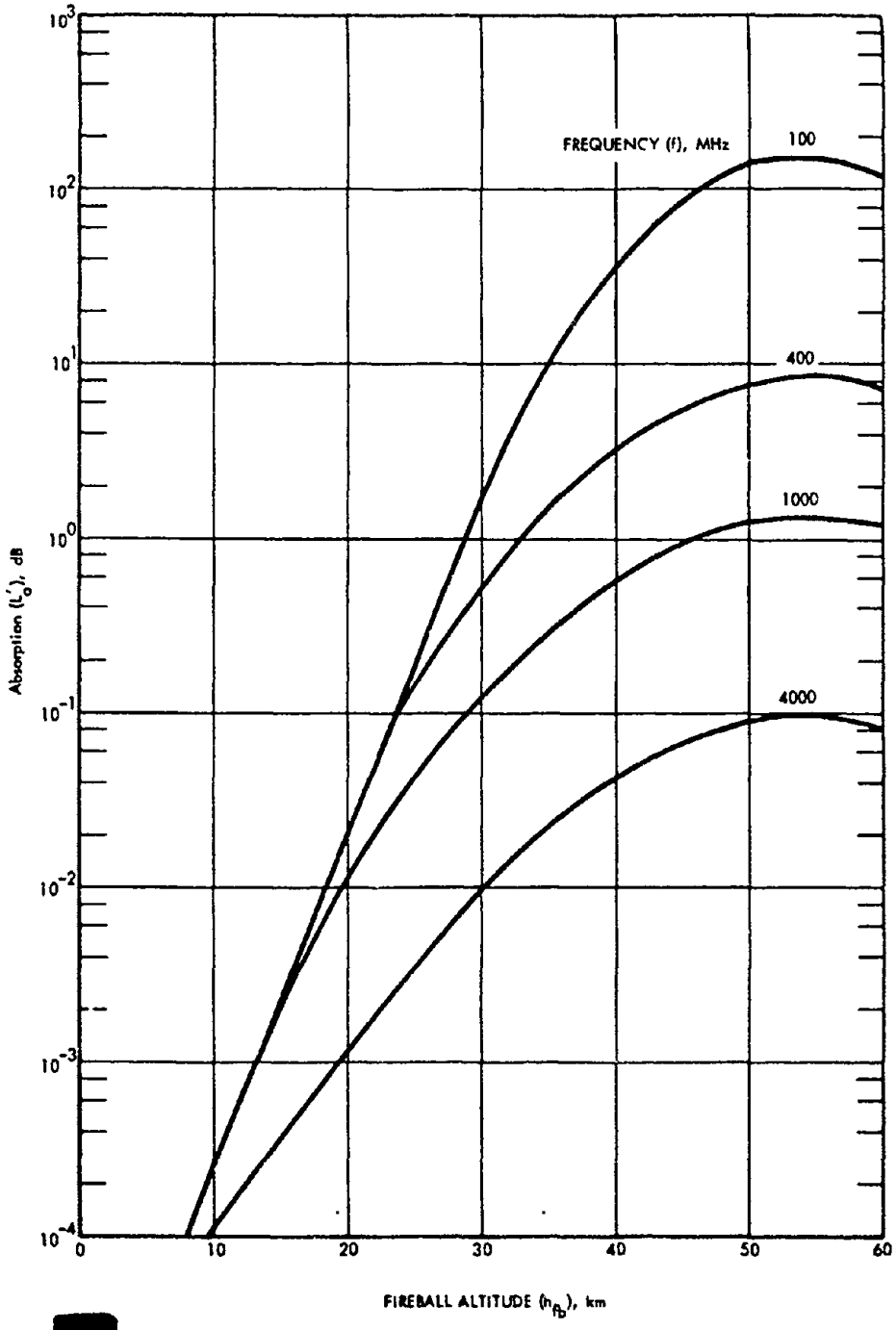

Figure 8-39. [redacted] One-Way Absorption Through Debris Region Due to Beta-Particle Ionization [redacted]

[redacted]

[redacted]

Problem 8-5 Absorption Due to Prompt Radiation Outside the Fireball [redacted]

[redacted] Figures 8-40 and 8-41 are used to obtain the one-way absorption along a propagation path caused by prompt radiation in terms of the one-way vertical absorption (the absorption for a single vertical traversal of the atmosphere) at a time t after burst. The absorption for the vertical path may be converted to that for an oblique path by using the secant of the angle of incidence at the altitude of peak absorption (approximately 65 km, see Problem 8-10).

[redacted] Using the detonation altitude and the ground range between the burst and the point where the propagation path intersects 65 km altitude, a reference yield W_r is obtained from Figure 8-40 (note that W_r differs for night and day). The location of the 65-km intersect point with respect to the propagation-path ground location can be determined from Figure 8-55 as described in Problem 8-10. If the actual weapon yield, W, is less than W_r, go to 2; otherwise go to 1.

1. Enter Figure 8-41 with time after burst in seconds and the radio frequency to obtain A_p', the one-way vertical absorption (note that the absorption differs for night and day). Go to 3.

2. Compute t_r:

$$t_r = \frac{W_r}{W} \text{ sec},$$

where W_r and W are both in Mt or kt. If $t > t_r$, go to 4; otherwise go to 3.

3. Enter Figure 8-41 with time after burst equal to t_r and the frequency to obtain $A_p'(t_r)$. Compute A_p':

$$A_p' = \frac{t_r A_p'(t_r)}{0.5t_r + 1.5t}.$$

Go to 5.

4. Enter Figure 8-41 with time after burst, t, and the frequency to obtain $A_p'(t)$. Compute A_p':

$$A_p' = \frac{tA_p'(t)}{t + t_r}.$$

5. Compute A_p, the one-way path absorption along the oblique path:

$$A_p = A_p' \sec \theta,$$

where $\sec \theta$ is the secant of the angle of incidence at 65 km determined from Figure 8-55.

[redacted] *Example 1* [redacted]

Given: A 1 Mt weapon detonated at an altitude of 300 km. The ground range between the burst and the propagation path is 800 km; the secant of the angle of incidence ($\sec \theta$) at 65 km is 3 for the propagation path.

Find: The one-way path absorption due to prompt radiation for a 100 MHz signal 10 seconds after the burst during the daytime.

Solution:

a. From Figure 8-40, W_r = 100 kt for a detonation altitude of 300 km and a ground range of 800 km.

b. Since $W_r < W$, A_p' is determined to be 12 dB from Figure 8-41.

c. $A_p = A_p' \sec \theta = (12)(3) = 36$ dB.

Answer: The one-way path absorption for a 100 MHz signal having a propagation path with an angle of incidence at 65 km whose secant is 3, resulting from prompt radiation from a 1 Mt weapon detonated at an altitude of 300 km, is 36 dB 10 seconds after burst at a ground range of 800 km from the burst point.

[redacted] *Example 2* [redacted]

Given: A 1 Mt weapon detonated at an

[redacted]

[redacted]

[redacted]

altitude of 200 km. The ground range between the burst and the propagation path is 1000 km; the secant of the angle of incidence (sec θ) at 65 km is 3 for the propagation path.

Find: The one-way path absorption due to prompt radiation for a 100 MHz signal 10 seconds after the burst during the daytime.

Solution:

a. From Figure 8-40, W_r = 5 Mt for a detonation altitude of 200 km and a ground range of 1000 km.

b. $t_r = \frac{W_r}{W} = 5.$

c. $t > t_r$; therefore, from Figure 8-41 $A_p'(t)$ = 12 dB, and

$$A_p' = \frac{tA_p'(t)}{t + t_r} = \frac{(10)(12)}{10 + 5} = 8 \text{ dB}.$$

d. $A_p = A_p' \sec \theta = (8)(3) = 24$ dB.

Answer: The one-way path absorption for a 100 MHz signal having a propagation path with an angle of incidence at 65 km whose secant is 3, resulting from prompt radiation from a 1 Mt weapon detonated at an altitude of 200 km, is 24 dB 10 seconds after burst at a ground range of 1000 km from the burst point.

[redacted] *Reliability* [redacted] The procedures given for computing absorption due to prompt radiation outside the fireball are based on simplified weapon design, atmospheric chemistry, and geometry models. More detailed models are required for specific communications and radar system problems.

[redacted] *Related Material* [redacted] See paragraph 8-2 and Problem 8-10.

[redacted]

[redacted]

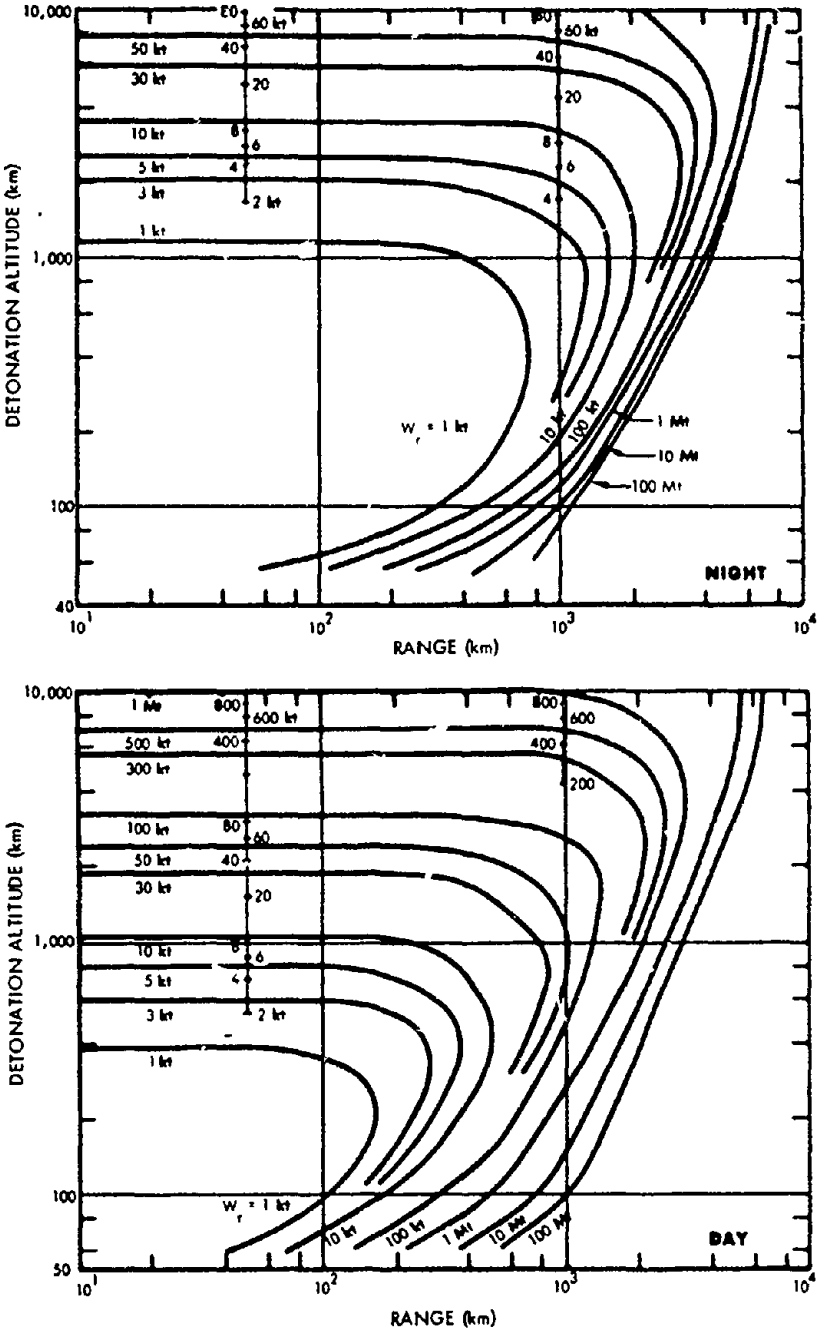

Figure 8-40. [redacted] Reference Weapon Yield W_r [redacted]

[redacted]

[redacted]

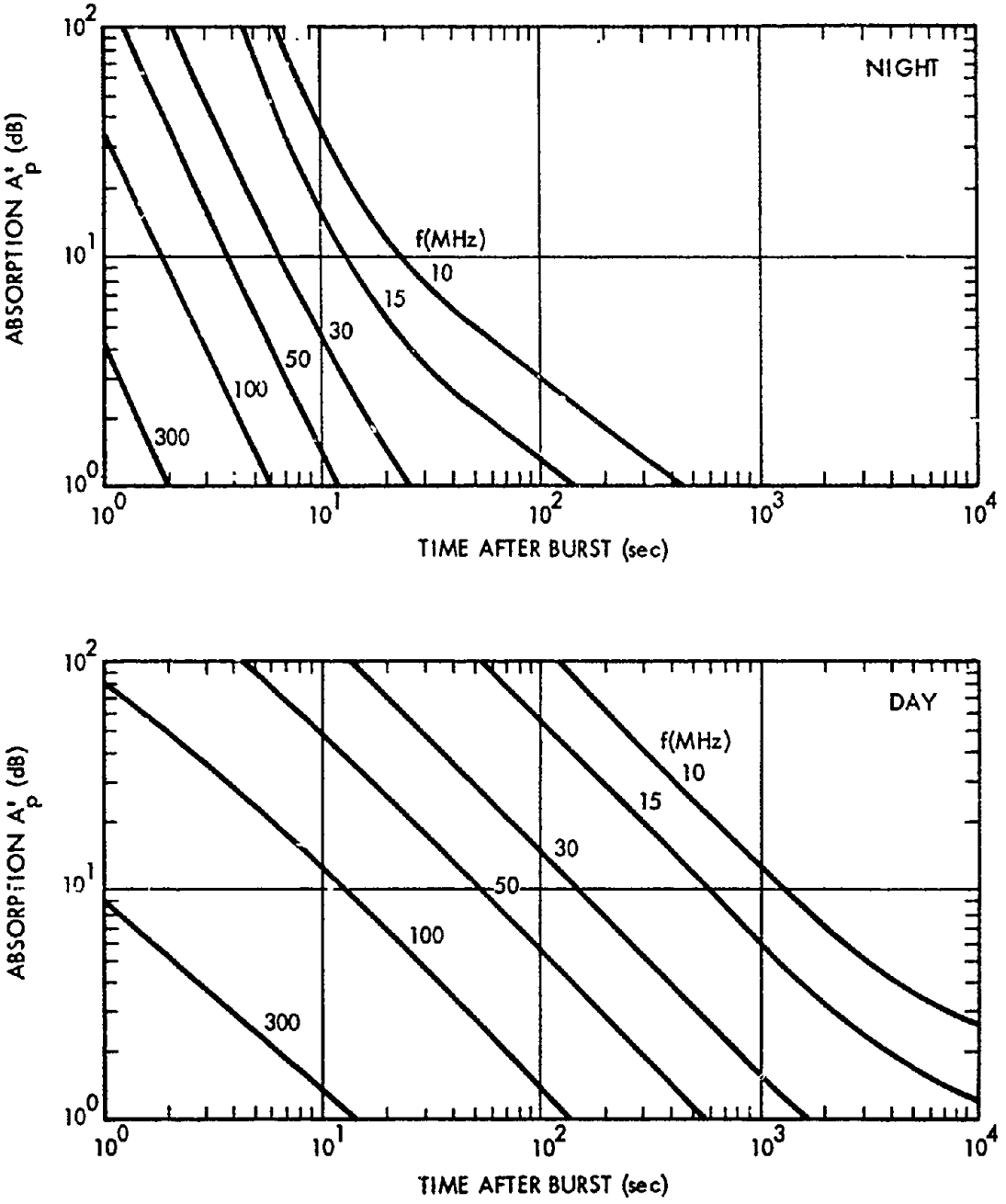

Figure 8-41. [redacted] One-Way Vertical Absorption Due to Prompt Radiation [redacted]

[redacted]

[redacted]

Problem 8-6 Absorption Outside the Fireball Due to Delayed Gamma Rays [redacted]

[redacted] Figures 8-42 through 8-48 are used to estimate the absorption caused by gamma rays emitted by the radioactive decay of fission debris. When the propagation path is within 100 km of the debris region and the debris region is below 120 km, the absorption depends on the orientation of the propagation path with respect to the debris region. Data are provided for three cases: a vertical path, a path passing above the debris region, and a path passing below the debris region. The geometry is illustrated in Figure 8-42.

[redacted] If the debris is at an altitude greater than 120 km or if the propagation path passes farther than 100 km from the debris region, absorption caused by gamma rays is given in terms of the gamma ray intensity parameter, I_γ. In determining I_γ, the debris region is modeled as a thin pancake region. Methods to determine the altitude and radius of the pancake debris region as a function of the burst parameters are described in Problems 8-1 through 8-3. If the altitude of detonation is below 85 km, the debris region is centered over the burst point (see Problem 8-1). For higher detonation altitudes, the center of the debris region is offset horizontally from the burst point toward the nearest magnetic pole after reaching maximum altitude (see Problem 8-2 and Figure 8-17). If the detonation altitude is greater than 120 km, up to three debris regions are defined (see Problem 8-3 and Figure 8-18).

[redacted] Figures 8-42 through 8-45 are used to obtain the one-way path absorption for bursts below 120 km and ground ranges from the debris less than 100 km. Choose the figure with the angle θ_d (see Figure 8-42) closest to the case of interest. Enter the figure with debris altitude, h_d, closest point of approach, X_d (see Figure 8-42), and time of day (day or night); obtain A'_γ, the one-way path absorption for a 1000 MHz signal 10 seconds after a 1 Mt fission yield detonation. Compute A_γ, the one-way path absorption:

$$A_\gamma = A'_\gamma W_F \frac{18}{(1 + t)^{1.2}} \frac{10^6}{f^2}$$

where W_F is the fission yield in Mt, t is the time in sec, and f is the propagation frequency in MHz.

[redacted] Figures 8-46 through 8-48 are used to obtain the one-way path absorption for bursts above 120 km or for cases where the ground range from the debris to the point where the propagation path intersects the altitude of 65 km is greater than 100 km. The following series of steps describe the procedure for obtaining the absorption.

1. Compute the quantity R', as follows:

$$R' = \begin{cases} \left[D^2 + (h_d - 60)^2\right]^{1/2} & D > R_d/2 \\ \left[\left(\frac{R_d}{2}\right)^2 + (h_d - 60)^2\right]^{1/2} & D \leq R_d/2 \end{cases}$$

where D is the ground range between the debris center and the point where the propagation path intersects 65 km altitude (see Figures 8-42 and 8-55 and Problem 8-10), and h_d and R_d are the debris altitude and radius, respectively (see Problems 8-1, 8-2, and 8-3).

2. Determine the debris-region fission yield W'_F:

$$W'_F = W_F \qquad h_o \leq 120 \text{ km}$$

$$W'_F = FF\ W_F \qquad h_o > 120 \text{ km}$$

where FF is the fraction of the total weapon fission yield in the debris region (see Problem 8-3).

[redacted]

3. Enter Figure 8-46 with debris-region fission yield (W_F'), time after burst t, and R' to obtain I_γ'.

4. Enter Figure 8-47 with debris altitude h_d, debris radius R_d, and the ground range where the propagation path intersects 65 km altitude D, to obtain C_γ. Compute I_γ:

$$I_\gamma = C_\gamma I_\gamma'.$$

If there is more than one debris region (if the detonation is above 120 km or if there are multiple bursts), the radiation intensity parametric I_γ should be found for each debris region and the sum of the radiation intensity parameters used to obtain the absorption.

5. Enter Figure 8-48 with I_γ, time of day (day or night), and frequency to obtain A_γ', the one-way vertical absorption. Compute A_γ, the one-way path absorption:

$$A_\gamma = A_\gamma' \sec \theta$$

where $\sec \theta$ is the secant of the angle of incidence at 65 km (see Problem 8-10).

[redacted] *Example 1* [redacted]

Given: A 1 Mt weapon, 50% fission (W_F = 0.5 Mt), detonated at an altitude of 30 km during the daytime.

Find: The one-way absorption resulting from gamma ray ionization for a 1000 MHz signal 2 min after burst if the ground range between debris center and the propagation path is less than 100 km, the closest point of approach of the propagation path to the debris center, X_d, is 20 km, and θ_d is 60° (see Figure 8-42).

Solution: By the methods described in Problem 8-1, the debris altitude is determined to be:

$$h_d = 49 \text{ km}.$$

From Figure 8-43, A_γ' = 14 dB for h_d = 49 km and X_d = 20 km. Therefore,

$$A_\gamma = A_\gamma' W_F \frac{18}{(1+t)^{1.2}} \frac{10^6}{f^2},$$

$$A_\gamma = (14)(0.5) \frac{18}{(121)^{1.2}} \frac{10^6}{10^6} = 0.4 \text{ dB}$$

Answer: The one-way path absorption for a 1000 MHz signal propagating on a path as described above 2 min after a daytime 1 Mt burst (W_F = 0.5 Mt) is 0.4 dB.

[redacted] *Example 2* [redacted]:

Given: A 1 Mt weapon, 50% fission, detonated at an altitude of 30 km during the nighttime.

Find: The one-way path absorption resulting from gamma ray ionization for a 100 MHz signal 2 min after burst if the ground range between the debris center and the point where the propagation path intersects 65 km is 200 km and sec θ = 3.

Solution:

a. By the methods described in Problem 8-1, the debris height, h_d, and radius, R_d, are determined to be:

$$h_d = 49 \text{ km},$$

$$R_d = 15 \text{ km}.$$

b. Since $D > R_d/2$,

$$R' = \left[D^2 + (h_d - 60)^2\right]^{1/2}$$

$$R' = \left[(200)^2 + (49 - 60)^2\right]^{1/2} \approx 200 \text{ km}$$

c. From Figure 8-46, I_γ' = 0.15 watts m^{-2}, for W_F = 0.5 Mt, $(1 + t)$ = 121 sec, and R' = 200 km.

d. From Figure 8-47, C_γ = 0.8 for $(D - R_d)$ = 185 km and h_d = 49 km. Therefore,

$$I_\gamma = C_\gamma' I_\gamma' = (0.8)(0.15) = 0.12 \text{ watts m}^{-2}$$

e. From Figure 8-48, $A_\gamma' = 1.0$ dB for $I_\gamma = 0.12$ watts m^{-2} and $f = 100$ MHz during the night. Therefore,

$$A_\gamma = A_\gamma' \sec\theta = 3.0 \text{ dB}.$$

Answer: The one-way path absorption for a 100 MHz signal propagating on a path as described above 2 min after a nighttime 1 Mt burst ($W_F = 0.5$ Mt) is 3.0 dB.

Example 3

Given: A 1 Mt weapon, 50% fission, detonated at an altitude of 300 km during the day at a location where the magnetic dip angle θ is 60°:

Find: The one-way path absorption resulting from gamma ray ionization for a 30 MHz signal 60 min after burst if the ground range between the point where the propagation path intersects 65 km is 1000 km due magnetic north of the burst point and sec $\theta = 3$.

Solution:

a. By the methods described in Problem 8-3, the height, h_d, radius, R_d, offset, Δd, and fraction of the debris, FF for the three debris regions (see Figure 8-18), are found to be:

Debris Region	h_d (km)	R_d (km)	Δ_d (km)	FF
1	390	170	75	0.25
2	550	500	125	0.2
3	390	170	75	0.35

Debris region 1 is centered 75 km magnetic north of the burst point. The ground range, D, between the debris center and the point where the propagation path intersects 65 km is 1000 – 75 = 925 km. The ground range between the center of debris region 2 and the propagation path is 875 km. Debris region 3 is offset 75 km south of the conjugate of the burst point and is too far from the propagation path to produce gamma ray ionization.

b. The quantity R' for debris region 1 is:

$$R_1' = \left[D^2 + (h_d - 60)^2\right]^{1/2}$$
$$= \left[(925)^2 + (330)^2\right]^{1/2} = 980 \text{ km}.$$

c. The debris region 1 fission yield is:

$$W_{F1}' = FF_1 \; W_F = 0.125 \text{ Mt}.$$

d. From Figure 8-46, $I_{\gamma 1}'$ is 2×10^{-5} watts m^{-2} for $W_{F1}' = 0.125$ Mt, $t = 3600$ sec, and $R_1' = 980$ km.

e. From Figure 8-47, $C_{\gamma 1}$ is 1 for $(D - R_d) = 775$ km and $h_d = 390$ km.

f. $I_{\gamma 1} = C_{\gamma 1} I_{\gamma 1}' = 2 \times 10^{-5}$ watts m^{-2}.

g. The quantity R' for debris region 2 is:

$$R_2' = \left[(875)^2 + (490)^2\right]^{1/2} = 1000 \text{ km}$$

h. The debris region 2 fission yield is:

$$W_{F2}' = FF_2 \; W_F = 0.1 \text{ Mt}$$

i. From Figure 8-46, $I_{\gamma 2}'$ is 1.5×10^{-5} watts m^{-2} for $W_{F2}' = 0.1$ Mt, $t = 3600$ sec, and $R_2' = 1000$ km.

j. From Figure 8-47, $C_{\gamma 2}$ is 1 for $(D - R_d) = 375$ km and $h_d = 550$ km.

k. $I_{\gamma 2} = C_{\gamma 2} I_{\gamma 2}' = 1.5 \times 10^{-5}$ watts m^{-2}.

l. $I_\gamma = I_{\gamma 1} + I_{\gamma 2} = 3.5 \times 10^{-5}$ watts m^{-2}.

m. From Figure 8-48, $A_\gamma' = 1$ dB for $I_\gamma = 3.5 \times 10^{-5}$ watts m^{-2} and $f = 30$ MHz.

n. $A_\gamma = A_\gamma' \sec\theta = 3$ dB.

Answer: The one-way path absorption for a 30 MHz signal propagating on a path as described above 60 min after a daytime burst ($W_F = 0.5$ Mt) is 3 dB. If the propagation path had been located near the conjugate of the burst point, gamma rays from debris regions 1 and 2 would not reach the path, and only debris region 3 would have been considered.

[redacted]

[redacted] *Reliability* [redacted] The procedures given for computing absorption due to gamma ray ionization are based on simplified-debris, atmospheric-chemistry, and geometry models. More detailed models are required for most radar and communication system problems.

[redacted] *Related Material* [redacted] See paragraphs 8-3, 8-8, 8-13, 8-14, and 8-15, and Problems 8-1, 3-2, and 8-3.

[redacted]

[redacted]

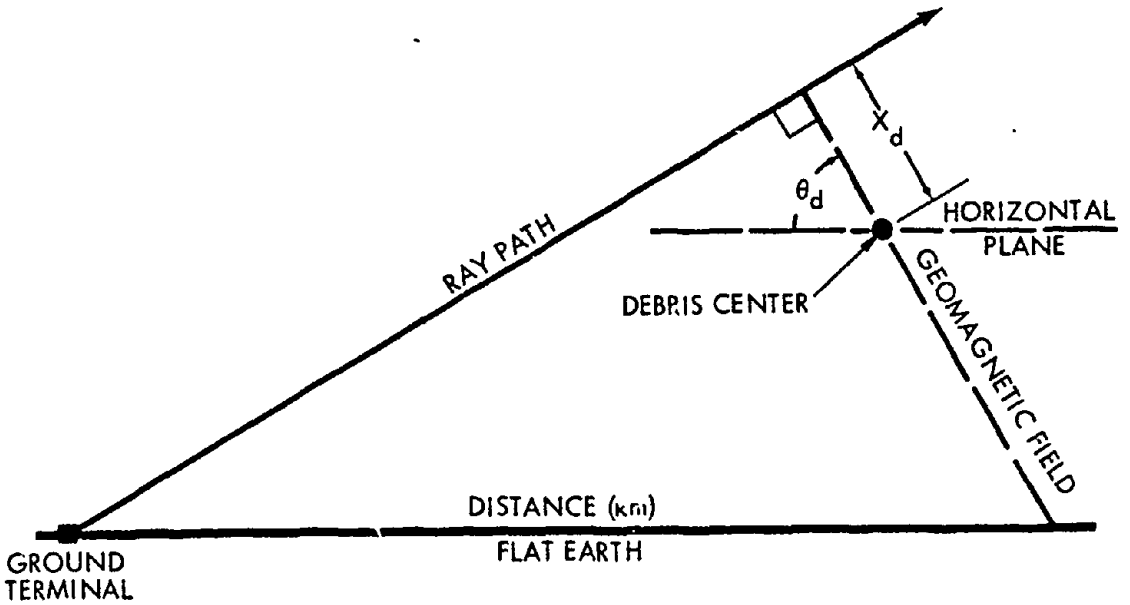

Figure 8-42. [redacted] Geometry for Gamma Ray Absorption [redacted]

[redacted]

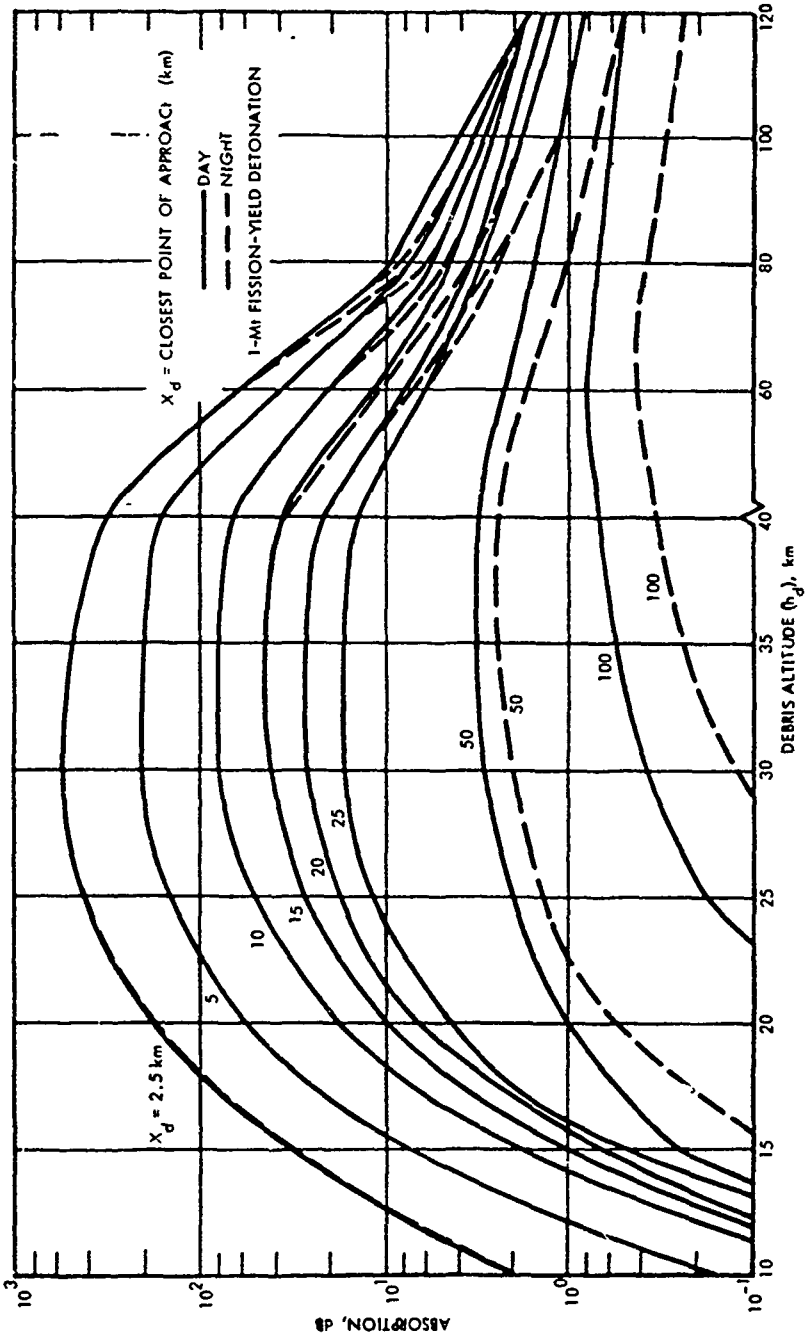

Figure 8-43. One-Way Absorption Due to Gamma Rays, f = 1000 MHz, θ_d = +60 Degrees

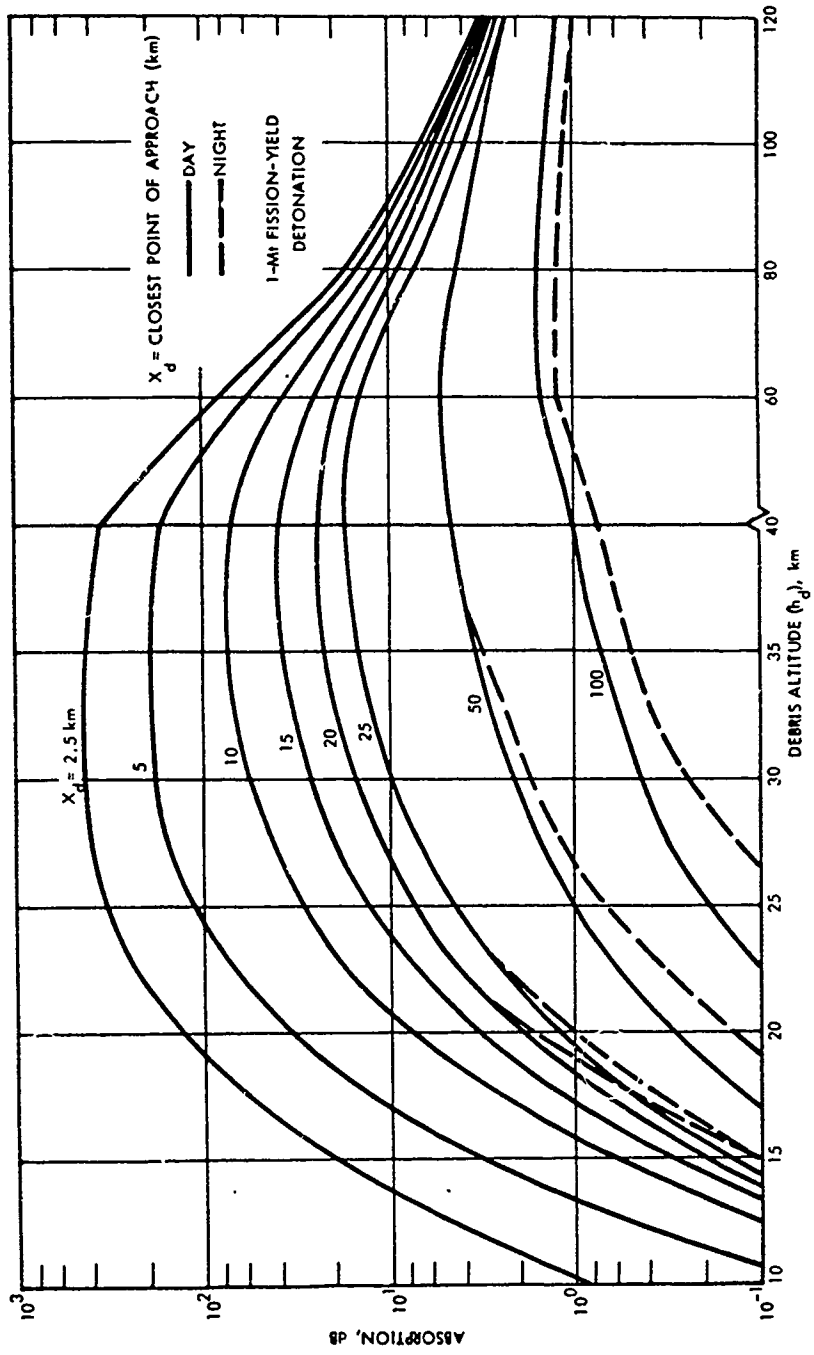

Figure 8-44. One-Way Absorption Due to Gamma Rays, f = 1000 MHz, θ_d = 0 Degrees

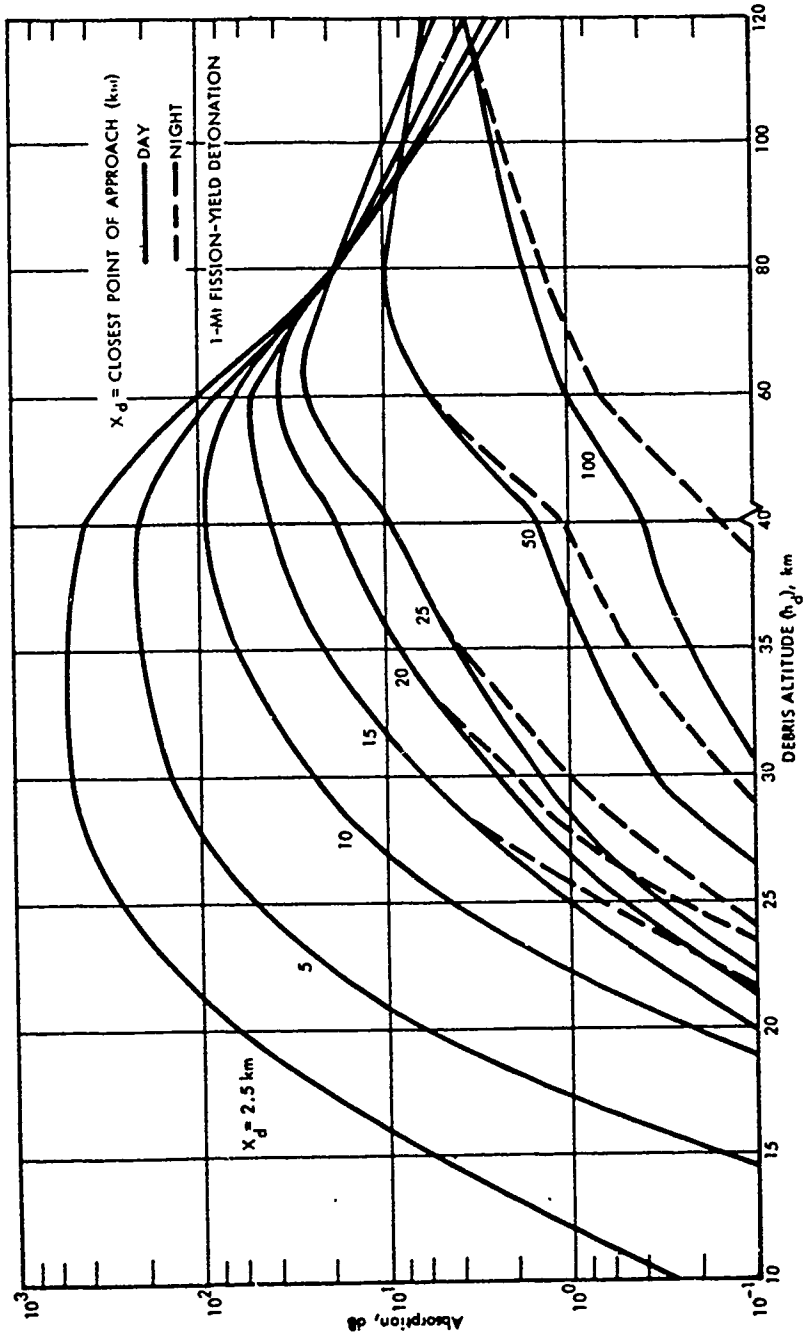

Figure 8-45. One-Way Absorption Due to Gamma Rays, f = 1000 MHz, θ_d = -60 Degrees

[redacted]

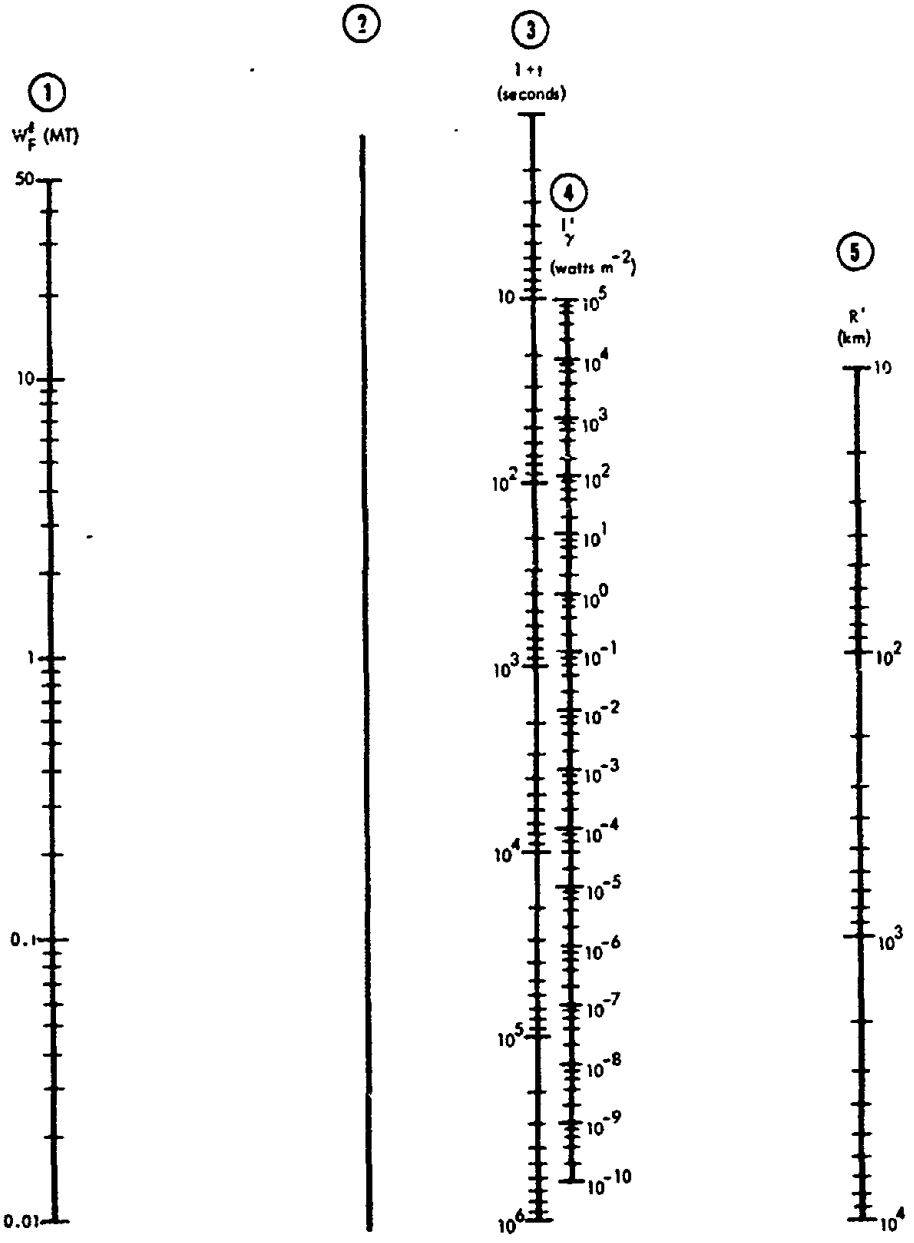

INSTRUCTIONS: To find I'_γ connect a straight line from fission yield (Scale 1) to time after detonation on Scale 3 (note this is a 1+t scale). Mark the intersection on Scale 2. Connect a straight line from the point determined on Scale 2 to the appropriate distance, R', on Scale 5. The intersection with Scale 4 is I'_γ.

Figure 8-46. [redacted] Gamma Radiation Intensity Nomogram [redacted]

[redacted]

[redacted]

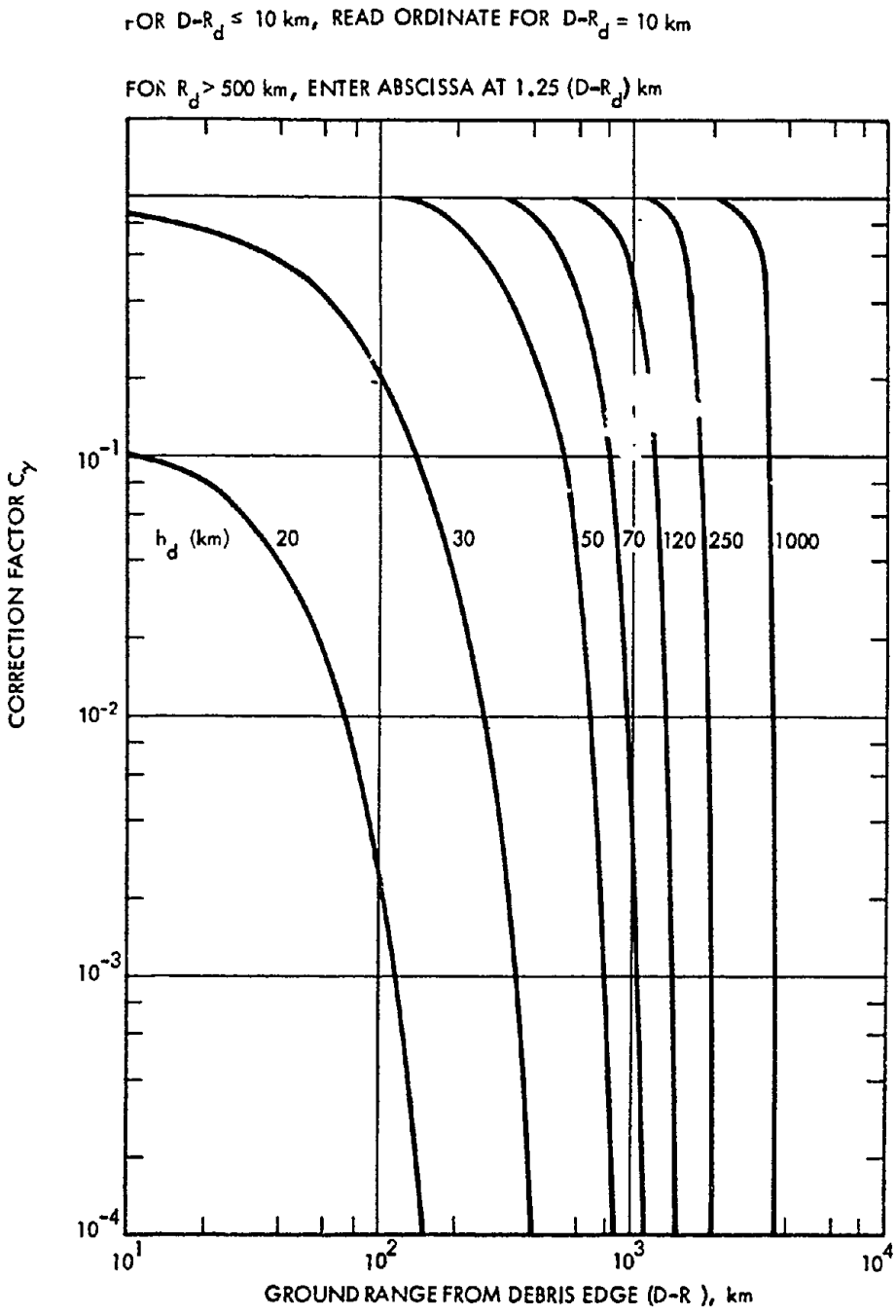

Figure 8-47. [redacted] Correction Factor for Gamma Ray Flux [redacted]

[redacted]

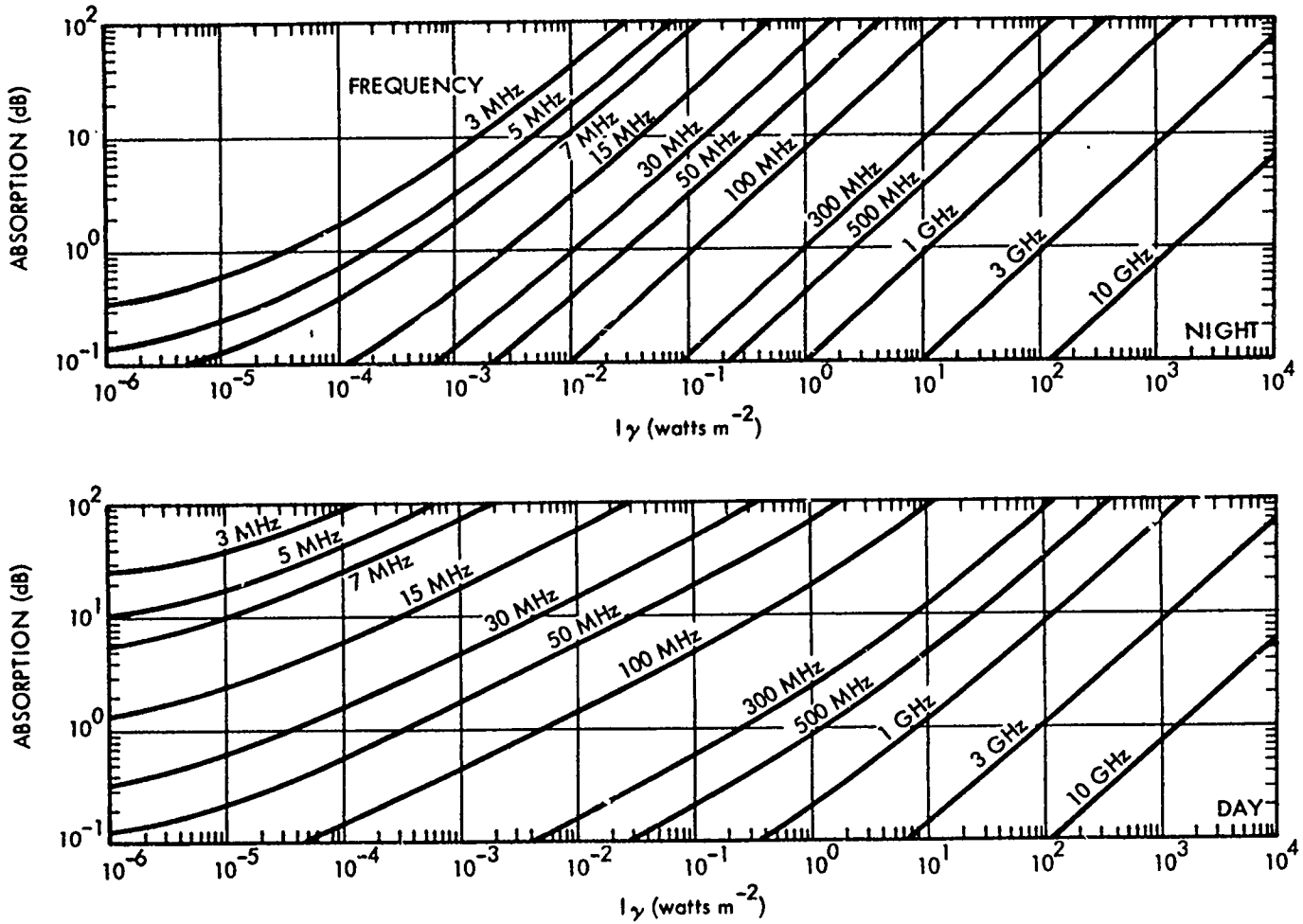

Figure 8-48. [redacted] One-Way Vertical Absorption Due to Gamma Rays [redacted]

Problem 8-7 Calculation of Absorption Outside the Fireball Due to Beta Particles

[redacted] Figures 8-49 through 8-51 are used to estimate the absorption outside the fireball region caused by beta particle ionization when the fission debris is above 60 km. If the debris is below 60 km, the absorption caused by beta particle ionization can be computed by the methods described in Problem 8-4.

[redacted] When the fission debris is above 60 km, the location of the beta particle absorption region with respect to the debris region is determined by the geomagnetic field (see paragraph 8-4). Most of the absorption occurs between the altitudes of 60 and 80 km. The predictions of absorption apply to beta particle radiation from fission debris that is uniformly distributed in a thin pancake-shaped region.

[redacted] Obtain the debris altitude, h_d, and debris radius, R_d, by the methods described in Problems 8-1, 8-2, or 8-3. If the detonation altitude, h_o, is greater than 85 km and the time after burst is greater than 10 minutes, determine the maximum debris altitude, h_m (km). Compute h:

$$h = h_d \quad \begin{cases} h_o < 85 \text{ or if} \\ h_o \geq 85 \text{ and } t < 10 \text{ minutes.} \end{cases}$$

$$h = h_m \qquad h_o \geq 85 \text{ and } t > 10 \text{ minutes.}$$

Enter Figure 8-49 with h and φ, the magnetic dip angle at the burst point to obtain Δ_β, the offset of the beta particle absorption region. If the magnetic dip angle at the burst point is not known, it can be obtained from Figure 8-54 as described in Problem 8-9.

[redacted] There are two beta particle absorption regions for each debris region; one is in the burst region and is offset a distance Δ_β from ground zero toward the nearest magnetic pole (see Figure 8-49), and the other is in the conjugate region and is offset from the conjugate of ground zero toward the nearest magnetic pole. Location of the conjugate of ground zero can be estimated from Figure 8-53 as described in Problem 8-8. The horizontal extent of the beta particle absorption region is approximately the same as that of the debris region (this neglects convergence of the magnetic field).

[redacted] If the propagation path passes through a beta particle absorption region, the one-way absorption can be found by the following procedure:

1. Determine the debris region fission yield, W_F':

$$W_F' = W_F \qquad h_o \leq 120 \text{ km}$$

$$W_F' = FF\ W_F \qquad h_o > 120 \text{ km}$$

where FF is the fraction of the total weapon fission yield in the debris region (see Problem 8-3).

2. Enter Figure 8-50 with debris region fission yield, W_F', time after burst, t, and debris radius, R_d, to obtain N_β. If the propagation path passes through more than one beta particle absorption region, compute the value of N_β for each region and use the sum to compute the one-way vertical absorption.

3. Enter Figure 8-51 with N_β, the frequency, f, and the time of day (day or night) to obtain A_β', the one-way vertical absorption. Compute A_β, the one-way absorption:

$$A_\beta = A_\beta' \sec \theta,$$

where $\sec \theta$ is the secant of the angle of incidence of the propagation path at 65 km which may be determined by the methods described in Problem 8-10.

[redacted]

[redacted]

Example 1

Given: A 1 Mt weapon, 50% fission, detonated at an altitude of 80 km at a location where the magnetic dip angle is 60° during daytime.

Find: The one-way absorption resulting from beta particle ionization for a 400 MHz signal 5 min after burst if sec $\theta = 3$.

Solution:

a. By the methods described in Problem 8-1, the debris height and radius are determined to be:

$$h_d = 305 \text{ km},$$

$$R_d = 200 \text{ km}.$$

b. Since $h_o < 85$ km,

$$h = h_d = 305 \text{ km}.$$

c. From Figure 8-49, $\Delta_\beta = 150$ km for $h = 305$ km, and $\theta = 60°$.

d. Since $h_o < 120$ km,

$$W_F' = W_F = 0.5 \text{ Mt}.$$

e. From Figure 8-50, $N_\beta = 4 \times 10^7$ betas cm^{-2} sec^{-1} for $W_F' = 0.5$ Mt, $t = 300$ sec, and $R_d = 200$ km.

f. From Figure 8-51, $A_\beta' = 2$ dB; therefore,

$$A_\beta = A_\beta' \sec \theta = 6 \text{ dB}.$$

Answer: There are two absorption regions caused by beta particle ionization. One is in the burst locale and is centered 150 km towards the nearest magnetic pole. The other is on the opposite side of the magnetic equator and is centered 150 km towards the nearest magnetic pole from the conjugate of the burst point. The horizontal radius of each absorption region is 200 km. The one-way path absorption for a 400 MHz signal passing through either absorption region is 6 dB.

Example 2

Given: A 1 Mt weapon, 50% fission, detonated at an altitude of 300 km at a location where the magnetic dip angle is 60° during daytime.

Find: The one-way absorption resulting from beta particle ionization for a 40 MHz signal 60 min after burst if the ground terminal is at burst ground zero, the propagation path is at an elevation of 15° along a zero degree magnetic azimuth, and sec $\theta = 3.4$.

Solution:

a. By the methods described in Problem 8-3, the height, h_d, radius, R_d, maximum altitude of rise, and fraction of the debris, FF, for the three debris regions (see Figure 8-18) are found to be:

Debris Region	h_d (km)	R_d (km)	h_m (km)	FF
1	390	170	550	0.25
2	550	500	800	0.2
3	390	170	550	0.35

b. Since $h_o > 85$ km and $t > 10$ min:

$$h_1 = h_{m1} = 550 \text{ km},$$

$$h_2 = h_{m2} = 800 \text{ km},$$

$$h_3 = h_{m3} = 550 \text{ km}.$$

c. From Figure 8-49, the beta particle absorption region offsets are:

$$\Delta_{\beta 1} = 300 \text{ km},$$

$$\Delta_{\beta 2} = 450 \text{ km},$$

$$\Delta_{\beta 3} = 300 \text{ km}.$$

d. Since $W_F = 0.5$ Mt, the fission yields contained in the debris regions are:

$$W_{F1}' = 0.125 \text{ Mt},$$

$$W_{F2}' = 0.1 \text{ Mt},$$

$$W_{F3}' = 0.175 \text{ Mt}.$$

[redacted]

[redacted]

e. Entering Figure 8-50 with the debris radii from "a," the fission yields from "d," and a time t = 3600 sec, the following values of N_β are obtained:

$$N_{\beta 1} = 10^6 \text{ betas cm}^{-2} \text{ sec}^{-1},$$

$$N_{\beta 2} = 8 \times 10^4 \text{ betas cm}^{-2} \text{ sec}^{-1},$$

$$N_{\beta 3} = 1.75 \times 10^6 \text{ betas cm}^{-2} \text{ sec}^{-1},$$

f. A sketch of the location of the absorption regions in the burst locale caused by beta particle ionization is shown in Figure 8-52. The propagation path chosen for this example traverses the absorption regions caused by all three debris regions. Thus, the values of N_β for each debris region are added together before finding the absorption.

$$N_\beta = N_{\beta 1} + N_{\beta 2} + N_{\beta 3}$$
$$= 2.8 \times 10^6 \text{ betas cm}^{-2} \text{ sec}^{-1}$$

g. From Figure 8-51, the one-way vertical absorption for a 40 MHz signal is

$$A'_\beta = 40 \text{ dB}$$

and

$$A_\beta = A_\beta \sec \theta = 136 \text{ dB}.$$

Answer: The one-way path absorption for a 40 MHz signal propagating on the path as described above 60 min after a 1 Mt (W_F = 0.5 Mt) daytime burst at 300 km is the sum of the absorptions caused by all three debris regions and is 136 dB.

[redacted] *Reliability* [redacted]: The procedures given for computing absorption due to beta particle ionization are based on simplified debris, atmospheric chemistry, and geometry models. More detailed models are required for most radar and communication system problems.

[redacted] *Related Material* [redacted]: See paragraphs 8-4, 8-5, 8-8, 8-13, 8-14, and 8-15, and Problems 8-1, 8-2, and 8-3.

[redacted]

[redacted]

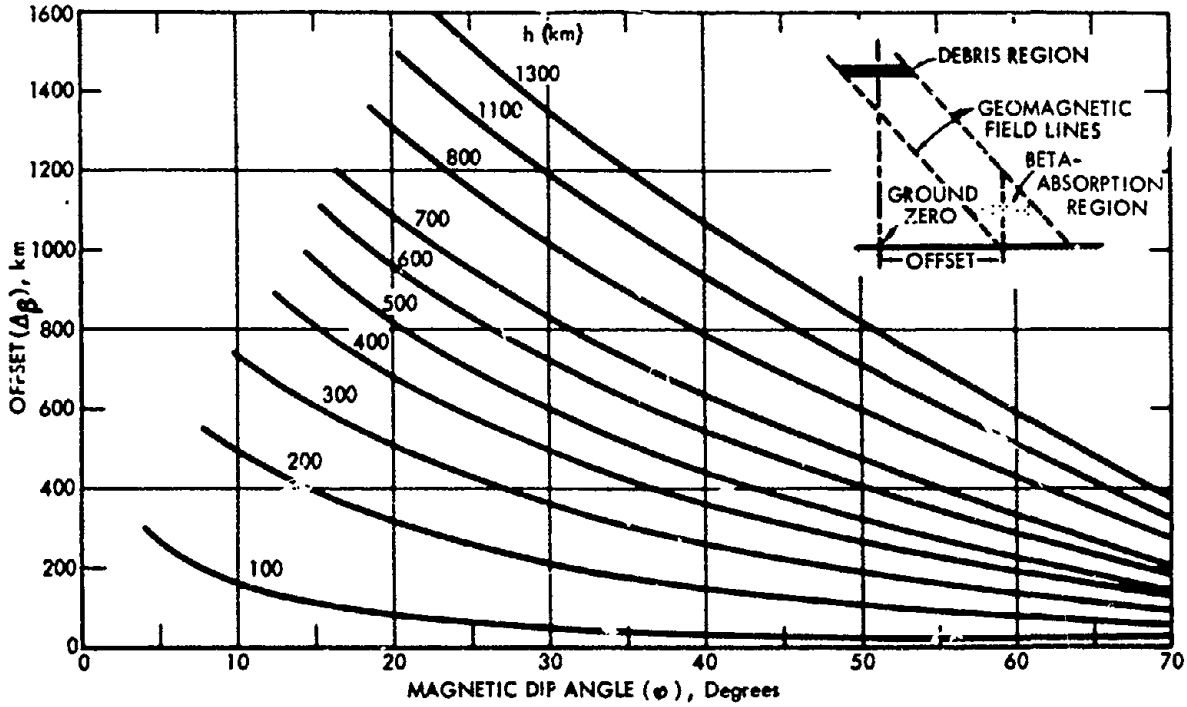

Figure 8-49. [redacted] Offset of Beta-Absorption Region [redacted]

[redacted]

[redacted]

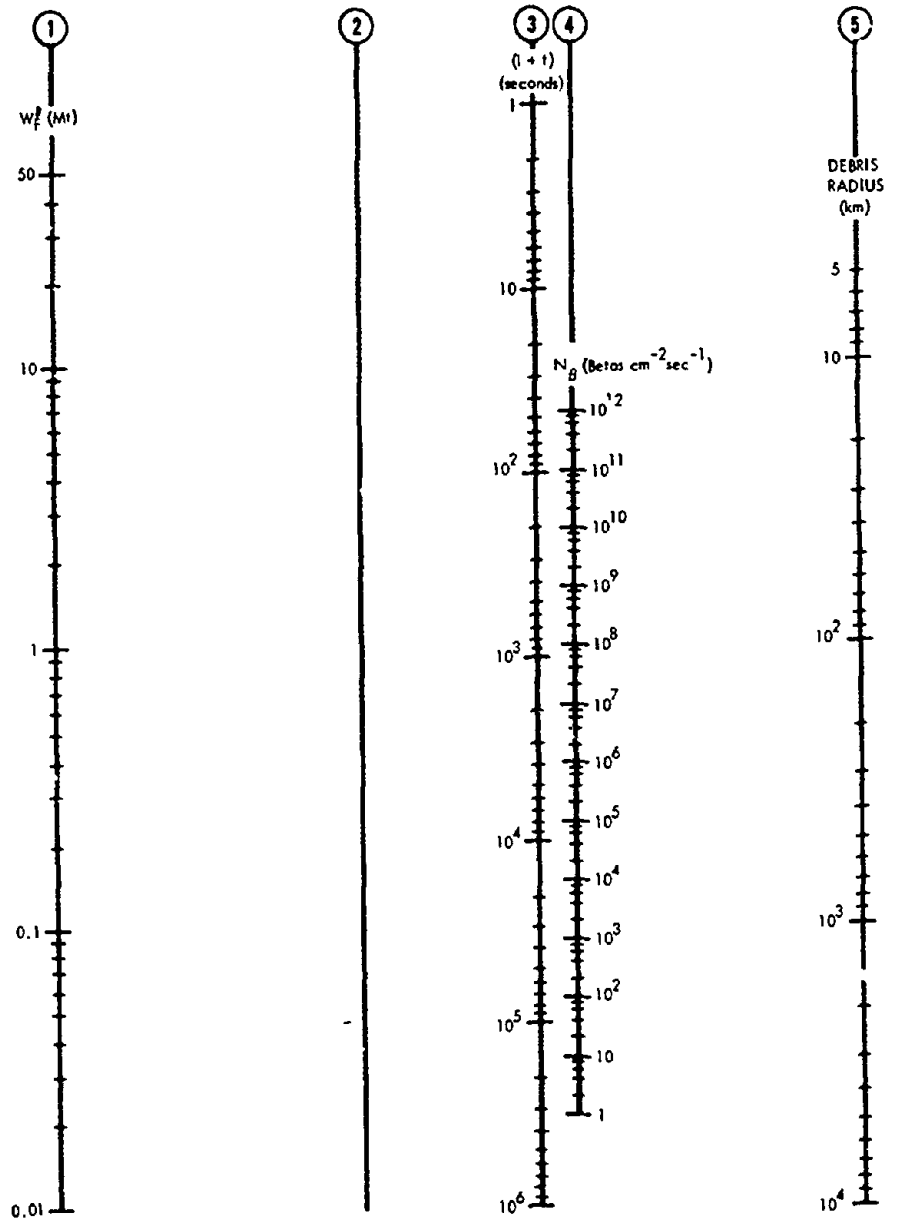

INSTRUCTIONS: To find N_β connect a straight line from fission yield (Scale 1) to time after detonation (Scale 3- this is a 1 + t scale). Mark the point of intersection of this line with Scale 2. Then draw a straight line from this point to the appropriate debris radius on Scale 5. The intersection of the latter line with Scale 4 is N_β.

Figure 8-50. [redacted] Beta Radiation Intensity Nomogram [redacted]

[redacted]

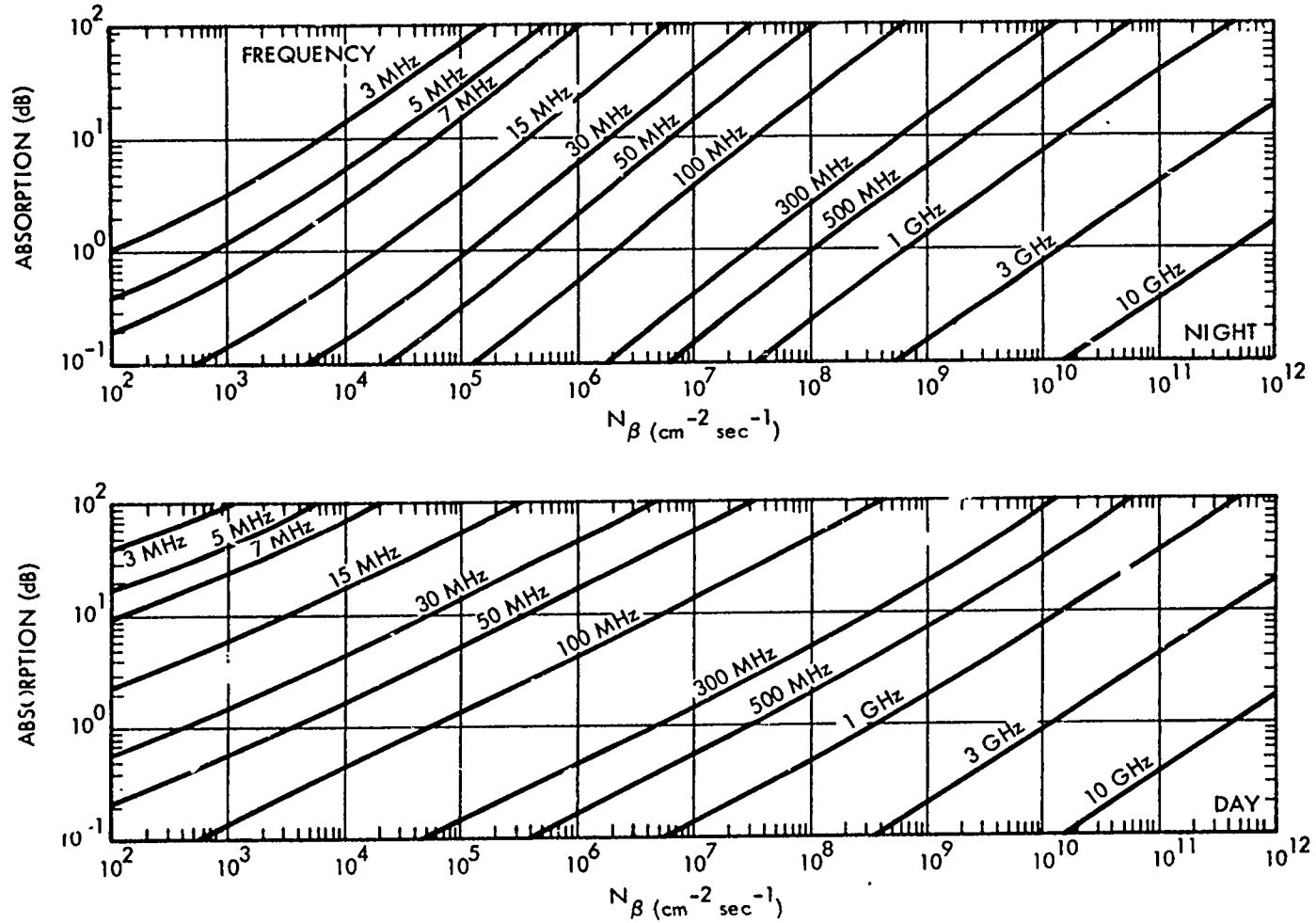

Figure 8-51. [redacted] One-Way Vertical Absorption Due to Beta Particles, Debris Altitude Above 60 km [redacted]

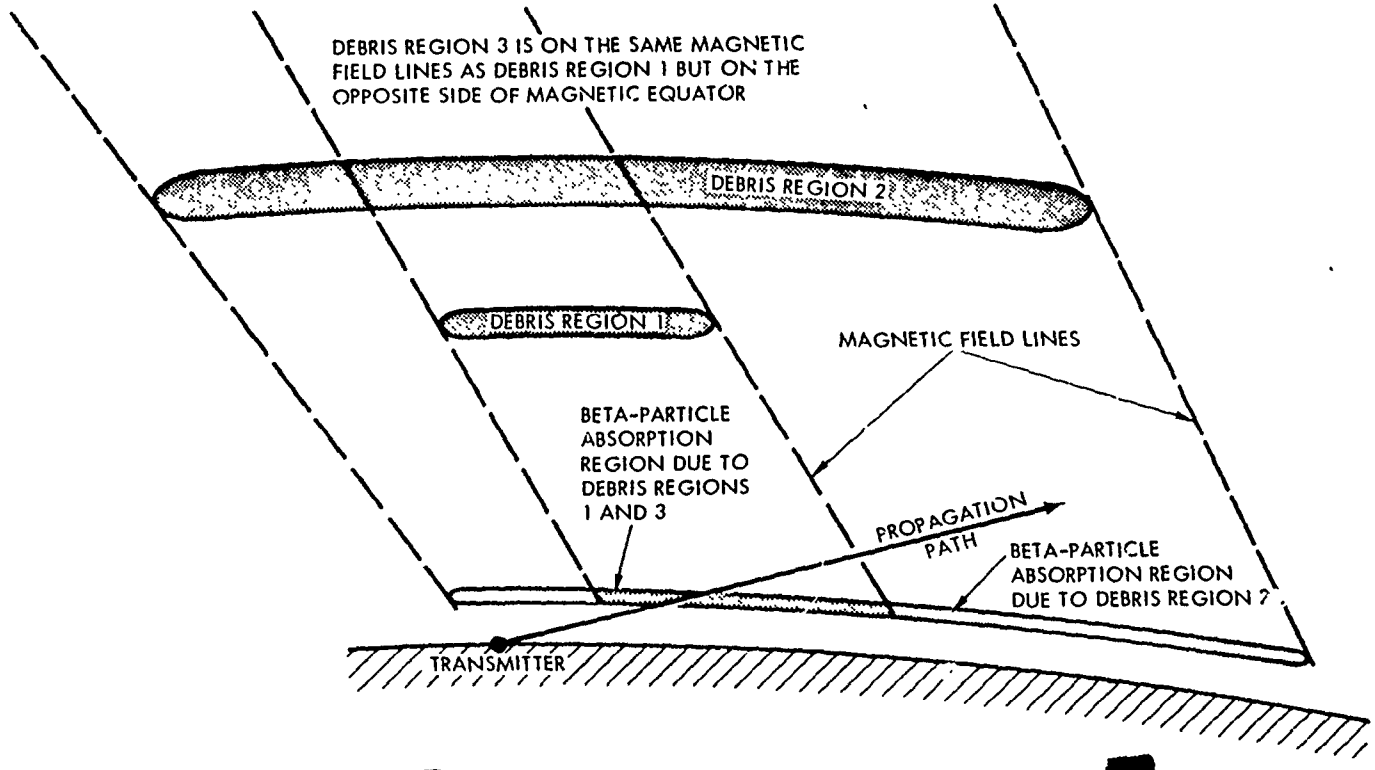

Figure 8-52. Sketch of Absorption-Region Geometry for Example 2

[redacted]

Problem 8-8 Magnetic Conjugate Map [redacted]

[redacted] Figure 8-53 presents the location of geomagnetic conjugate points on the earth's surface. Using the geographic coordinates of a given point, enter Figure 8-53 on the straight-line rectangular grid, and read the geographic coordinates of the magnetic conjugate point on the heavy curved grid.

[redacted] In reading Figure 8-53, note that the east-west curved dashed lines indicate conjugate latitude, plus for degrees north latitude and minus for degrees south latitude. Similarly, the north-south curved solid lines indicate conjugate longitude, plus for degrees east longitude and minus for degrees west longitude:

[redacted] *Example* [redacted]

Given: Geographic coordinates 45°N, 77°W (point near Ottawa, Canada).

Find: The coordinate of the conjugate point.

Solution: The given coordinates occur at the intersection of the -71° and -93° heavy grid lines.

Answer: The approximate geographic coordinates of the conjugate point are 71°S and 93°W.

[redacted] *Reliability* [redacted] In addition to uncertainties in the geomagnetic field, distortions of the geomagnetic field caused by the burst may persist for tens of seconds. Thus, the locations of conjugate debris and beta particle ionization regions may be significantly different than predicted by Figure 8-53.

[redacted] *Related Material* [redacted] See paragraph 8-4.

[redacted]

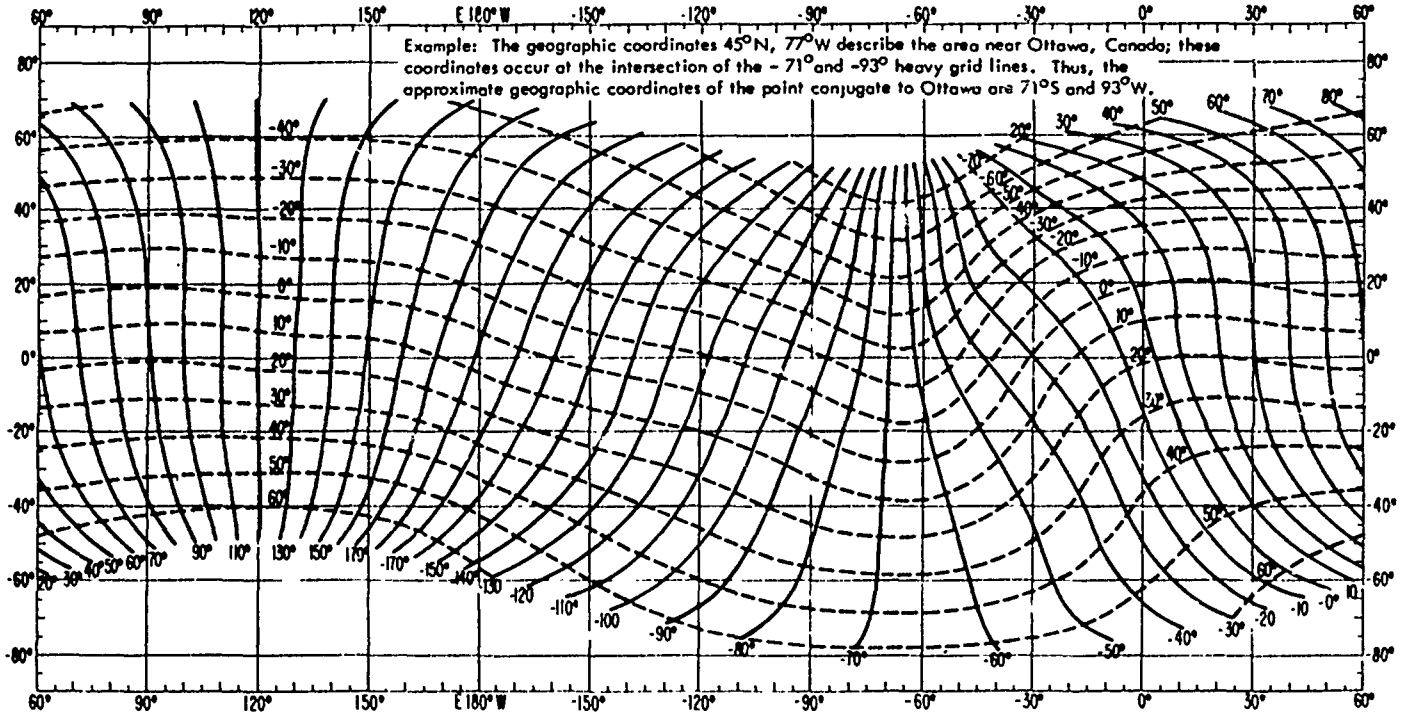

Figure 8-53. [redacted] Magnetic Conjugate Map [redacted]

[redacted]

Problem 8-9 Geomagnetic Dip Angle Map [redacted]

[redacted] Figure 8-54 presents the geomagnetic dip angle (declination) as a function of the geographic coordinates of a position on the earth's surface.

[redacted] *Example* [redacted]

Given: A point with geographic coordinates 40°N latitude, 100°W longitude.

Find: The geomagnetic dip angle.

Answer: From Figure 8-54 the magnetic dip angle is 70°.

[redacted] *Reliability* [redacted] Figure 8-54 shows the geomagnetic dip angle for undisturbed magnetic field conditions. The geomagnetic field may be distorted for tens of seconds after a nuclear detonation. Therefore, the locations of the debris and beta particle ionization regions may differ significantly from those predicted by Figure 8-54.

[redacted] *Related Material* [redacted] See paragraph 8-4.

[redacted]

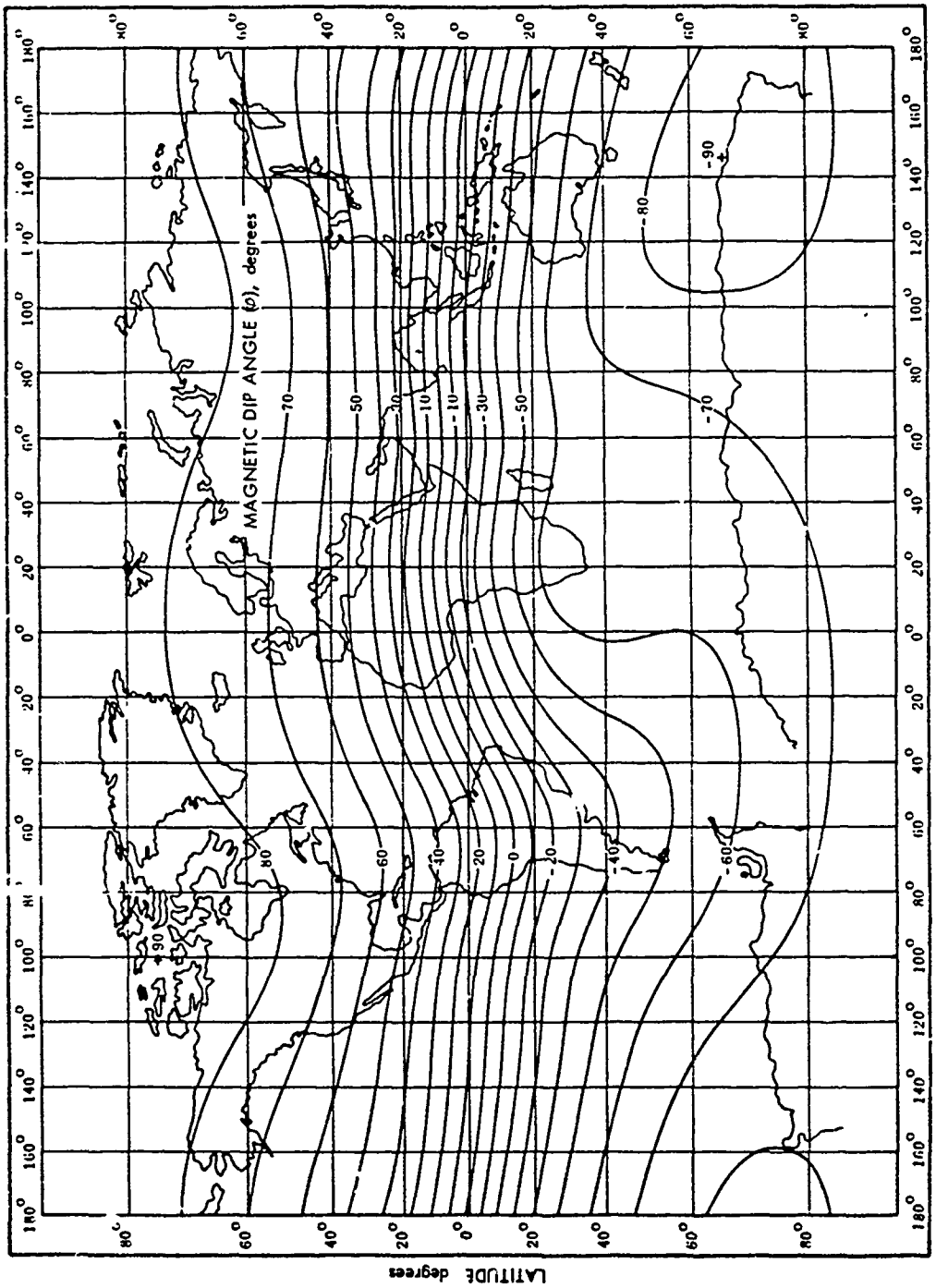

Figure 8-54. [redacted] World Map of Magnetic Dip [redacted]

[redacted]

Problem 8-10 Secant θ Chart [redacted]

[redacted] Figure 8-55 presents the secant of the angle of incidence of a ray path at 65 km altitude as a function of elevation angle or distance from the ground terminal to E- and F-region reflection points. The angle of incidence, θ, is illustrated in the sketch in Figure 8-55.

[redacted] *Example 1* [redacted]

Given: A propagation path with a 10-degree elevation angle (β).

Find: The horizontal distance from the ground terminal to the point where the propagation path intersects 65 km altitude, and the secant of the angle of incidence θ at the intersection.

Solution: Enter Figure 8-55 on the line sloping downward to the right labeled 10 degrees. Locate the intersection of this line with the line sloping upward to the right labeled h = 65 km. The abscissa of this intersection is the horizontal distance, and the ordinate is secant θ.

Answer: The horizontal distance from the ground terminal to the point where the propagation path intersects 65 km altitude is 320 km. The secant of the angle of incidence at the intersection is 4.6.

[redacted] *Example 2* [redacted]

Given: A HF propagation path that reflects from the F-region (300 km), 1500 km from the ground terminal.

Find: The horizontal distance from the ground terminal to the point where the propagation path intersects 65 km altitude, and secant θ at the intersection.

Solution: Enter the abscissa of Figure 8-55 at 1500 km. Proceed upward to the line labeled F-region Reflection Altitude (300 km). Note the elevation angle (β) corresponding to this point. Find the intersection of the elevation angle line with the line labeled D-region Absorption Altitude (65 km). The abscissa of this intersection is the desired horizontal distance, and the ordinate is secant θ.

Answer: The horizontal distance from the ground terminal to the point where the propagation path intersects 65 km altitude is 500 km. The secant of the angle of incidence at the intersection is 6.

[redacted] *Reliability* [redacted] The curves of Figure 8-55 are accurate for the simplified geometry assumed; however, the D, E, and F absorption and reflection altitudes are not single lines but occupy a volume of space which changes in ltitude with time of day and which may be affected by solar activity. Therefore, more detailed models are generally required for radar and communication system problems.

[redacted] *Related Material* [redacted] See paragraphs 8-1, 8-3, 8-4, 8-6, 8-7, 8-8, and Problems 8-1 through 8-6.

[redacted]

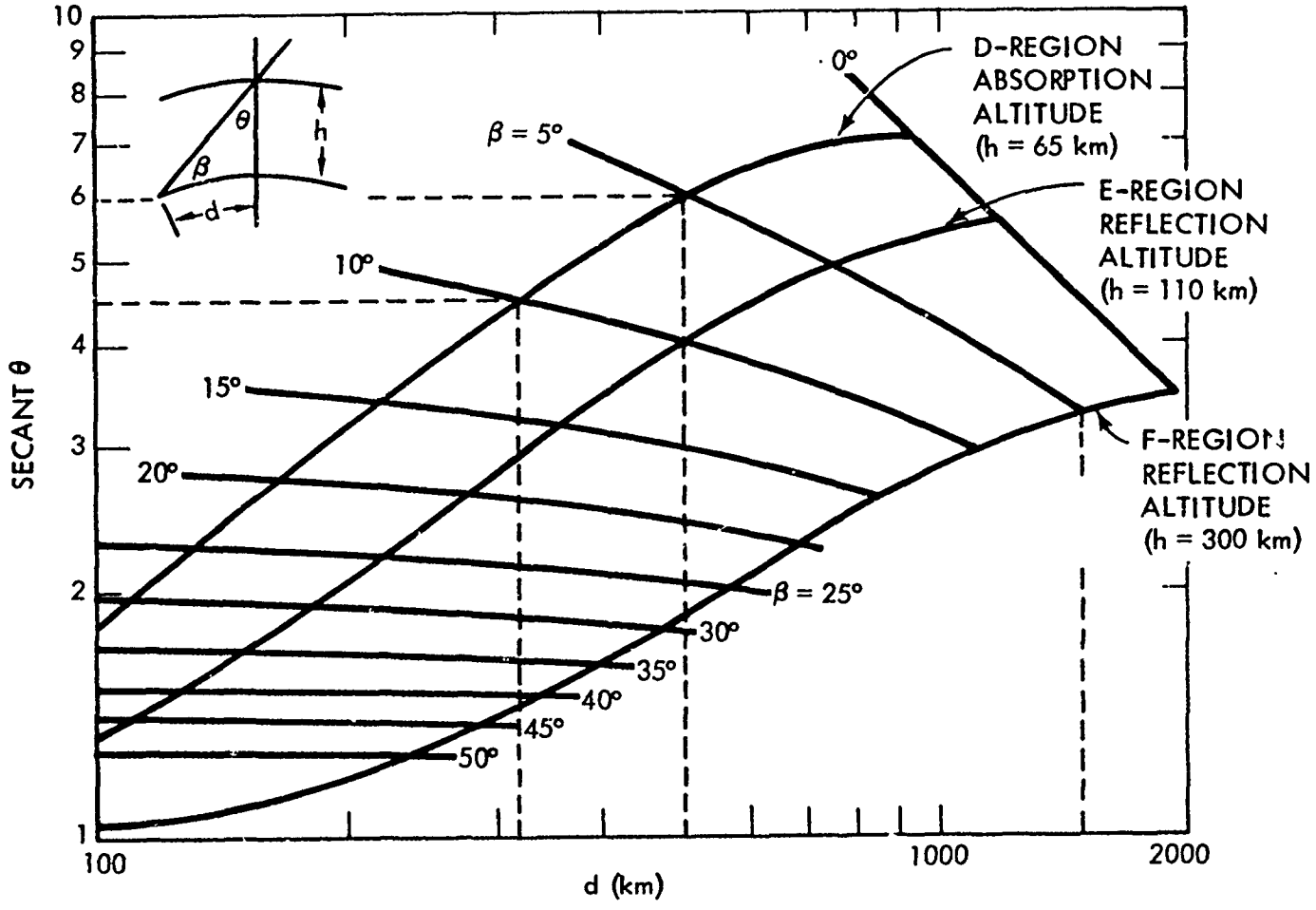

Figure 8-55. [redacted] Secant θ Chart [redacted]

[redacted]

[redacted] BIBLIOGRAPHY [redacted]

Atmospheric Ionization and Effects on Radar and Communications, A Bibliography, DASA 2069, Defense Atomic Support Agency, Washington, D.C., January 1968 [redacted]

Bibliography of Open and Unclassified Literature Pertaining to the Effects of High Altitude Nuclear Explosions, Parts I and II, Final Report, DASA 1795, Defense Atomic Support Agency, Washington, D.C., May 1966 [redacted]

DASA Reaction Rate Handbook, DASA 1948, Defense Atomic Support Agency, Washington, D.C., October 1967 [redacted] (will be revised as DNA 1948H during calendar year 1972).

Electromagnetic Blackout Handbook [redacted] Second Edition, Volume I: *Guide to Systems Effects* [redacted] DASA 1580, Defense Atomic Support Agency, Washington, D.C., December 1964 [redacted]

Electromagnetic Blackout Handbook [redacted] Second Edition, Volume II: *Nuclear Weapons Effects* [redacted] DASA 1580-1, Defense Atomic Support Agency, Washington, D.C., February 1965 [redacted]

High Altitude Tests Measurement Summary [redacted] DASA 1970, Defense Atomic Support Agency, Washington, D.C., September 1967 [redacted]

Knapp, W. S., and P. G. Fischer, *Aids for the Study of Electromagnetic Blackout*, DASA 2499, General Electric, TEMPO, Santa Barbara, Calif., July 1970 [redacted]

RANC IV, Computer Simulation of Radar Propagation in a Nuclear Environment, Volume I: *Computational Models*, DASA 2497-1, Defense Atomic Support Agency, Washington, D.C., July 1970 [redacted]

Weapon Effects Computer Code Directory, DASA 1727, Special Report 43, Defense Atomic Support Agency, Washington, D.C., April 1969 [redacted]

[redacted]

NTIS DISCLAIMER